Efficient Embeddings of Meshes and Hypercubes on A Group of Future Network Architectures

Yawen Chen

The School of Computer Science

The University of Adelaide

28 November, 2008

Contents

List of Figures

List of Tables

Abstract

Meshes and hypercubes are two most important communication and computation structures used in parallel computing. Network embedding problems for meshes and hypercubes on traditional network architectures have been intensively studied during the past years. With the emergence of new network architectures, the traditional network embedding results are not enough to solve the new requirements. The main objective of this thesis is to design efficient network embedding schemes for realizing meshes and hypercubes on a group of future network architectures. This thesis is organized into two parts.

The first part focuses on embedding meshes/tori on a group of double-loop networks by evaluating the traditional embedding metrics, since double-loop networks have been intensively studied and proven to have many desirable properties for future network architecture. We propose a novel tessellation approach to partition the geometric plane of double-loop networks into a set of parallelogram tiles, called *P-shape*. Based on the characteristics of P-shape, we design a simple embedding scheme, namely *P-shape embedding*, that embeds arbitrary-shape meshes and tori on double-loop networks in a systematic way. A main merit of P-shape embedding is that a large fraction of embedded mesh/torus edges have edge dilation 1, resulting in a low average dilation. These are the first results, to our knowledge, on embedding meshes and tori on general double-loop networks which is of great significance due to the popularity of these architectures. Our P-shape construction bridges between regular graphs and double-loop networks, and provides a powerful tool for studying the topological properties of double-loop networks.

In the second part, we study efficient embedding schemes for realizing hypercubes on a group of array-based WDM optical networks by analyzing the new embedding metric of wavelength requirement, as WDM optical networking is becoming a promising technology for deployment in many applications in advanced telecommunication and parallel computing. We first design routing and wavelength assignments of both bidirectional and unidirectional hypercubes on WDM optical linear arrays, rings, meshes

and tori with the consideration of communication directions. For each case, we identify a lower bound on the number of wavelengths required, and design the embedding scheme and wavelength assignment algorithm that uses a provably near-optimal number of wavelengths. To further reduce the wavelength requirement, we extend the results to WDM ring networks with additional links, namely WDM chordal rings. Based on our proposed embedding schemes, we provide the analysis of chord length with optimal number of wavelengths to realize hypercubes on 3-degree and 4-degree WDM chordal rings. Furthermore, we propose an embedding scheme for realizing dimensional hypercubes on WDM optical arrays by considering the hypercubes dimension by dimension, called lattice embedding, instead of embedding hypercubes with all dimensions. Based on lattice embedding, the number of wavelengths required to realize dimensional hypercube on WDM arrays can been significantly reduced compared to the previous results. By our embedding schemes, many communications and computations, originally designed based on hypercubes, can be directly implemented in WDM optical networks, and the wavelength requirements can be easily derived using our obtained results.

Keywords: Network Embedding, Parallel Computing, Optical Networks, Mesh, Hypercube, Double-loop Networks

Declaration

This work contains no material which has been accepted for the award of any other degree or diploma in any university or other tertiary institution and, to the best of my knowledge and belief, contains no material previously published or written by another person, except where due reference has been made in the text.

I give consent to this copy of my thesis when deposited in the University Library, being made available for loan and photocopying with respect to copyright where applicable.

Singed:

Yawen Chen

Acknowledgments

I first thank my principal supervisor Prof. Hong Shen for guiding my research. He has been part of my research in all the stages, starting from problem definition to publication of our solutions. Prof. Shen has provided me with encouragement and an endless source of ideas. His breadth of knowledge and his enthusiasm for research amaze and inspire me. I also would like to thank My co-supervisor, Professor Mike Brooks, for his support on my final year of my Ph.D study in the University of Adelaide. Thanks to Mr. Phillip Thomas for his help with editing assistance. Special thanks to Ms. Tracey Young and Mr. Yidong Li for their sincere help for complete this final version.

I am deeply indebted to school of computer science at the University of Adelaide, and the 21^{th} COE program in Japan Advanced Institute of Science and Technology (JAIST) for granting me scholarships, which enable me to pursue Ph.D study. Thanks them also for supporting me to present our work at some international conferences.

I would like to thank my friends and colleagues, especially Zonghua Zhang, Yingpeng Sang, Hui Tian, Shihong Xu and Yidong Li, for their insightful suggestions on study and life, which has been a great help for my future research career.

I owe a special debt of gratitude to my parents and family. They have, more than anyone else, been the reason I have been able to get this far. Words cannot express my gratitude to my parents, who give me their support and love from across the seas. My husband, Haibo Zhang, gives me his selfless support and love that make me want to excel.

Finally, I would like to thank all the people who either directly or indirectly provide me knowledge, experience, and support.

Thank you all, very much.

Publications

Published Papers

(1) Yawen Chen and Hong Shen. RWA of Hypercube Communications Embedded on A Family of Optical Double-Loop Networks. *15th IEEE International Conference on Networks (ICON)*, Adelaide, Australia, 2007.

(2) Yawen Chen and Hong Shen. Wavelength Assignment for Directional Hypercube Communications on a Class of WDM Optical Networks. *36th International Conference on Parallel Processing (ICPP)*, Xi-An, China, 2007.

(3) Yawen Chen, Hong Shen and Haibo Zhang. Embedding Hypercube Communications on Optical Chordal Ring Networks of Degree 4. *31st IEEE Conference on Local Computer Networks (LCN)*, Tampa, Florida, USA, 2006.

(4) Yawen Chen, Hong Shen and Haibo Zhang. Hypercube Communication Realized on Optical Chordal Ring Networks with Chord Length of 3. *11th Asia-Pacific Computer Systems Architecture Conference (ACSAC)*, Shanghai, China, 2006.

(5) Yawen Chen and Hong Shen. An Improved Scheme of Wavelength Assignment for Parallel FFT Communication Pattern on a Class of Regular Optical Networks. *International Conference on Network and Parallel Computing (NPC)*, Beijing, China, 2005.

(6) Yawen Chen and Hong Shen. Wavelength assignment for parallel FFT communication pattern on linear arrays by lattice embedding. *Fifth International Conference on Parallel and Distributed Computing, Applications and Technologies (PDCAT)*, Dalian, China, 2005.

Submitted Papers

(1) Yawen Chen and Hong Shen. Embeddings of Meshes and Tori on Double-loop Networks. Submit to **Journal of Computer and System Sciences**.

(2) Yawen Chen and Hong Shen. Routing and Wavelength Assignment for Directional Hypercubes on a Class of Array-based Optical Networks. Submitted to **Journal of Parallel and Distributed Computing**.

(3) Yawen Chen and Hong Shen. Routing and Wavelength Requirement of Hy-

percube Communication Pattern on Chordal Rings of Degrees 3 and 4. Submitted to **Computer Communication**.

Chapter 1

Introduction

Network embedding is widely used as a method for simulations between networks of different topological structures. The concept of network embedding has proven to be a successful one in understanding relationships between different architectures [76][111] [80]. This chapter introduces the concept of network embedding, and provides the preliminary knowledge used in this thesis.

1.1 Network Embedding

1.1.1 Definitions and Embedding Metrics for Network Embedding

One of the essential issues in evaluating a network is to study the graph embedding problem, which is a technique in graph theory [124]. Graph embedding has applications in a wide variety of computational situations [125] [71] [58] [98]. For example, the flow of information in a parallel algorithm defines a program graph, and embedding this into a networks is to organize the computation on the networks. Other problems that can be formulated as graph embedding problems are laying out circuits on chips, representing data structures in computer memory, and finding efficient program control structures.

Network embedding has many important applications in parallel processing, and provides the theoretical foundation for evaluating the relative performance of two different classes of interconnection networks [80] [71]. Networks are often organized into

various architectures, which can be represented as graphs. Network embedding in parallel computing concerns mapping the nodes of a *guest graph* G, which represents the communication requirement of a parallel algorithm, to the nodes of a *host graph* H, which models a static network. That is, the nodes in the guest graph represent the processes of a parallel task and the edges represent the need for data communication between the corresponding nodes.

Network embedding of one interconnection network into another is a very important issue in the design and analysis of parallel architectures [76]. Processor utilization and communication time are two important considerations in selecting data structures and algorithms for architectures assembled out of a large number of processors. Communication is one of the most expensive resources in such an architecture, and its efficient utilization is imperative [70]. In studying the efficient utilization of the communication system, the communication needs of the computations are modeled by a graph, which is usually referred to as the guest graph. This graph discloses the interaction between the data elements of the computation. Similarly, the topology of the architecture is captured by a host graph. Each vertex represents a processor with local storage and each edge a communication link between processors. The guest graph is embedded in the host graph for execution.

Through network embedding, the algorithms originally developed for one architecture can be directly mapped to another architecture. If the properties and structure of the underlying graph are used effectively, the computation and communication speeds can be significantly improved. There is much motivation behind embedding other parallel architectures [64]. First, efficient parallel algorithms may exist for some architectures which suit the needs of these algorithms perfectly, and we may wish to implement these algorithms on other network architectures. Second, the proof of embedding for an architecture shows that all algorithms should be implemented in new architecture with a level of efficiency determined only by the cost associated with the embedding. Furthermore, since the embedded architecture is usually easier to understand and visualize, it is often easier to design algorithms for the simpler architecture. In this sense, the embedded architecture can be considered as an abstraction from the guest architecture,

where the irrelevant connections are masked out. Finally, embedded architectures can be considered as parallel data structures for parallel architectures. Besides the inherent mathematical interest for network embedding problems, motivation for this study is derived from many concerns of computer science that can be effectively modeled by the following graph theoretical abstraction [46].

An *embedding* of a graph $G = (V_G, E_G)$, called *guest graph*, into a graph $H = (V_H, E_H)$, called *host graph*, is a mapping $f : G \rightarrow H$ consisting of two mappings $f_V : V_G \rightarrow V_H$ and $f_E : E_G \rightarrow P_H$, where P_H denotes the set of paths in the graph H. The mapping f_E maps edge $(u, v) \in E_G$ to a path $p \in P_G$ connecting $f_V(u)$ and $f_V(v)$ [67].

Using an embedding of guest network G into host network H, one can automatically transform any algorithms developed for a multiprocessor system connected by G into an algorithm for the multiprocessor system connected by H. Efficiency of an embedding is commonly measured by *expansion*, *dilation* and *congestion* [80]. These embedding parameters, defined as follows [68] [67] [46], strongly influence the effectiveness of the simulation.

- *Expansion* of the embedding is $|V_G|/|V_H|$, which is the ratio of the number of nodes in the guest graph compared to the number of nodes in the host graph.

- *Edge dilation* of edge $e_G \in E_G$ under an embedding f is the length of the path $f_E(e_G)$, where the length of a path p is the number of its edges. Let $E[f_E(e_G)]$ denote the set of edges in the path $f_E(e_G)$. The dilation of edge $e_G \in E_G$ under an embedding f is the length of the path $f_E(e_G)$: $dil_f(e_G) =\mid E[f_E(e_G)] \mid$.

- *Dilation* of an embedding f is the maximum dilation of an edge in G: $dil_f(G) = max_{\forall e_G \in E_G} dil_f(e_G)$.

- *Average dilation* has been used as a standard performance metric in practical evaluations of embedding [35], and represents the average length of an edge in guest network corresponding to a link in the host networks: $adil_f(G) = \frac{1}{|E_G|} \sum_{\forall e_G \in E_G} dil_f(e_G)$.

- *Edge Congestion* of an edge $e_H \in E_H$, $cong(e_H)$, is the number of paths in $\{f_E(e_G) \mid e_G \in E_G\}$ that contains e_H.

- *Congestion* of an embedding is the maximum congestion over all edges in H.

The delay is caused by the sum of dilation and congestion [80]. Dilation is the maximum distance in H between adjacent vertices (processes) in G and congestion is the maximum load on the edges (communication links) of H. A good mapping is said to exist when adjacent processors in the guest network are mapped to reasonably close processors in the host network (i.e. small dilation). Furthermore, the paths between adjacent processors in the guest network are chosen in such a way that the congestion at each host node and across each host edge is moderately small (i.e. small edge congestion). In the case of mapping guest networks onto smaller hosts, the processors of the host have to be assigned to about the same number of processes from the guest (i.e. small expansion). The general goal of graph embeddings is, given a guest graph G and a host graph H, to find an embedding function f that minimizes the dilation and congestion.

Network embedding problems on different types of topologies have been studied on various architectures over the past few decades. Embeddings of networks such as rings, meshes, complete trees, binomial trees, pyramids, X-trees, hypercubes and so on, have been investigated by numerous researchers. Most of the results are surveyed in [37], [80], [77] and [76]. Some embedding results are shown as follows. In [62], embeddings of complete binary trees into butterfly networks were studied. In [6], embedding of an arbitrary binary tree into the star graph was designed. The problem of embedding complete binary trees in product graphs was discussed in [44]. In [5], the embedding for fault-tolerant capabilities of networks whose underlying topology is k-array n-cube was studied. In [94], Monien demonstrated how to embed an arbitrary binary tree with dilation 11 and optimal expansion into an X-tree. In [66], it is proven that the complete binary tree can be embedded into the square grid of the same size with almost optimal dilation. In [13], the embedding of caterpillars, which is a special type of trees where vertices of degree 3 or greater lie on a single path, into the hypercube was exam-

ined. In [78], it is shown that large cube-connected-cycles and butterfly networks can be simulated very efficiently on smaller ones. In [111], the general relation, bounds and inequalities were discussed for the studied parameters and their special cases stressing the similarity and duality between them instead of discussing the results on specific graphs.

1.1.2 Embeddings of Meshes and Hypercubes

Meshes and Hypercubes are two of the most important and popular structures used in parallel computing. One of the biggest reasons for the popularity of meshes and hypercubes is their ability to efficiently embed a large number of parallel structures.

1.1.2.1 Meshes

Mesh is the best-known and easiest-to-build interconnection network for parallel computers, as it enjoys efficient VLSI layouts, simplicity of topology, and a large number of parallel algorithms that can be efficiently executed on mesh. For example, most of the problems, which utilize parallel processing, use n-dimensional matrices as one of the primary data structure. This is especially true in the area of numerical analysis, image processing, computer vision and pattern recognition. These applications require operations which utilize data from the point of view of the mesh topology, and most of the matrix algorithms use a mesh connected abstraction. Thus efficient embedding of meshes is an important issue of any general purpose interconnection network [110]. Figure 1.1 shows a 2-dimensional 4×4 mesh.

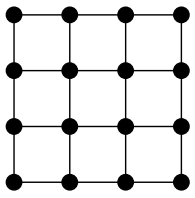

Figure 1.1: A 4×4 mesh

Many results have been obtained for embedding of meshes. In [119], [47], [92] and [45], embeddings from 2-dimensional meshes into other 2-dimensional meshes were

discussed. Embeddings from 2-dimensional meshes into hypercubes were studied in [112] [86], and 3-dimensional meshes into hypercubes in [113] and [26]. In [96], 3-dimensional meshes embedded in hypercubes with link and/or node failures were investigated. In [69], embeddings of multidimensional meshes into minimal Boolean cubes were addressed by graph decomposition. In [46], many to one embeddings from meshes into cylinders, tori, and hypercubes were studied. In [41] and [49], embeddings of meshes in crossed cubes, which are important variants of hypercubes, were designed with dilation 1. In [123], embedding of meshes in Mobius cubes was proposed, as Mobius cubes form a class of hypercube variants. In [110], embedding algorithms were designed for mapping n-dimensional meshes onto a star graph of degree n with expansion 1 and dilation 3; and it highlighted that an n-degree star graph can efficiently simulate an n-dimensional mesh. In [103], a class of algorithms were developed for mesh structures embedded in rotator graphs, which were proposed as an alternative to the star and pancake graphs for multiprocessor interconnection networks. In [50], simple and snake-like embeddings were designed for meshes and tori networks onto 4 degree chordal rings. In the first part of this thesis, the embeddings for 2-dimensional meshes/tori on a family of double-loop networks are systematically studied, in such a way that a large fraction of embedded mesh/torus edges have edge dilation 1 with a low average dilation.

1.1.2.2 Hypercubes

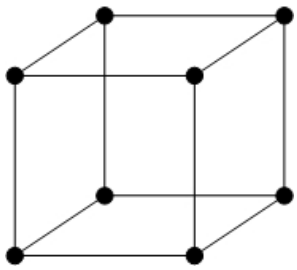

Figure 1.2: An 8-node hypercube

Hypercube structure is a widely used and well-known interconnection model since it possesses many attractive properties [80][114]. The n-dimensional hypercube H_n is a graph with 2^n nodes, each node with a distinct binary string $x_1x_2...x_n$ on the set $\{0, 1\}$.

Two nodes are linked by an edge if and only if their strings differ in exactly one bit. Hypercube features low diameter and high connectivity, as it requires $O(nlogn)$ wires to interconnect $O(n)$ processors, and has a diameter of $O(logn)$. Figure 1.2 shows a 3-dimensional hypercube.

Hypercube is one of the most flexible and powerful parallel architectures, which is well-suited for both special-purpose and general-purpose tasks, and can efficiently simulate any other network of the same size [80]. Furthermore, it has been shown to support an extremely large and rich class of algorithms during the last two decades. Specifically, a large number of parallel algorithms can be directly implemented on the hypercube without significantly affecting the number of processors or running time. Hence, hypercube is an excellent and popular choice for the traditional architecture of a multi-purpose parallel machine. In [80], the properties and the usefulness of hypercube have been intensively researched. It is shown that hypercube can efficiently simulate all arrays, binary tree, and meshes of trees. In fact, the hypercube contains or nearly contains almost every network yet discovered for parallel computation. Moreover, it has been shown that hypercubes offer very efficient non-blocking solutions for all-to-all broadcast operations, which would be very attractive for control plane implementation. Together with the hypercube, an interesting and powerful class of networks is commonly known as hypercubic networks. The most popular derivative networks are the butterfly, shuffle-exchange graph, de Bruijin graph, Benes network, and cube-connected-cycles (CCC). Another reason that hypercubic networks are so commonly used in parallel machines is that they can efficiently simulate any bounded-degree communication network. This is because hypercubic networks can solve arbitrary message-routing problems in $O(logN)$ steps [80].

Hypercube is one of the most versatile and efficient interconnection networks yet discovered for parallel computation. One of the biggest reasons for the popularity of the hypercube is its ability to efficiently embed many parallel architectures. The embedding of other graphs into hypercube has been given much attention during the past decade because it has many applications on parallel computers of hypercube structure [24][25]. Embeddings of meshes into hypercubes have been studied in [24] and [25]. Embed-

dings of trees into hypercubes have been discussed in [67], [63], [15] and [16]. In [130], fault-tolerant cycle embeddings of hypercubes were designed. In [12], embeddings of star networks into hypercubes were investigated. In [25], an embedding scheme for an infinite class of two-dimensional grids embedded in hypercubes was developed. In [65], a new embedding method, based on matrix transformations, was proposed for optimally embedding hierarchical hypercube networks into hypercubes. In [68] and [70], embedding hyperpyramids into hypercubes was studied. On the other hand, the embeddings of hypercubes on other networks have also been of great interest. In [56], embedding hypercubes into pancake, cycle prefix and substring reversal networks were studied. In [41] and [49], the embedding problems on crossed cube, which is an important variant of the hypercube, have been analyzed in recent years. In [14], the problem of embedding the n-dimensional hypercube into a rectangular grid with 2^n vertices was studied to minimize the congestion. Other related research includes embedding hypercubes on de Bruijn graphs [2], Cayley graphs [93].

1.1.3 Challenges for Embedding on Double-loop Networks

Loop networks were studied in the literature as well as used in practical applications (Illiac IV, 802.5 token ring, the fiber distributed data interface (FDDI) network, the distributed queue dual bus (DQDB) with redundancy, SILK rings, and synchronous optical network (SONET) ring)[102][39]. Double loop networks are extensions of the ring networks and are widely used in the design and implementation of local area networks and parallel processing architectures [73]. In the design and implementation of local area networks, the ring topology has been used frequently due to its simplicity, expendability and regularity. The switching mechanism at each node can easily be implemented using building blocks of the same specification. Moreover, a token or message can be passed over the ring in a uniform way. However, the ring network has a low degree of reliability and hence very high vulnerability. More specifically, the connectivity of an unidirectional ring network of n nodes is 1 since the breakdown of any node i would disable any directed path from node $i-1$ to node $i+1$ taken modulo n. Another way

of measuring the performance is the maximum distance among any pair of nodes. A large distance would contribute to the transmission delay between these two nodes. One common way to improve the performance of a network is to increase its connectivity and decrease its diameter. That can be done by adding links to the network. A popular variation of the ring network is the double-loop network [87].

Double-loop networks have become popular in the design of computer networks and distributed memory multiprocessor systems [61]. Many researchers are interested in the double-loop networks (see [73], [28], [27], [61], [87], [102], [36], [121], [39] and [128]), which have been researched and proven to have many desirable properties for future network architecture such as scalability, fixed node degree, node symmetry (i.e. vertex transitivity), regularity, reasonable diameter, and reliability. The diameter problem on double-loop networks was studied in [32] and [3]. The message routing and fault-tolerant message routing problems on double-loop networks were discussed in [40], [36], [61], [87] and [102]. The permutation routing problem on double-loop networks was discussed in [39]. In [121], the fault tolerant embedding of rings on double-loop networks was studied, and the hamiltonian cycle problem on double-loop networks with exactly one faulty element was solved.

Although double-loop networks are widely used in the design and implementation of local area networks and parallel processing architectures [73], little work has been done on the embedding problems of double-loop networks due to the complexity of double-loop networks. As a large number of parallel algorithms, originally designed on existing structures, can be applied to double-loop networks by embedding techniques, it is of great practical significance to investigate the embedding results on double-loop networks. Although meshes and double-loop networks have all been widely studied and used in parallel computing, the embedding for meshes and tori on double-loop networks was not well studied. Since meshes have the same node degree with double-loop networks, it is of great theoretical interest to find how meshes and tori can be embedded on double-loop networks from the topological point of view. Therefore, the problem of embedding meshes on double-loop networks has both practical and theoretical significance.

In [50], simple and snake-like embeddings of meshes and tori networks onto degree-four chordal rings, which is equivalent to a special case of double-loop networks, were designed. However, the embedding method is limited and its performance is not satisfactory because the average dilation becomes prohibitively large when the system size increases. In this thesis, we propose an efficient scheme to embed meshes on double-loop networks using a novel tessellation approach to partition the geometric plane of double-loop networks into a set of parallelogram tiles, called *P-shape*, which is a powerful tool to illustrate the embedding on double-loop networks. As a bridge between regular graphs and double-loop networks, P-shape provides a new way of geometrical representation of double-loop networks.

1.2 Network Embedding on Optical Networks

1.2.1 WDM Optical Networks

1.2.1.1 WDM Technology and RWA Problem

Optical networks offer the possibility of interconnecting hundreds to thousands of users, covering local to wide areas, and providing capacities exceeding substantially those of conventional technologies [8]. Traditional networks use the electrical form to switch signals which can be modulated electronically at a maximum bit rate of the order of 10 Gbps, while the optical fiber bandwidth is about 10 Tbps, thus several orders of magnitude higher. Optics is thus emerging as a key technology in state of the art communication networks and is expected to dominate many applications, such as video conferencing, scientific visualization and real-time medical imaging, highspeed super-computing and distributed computing.

Multi-wavelength communication, which is implemented through Wavelength Division Multiplexing (WDM), has become a promising technology for many emerging networking and parallel/distributed computing applications because of its huge bandwidth [34][138]. In WDM optical networks, the bandwidth in optical fiber is partitioned into multiple data channels, in which different stream of data can be transmitted simul-

NOTE: This figure is included on page 25 in the print copy of the thesis held in the University of Adelaide Library.

Figure 1.3: A WDM network consisting of wavelength routers interconnected by pointto-point fiber-optic links [1]

taneously using different wavelengths. Once the data stream has been transmitted in the form of light, it continues without conversion to electronic form until it reaches its destination. In general, an optical WDM network consists of routing nodes interconnected by point-to-point fiber links (Figure 1.3 [1]), which can support a certain number of wavelengths. Each wavelength can carry a separate stream of data. To efficiently utilize the bandwidth resources and to eliminate the high cost and bottleneck caused by optoelectrical conversion and processing at intermediate nodes, end-to-end lightpaths are usually set up between each pair of source-destination nodes. A *connection* or a *lightpath* in aWDMnetwork is an ordered pair of nodes (*x; y*) corresponding to transmission of a packet from source *x* to destination *y*. For a packet transmission, a transmitter at the source must be tuned to the same wavelength as the receiver at the destination for the duration of the packet transmission and no data stream collision may occur at any fiber.

Optical bandwidth is the number of available wavelengths, and the wavelength resource is very limited. State of the art technology allows several hundreds of wavelengths per fiber in the laboratory, while the available wavelengths are much less in manufacturing. However, there is no anticipation for dramatic progress in the near future. Thus, one of the most important issues to be solved in WDM optical networks is to establish communication between pairs of nodes so that the total number of wave-

lengths used is minimized. The resulting problem is referred to as *Routing and Wavelength Assignment* (RWA) [134], which is a key problem for increasing the efficiency of wavelength-routed all-optical networks. If the number of wavelengths required to realize an all-optical process in one round is greater than the available number of wavelengths, then several all-optical rounds are needed [8]. Routing and Wavelength Assignment problem is defined below:

Given a physical network structure and the required connections, the problem of RWA is to select a suitable path and wavelength among many possible choices for each connection so that no two paths sharing a link are assigned the same wavelength. Therefore, routing and wavelength assignment for the connections are subject to the following two constraints [134]:

1. *Wavelength continuity constraint*: a lightpath must use the same wavelength on all the links along its path from source to destination node.

2. *Distinct wavelength constraint*: all lightpaths using the same link (fiber) must be assigned distinct wavelengths.

As illustrated in Figure 1.3 [1], a connection between node A and node C is carried on wavelength λ_1, but a connection between node B and node D must be carried on different wavelength λ_2.

Due to these two constraints, traditional embedding techniques, which pay attention to the congestion of the embedding, are not sufficient to minimize the number of wavelengths required to realize communication patterns on WDM optical networks. While the number of wavelengths in a real network is very limited, the objective of RWA is to minimize the number of wavelengths for realizing a communication requirement by taking into consideration both routing options and wavelength assignment options. Numerous studies have been conducted on the RWA problem [34][134]. Several RWA schemes have been proposed that differ in the assumptions on the traffic pattern, availability of the wavelength converters, and desired objectives. The traffic assumptions generally fall into one of two categories: static or dynamic. In static RWA models, it is assumed that the demand is fixed and known, i.e. all the lightpaths that are to be set up in the network are known beforehand. Even in the simpler static case, typical

proposed formulations for optimal lightpath establishment turn out to be difficult mixed integer linear programs. In particular, the optimal static lightpath establishment problem without wavelength converters was proven to be NP-complete in [115] by showing the equivalence of the problem to the graph-coloring problem.

1.2.1.2 Optical Architectures for Parallel Computing

Current development activities indicate that WDM network will be deployed mainly as a backbone network for large regions, e.g. for nationwide or global. A number of experimental prototypes have been and are currently being developed, deployed, and tested mainly by telecommunication providers including a plethora of startup companies. It is anticipated that the next generation of the Internet will employ WDM-based optical backbones. As optics becomes a major networking media in all communications needs, optical interconnects will inevitably play an important role in interconnecting processors in parallel and distributed computing systems [131]. Currently, copper wires are the most cost effective and reliable interconnect in parallel machines. However, as machines grow more powerful, wire density becomes critical making fiber possible alternatives due to their small wire size. On a single optical fiber, information/data can be transmitted concurrently, and over 1000 high bandwidth (100-200 Mb/s) independent channels or busses can be supported in parallel. Fiber links allow a number of high speed serial links to replace a large number of electrical lines, and the use of fiber is space saving.

Advances in optical technologies have made it possible to implement optical interconnections in future massively parallel processing systems [82][88]. There are many desirable characteristics of optical interconnects, such as high speed, high bandwidth, high reliability, longer interconnection lengths, low power requirements, and possibly a significant reduction in design complexity through the use of multiple access techniques and wavelength division multiplexing techniques. The effectiveness of optical interconnects has been extensively examined [88][42][83]. As mentioned in [91], all-optical technology is an attractive way to support the ever-growing demand of fast interconnections in multiprocessor systems. All-optical communication benefits from a number of

good characteristics such as no optoelectronic conversion, high noise immunity, and low latency. Moreover, WDM mechanism theoretically enables an aggregate system capacity of several terabits per second on just one physical fiber, and is a promising alternative to multiple bus and fixed topology systems with respect to scalability, modularity, and reconfigurability [17].

Parallel processing using WDM optical interconnections poses new challenges. New system configurations need to be designed, data communication schemes based on new resource metrics need to be investigated, and algorithms for a wide variety of applications need to be developed under the novel computation models using optical interconnections. The parallel transmission characteristic offered by WDM optical technology provides the means for implementing parallel communication among a large number of processors. As mentioned in [17], using WDM-based networks for communication has many advantages over the conventional electric bus and interconnect, as outlined below.

- Bandwidth: The total usable bandwidth of a fiber can be multiplexed into approximately 200 WDM channels, each operating at 1 gigabit per second.

- Scalability: Power loss on a common bus grows linearly with the number of processors on that bus.

- Modularity: In most single-hop systems, a single node can be added to the network at any time without redesigning the entire system. However, in most multihop systems, this is not possible.

- Reliability: Optical fiber is an inherently low loss medium, and the length of fiber needed for a multiprocessor interconnect is sufficiently small so that there is no need for optical amplification.

- Arbitrary virtual topologies: By fixing the transmitters and receivers of each processor to the proper wavelength, any virtual multihop topology may be created. A WDM-based multiprocessor could even be divided into two or more subnets, each used for independent computations.

- Reconfigurability: The transmitters and receivers can be retuned dynamically at the user or the operating system level, allowing the system to switch between virtual topologies dynamically.

- Protocol transparency: Each channel may be operated independently and may use a different protocol for communication. There is no fixed frame length or data configuration requirement on the multiple channels in a WDM network.

- Muticasting: Broadcasting and multicsting are easily facilitated in any WDM based interconnect.

Many studies have been conducted on optical interconnection network for parallel computing. In [82], parallel computing using optical interconnections was discussed from high-level architecture design and algorithmic points of view, and pointed out directions for further research and development. In [23], an optical interconnection network, Gemini, was designed for parallel processing. The following are three examples of optical architectures proposed for parallel computing.

- Multiple Channel Architecture (MCA)

  Multiple Channel Architecture (MCA)[126][137][101] was a proposed architecture which uses fiber optic communications to overcome many of the problems associated with interconnection networks. Multiple Channel Architecture (MCA) is an optical interconnection strategy for parallel processing. The architecture seeks to exploit the high bandwidth available in optical communications by supporting multiple virtual buses or selectable channel on a single fiber. Arbitrary interconnection patterns and machine partitions can be emulated via appropriate channel assignment.

- Hybrid Multiprocessing Using WDM Optical Fiber Interconnections

  Hybrid multiprocessing using WDM optical fiber interconnections [22] is almost similar to the MCA except that it uses receivers and transmitters tuned to fixed frequencies rather than using of tunable components. The design of a wavelength

division multiplexed fiber optic bus for multiprocessors allows both the shared memory model and the distributed memory model to be supported efficiently. Some of the engineering issues are also discussed in the design of WDM fiber bus approaches for cutting the cost of the optical components.

- Spanning Multichannel Linked Hypercube (SMLH)

  In [89], a new scalable interconnection topology called the Spanning Multichannel Linked Hypercube (SMLH) was proposed along with an optical implementation methodology that combines both the advantages of free space optics with those of wavelength division multiplexing techniques. The SMLH uses the hypercube topology as a basic building block and connects such building blocks using two-dimensional multichannel links. The SMLH topology supports many communication patterns found in different classes of computation, such as bus-based, mesh-based, and tree-based problems as well as hypercube-based problems.

However, optical technology is not yet as mature as conventional technology, and most of these machines are still in their experimental stages and are not yet commercially used. There are limits as to how sophisticated optical processing at each node can be done [43]. Below are some limitations for the WDM-based multiprocessor.

- Cost: While optical fiber is relatively inexpensive, the optical components, such as transmitters and receivers, are prohibitively expensive. As the technology improves, and these devices become mass produced for local and metropolitan area network use, they are expected to become affordable [17].

- Optical Storage: Optical media is more durable and less vulnerable to environmental conditions. On the other hand, it offer lower storage capacities. One important problem need to be effectively solved is light storage. A lot of light storage techniques are still in experimental stage. With the development of new effective storage methods, WDM-based multiprocessor architecture is expected to replace the traditional multiprocessor architecture.

NOTE: This figure is included on page 31 in the print copy of the thesis held in the University of Adelaide Library.

Figure 1.4: Difference between congestion and RWA [133]

1.2.2 Embedding from Logical Topology to Physical Topology

The connectivity of the traffic pattern is represented by the logical topology, which is a graph consisting of the nodes in the network with an edge between two nodes if a connection is set up between the two nodes using some wavelength and path in the physical topology. The logical topology consists of the same set of nodes as the physical topology. The edges of the logical topology correspond to the set of lightpaths that are established over the physical topology. This model has been widely used in analysis the communication problems in optical networks [129][79][109]. A logical topology can be embedded into a physical topology by establishing logical connections. Two nonadjacent nodes in the host network can be connected by a lightpath to form a logically adjacent pair of nodes in the guest network. This problem of embedding a desired logical topology on a given physical topology (fiber network) has been formally stated in [95]. As optical fiber has a high transmission rate, the dilation of embedding is not that critical due to low latency. One of the most important metrics in optical network embedding is the number of wavelengths, as wavelength is the main resource in optical networks.

In [8], graph problems arising from WDM in all-optical networks have been studied in the graph theory point of view. The optical network can be modeled as a directed graph $G(V;E)$. Nodes in V are switches and edges in E are links. Given a network G and communication pattern G_0, the congestion for embedding G_0 in G is the minimum

among all the embedding schemes for maximum number of paths in G' that use the links in G. Let $Cong(G', G)$ denote the congestion of graph G' embedded in graph G, and $\lambda_e(G', G)$ denote the number of wavelengths required for realizing communication pattern of G' in optical network G by embedding scheme e. The relevance between congestion and the number of wavelengths is shown by the following lemma [8]:

Lemma 1. $\lambda_e(G', G) \geq Cong(G', G)$.

In other words, to solve a given RWA problem, one has to use a number of wavelengths at least equal to the congestion of the embedding. In general, minimizing the number of wavelengths is not the same problem as minimizing congestion of embedding. In fact, RWA problem is much harder due to the further requirement of wavelengths assignment [8]. In order to obtain equality in Lemma 1, the optimal solution for RWA is to find a routing and wavelength assignment scheme such that the equality is achieved.

Traditional network embeddings that minimize the congestion for a given communication pattern are not adequate for minimizing the number of wavelengths (channels) to realize the communication requirement [134]. The wavelength requirement is usually larger than the congestion of network embedding. As shown in Figure 1.4, the congestion of embedding the communications is 2, while the number of wavelengths required is 3. To efficiently realize a logical topology in an optical network, both routing and channel assignment options must be taken into consideration.

Much work concerning WDM networks is based on the static model [1] [11] [57] [108] [99]. In this model, the route of each request is given and the problem is to find the minimum number of wavelengths to satisfy a given request set. Since wavelength converters are still expensive and difficult to implement, most of the literature on the RWA problem considers networks without any wavelength converters. A summary of graph theoretical problems associated with routing in optical networks can be found in [8] and [58]. There is a vast literature dealing with the problem of minimizing the number of wavelengths to set up lightpaths for (classes of) communication requests. Related results for all-to-all and multicast communication realized on optical networks

are summarized below.

All-to-all broadcast (gossiping) is a fundamental communication application on computer/communication networks. All-to-all routing on a single hop model has been studied for rings, tori, meshes, hypercubes, and trees of rings in [9], [11], [117] and [135]. The number of wavelengths needed in a d-dimensional torus with n nodes in each dimension was obtained in [9]. In [11], all-to-all communication realized on rings was studied. In [117], the number of wavelengths for realizing all-to-all communication on some special product graphs were derived. In [97], all-to-all routing for a family of chordal rings of degree 4 was studied. In [135], the problem of scheduling all-to-all personalized connections in WDM rings was discussed. All-to-all communication realized on multi-hop optical networks was also studied in [85], [60] and [100]. In [100], the uniform all-to-all routing problem for a symmetric directed ring was studied, and the numbers of wavelengths were derived for a uniform 2-hop, 3-hop and 4-hop model respectively. In [60], the all-to-all routing problem was studied in several specific mulit-hop WDM optical networks including lines, rings, 2-D square tori, and 3-D square tori. In [85], a generic method was proposed for realizing all-to-all routing for a given networks with k-hop routing.

Currently, many bandwidth-intensive applications require multicast services for efficiency purposes. In particular, as wavelength division multiplexing (WDM) technique emerges as a promising solution to meet the rapidly growing demands on bandwidth in present communication networks, supporting multicast at the WDM layer becomes an important yet challenging issue [107]. In [139] and [107], the wavelength requirement for a multicast connection in some special topology networks, such as rings, meshes, and hypercubes, was analyzed. Finding multi-trees for a multicast connection was also discussed in [59] and [106]. A greedy algorithm was proposed in [106] to find multi-trees, such that each tree uses the same wavelength and the total cost of multi-trees is minimized. In [136], a set of algorithms were designed to construct a source-based multicast light-forest consisting of one or more multicast trees to minimize the number of wavelengths and the number of hops. Multicast wavelength assignment with wavelength conversion in WDM networks was studied in [140] and [104]. In [81], the routing

problem to minimize wavelength cost is formalized as the wavelength cover problem in which a multiλ-light-tree is to be found for the given multicast request. The routing problem to minimize both wavelength cost and wavelength conversion cost was studied in [84]. A further generalization was made by considering the transmission delay in [118]. In [141], the conversion delay instead of transmission delay was taken into account. A survey on multicast realizing on optical networks has been conducted in [38].

Besides all-to-all and multicast communications, there are many results on other communication patterns designed to embed on optical networks. In [20], the optimal embeddings were designed for complete graphs, meshes, and hypercube on WDM optical passive star networks with tunable transmitters of limited tuning range and fixed wavelength receivers. In [19], the problem of embedding a virtual de Bruijn topology in a physical optical passive star time and wavelength division multiplexed (TWDM) network was studied. In [105] and [106], permutation embedding and scheduling in multiplexed optical networks with regular topologies were discussed.

1.2.3 Challenges for Embedding Hypercubes on WDM Optical Networks

Hypercube has become one of the most popular communication patterns shared by a large number of computational problems [80]. Moreover, hypercube is one of the most flexible and powerful parallel architectures, which has been shown to support an extremely large and rich class of algorithms during the last two decades. Therefore, hypercube has received considerable attention due to its good topological characteristics (small diameter, regularity, high connectivity, simple control and routing, symmetry, and fault tolerance) and its ability to efficiently permit the embedding of numerous topologies, such as rings, trees, meshes, and shuffle-exchange, among others [80]. However, a drawback of the hypercube is its lack of scalability, which limits its use in building large size systems out of smaller size systems. The lack of scalability of the hypercube stems from the fact that the node degree is not bounded and varies as $\log N$, where N

is the total number of nodes. This property makes the hypercube cost prohibitive for large N due to the inherent drawbacks such as the high cost and complexity of building large hypercubes [114]. Since WDM divides the bandwidth of an optical fiber into multiple wavelength channels so that multiple devices can transmit on distinct wavelengths through the same fiber concurrently, physical topologies for realizing hypercube connections can be significantly simplified by realizing the connections of hypercube on WDM optical networks. Therefore, the existing results on hypercube can be incorporated into the optical networks with simple topologies such as linear array and rings by taking advantages of the parallel transmission characteristic of optical communication. In addition, the computational efficiency can be improved compared to the traditional electric networks, because optical technology can provide for parallel computing systems with an enormous amount of bandwidth and low latency. Many studies have been conducted by combining the optical fiber technology and hypercube. In [20], [120] and [122], hypercube on WDM partitioned optical passive star networks was studied. In [91], a solution for embedding a virtual unidirectional incomplete hypercube into optical networks was presented. In [132], wavelength assignments for hypercube communications on mesh-like optical networks were studied. However, the results obtained in [132] were based on a traditional standard embedding scheme. As mentioned in [132], optimal node numbering (and its RWA) is a much more complex problem. In Chapters 3, 4 and 5, we study the embeddings of hypercubes on a class of WDM optical networks, and improve on the previous results.

1.3 Main Contributions

In this thesis, we study the embedding of meshes and hypercubes on a group of future network architectures. The main contents and contributions are summarized below.

1.3.1 Embedding Meshes/Tori on Double-loop Networks

In Chapter 2, we study the embeddings of meshes/tori on a group of double-loop networks by evaluating the traditional embedding metrics, since double-loop networks have

been intensively studied and proven to have many desirable properties for future network architecture. The key contributions of this part are summarized as follows.

- We propose a novel tessellation approach to partition the geometric plane of double-loop networks into a set of parallelogram shaped tiles, called P-shape, which is a powerful tool to illustrate the embedding of meshes and tori on double-loop networks. As a bridge between regular networks and double-loop networks, P-shape provides a new way of geometrical representation of double-loop networks.

- We construct P-shape for $DL(N; 1, s)$, and show that meshes and tori can be embedded on $DL(N; 1, s)$ by simply embedding the nodes of meshes and tori on the nodes in P-shape, called P-shape embedding, which significantly improves the previous scheme [50] on $DL(N; 1, s)$.

- We further extend the construction of P-shape to the general case of $DL(N; s_1, s_2)$, thus allowing meshes and tori to be embedded on $DL(N; s_1, s_2)$ in a systematic way. To the best of our knowledge, this is the first result for embedding meshes and tori on $DL(N; s_1, s_2)$.

- We evaluate the embedding metrics of dilation, average dilation and congestion, and derive the conditions for achieving optimal or near-optimal embeddings of meshes and tori on double-loop networks. Our results show that a large fraction of edges in meshes and tori have dilation 1 by P-shape embedding, resulting in a low average dilation. In addition, the performance of our P-shape embedding depends on the parameters of P-shape, instead of the system size.

1.3.2 Embedding Hypercubes on WDM Optical Networks

The second part is based on embedding hypercubes on a class of array-based WDM optical networks by analyzing the new embedding metric of wavelength requirement. Optical networks offer the possibility of interconnecting hundreds to thousands of

users, and represent a promising technology for many emerging networking and parallel/distributed computing applications. The key contributions are summarized below.

- We study routing and wavelength assignment for embedding hypercubes on WDM optical networks including linear arrays and rings with the consideration of communication directions. Specifically, we analyze this problem for both bidirectional and unidirectional hypercubes. In each case, we identify a lower bound on the number of wavelengths required, and design the embedding scheme and wavelength assignment algorithm that uses a provably near-optimal number of wavelengths. In addition, we extend the results to meshes and tori. The results regarding bidirectional cases have improved on the previous results [133].

- We design an embedding scheme for hypercubes on WDM optical chordal ring networks of degree 3, and derive the number of wavelengths required for different chord length. Based on embedding scheme of double cycle embedding, we also provide the analysis of chord length with an optimal number of wavelengths to realize hypercube communications on 3-degree chordal rings.

- We design the embedding schemes of symmetric embedding and cyclic permutation embedding schemes for hypercubes on 4-degree WDM optical chordal ring networks, and derive the numbers of wavelengths required. Based on our proposed embedding schemes, we analyze chord length with the optimal number of wavelengths to realize hypercubes on 4-degree chordal rings.

- We design an embedding scheme for realizing parallel FFT (dimensional hypercube) on WDM optical linear array by considering the hypercube communication dimension by dimension. Based on our proposed embedding scheme, called *lattice embedding*, the number of wavelengths required to realize parallel FFT communication pattern on optical linear array has been significantly reduced compared to the previous results [31] [29].

1.4 Impact of This Research

This thesis analyzes the efficient solutions on network embedding for meshes and hypercubes on a group of network architectures, which have great potential to be used in the future. This work has more theoretical practical significance. From the graph theory point of view, we provide solutions for the network embedding problems of meshes/tori on double-loop networks. As previous solutions are only proposed on some special case of double-loop graphs, our work is the first solution for embedding meshes/tori on general double-loop graphs. We also provide embedding solutions for hypercubes on array-based optical networks by analyzing the wavelength requirement with the consideration of communication directions, since previous results are only based on the bidirectional cases. In addition, we also design the embedding schemes for hypercubes on 3-degree and 4-degree chordal ring graphs, which has not been discussed in graph embedding theory as far as we know. All these results are of great theoretical interest from the graph theory point of view. Graph embedding problems have a wide variety of applications such as laying out circuits on chips, representing data structures in computer memory, and finding an efficient program control structure. Our proposed embedding solutions have great potential theoretical usefulness in future applications.

Meshes and hypercubes are two most important architectures used in traditional network architectures. An extremely large number of algorithms and applications are designed based on these topologies in practice. Double-loop networks have been intensively studied and proven to have many desirable properties for future network architecture, and WDM optical networks are promising technologies that may be deployed in many applications in parallel computing. It is of practical importance to investigate the embedding problems for meshes and hypercubes on these topologies for future architectures, since the algorithms originally developed for one architecture can be directly mapped onto another architecture under an embedding. If the properties and structure of the underlying graph are used effectively, the computation and communication speeds can be significantly improved. Our solutions not only provide an evaluation of two architectures, but also identify the feasibility of embedding performance, which will in-

struct the implementation of the virtual topology or algorithms to the physical topology in practice.

1.5 Thesis Outline

This chapter provides the important preliminaries and concepts used in this thesis, which is organized as follows.

In Chapter 2, network embeddings of meshes/tori on a family of double-loop networks are proposed.

In Chapter 3, network embeddings of hypercubes on a group of simple WDM optical networks are studied including linear array, rings, meshes and tori.

Extensions for embedding hypercubes on optical chordal ring of degree 3 and degree 4 are discussed in Chapter 4.

In Chapter 5, the efficient realization of n-dimensional hypercube embedded on optical linear arrays is discussed.

Chapter 6 concludes this thesis and discusses the directions for future work.

Chapter 2

Embedding of Meshes and Tori on Double-Loop Networks

In this chapter, we address the embedding of meshes/tori on double-loop networks by proposing a novel tessellation approach to partition the geometric plane of double-loop networks into a set of parallelogram tiles, called *P-shape*. Based on the characteristics of P-shape, we design a simple embedding scheme, namely *P-shape embedding*, that embeds meshes and tori on double-loop networks in a systematic way. Under P-shape embedding, we evaluate the embedding metrics of dilation, average dilation and congestion, which depend heavily on the parameters of P-shape. In particular, we derive the families of double-loop networks that can achieve optimal and near optimal embedding of a given mesh or torus using our P-shape embedding.

2.1 Introduction

Double loop computer networks are extensions of ring networks and are widely used in the design and implementation of local area networks and parallel processing architectures [10] [73]. Wong and Coppersmith [127] introduced the network $DL(N; 1, s)$ with each node i connected to node $i + 1 \pmod N$ and node $i + s \pmod N$, where $i = 0, 1, ..., N - 1$. Fiol *et al.* [51] extended $DL(N; 1, s)$ to $DL(N; s_1, s_2)$, generally known as the double-loop network, with each node i connected to $i + s_1 \pmod N$ and

$i + s_2 \pmod N$. A great deal of research on routing [102][87][36], diameters [73][127] and designs of optimal double-loop has been intensively conducted because of their relevance to the design of some interconnection and communication computer networks [27]. However, the embedding problems on double-loop networks has not been well studied due to the topological complexity of double-loop networks. Although L-shape [28] for double-loop networks has been regarded as an important tool for studying the diameter and distance properties of double-loop networks, it is difficult to use L-shape to study the embedding problems for regular graphs on double-loop networks due to the asymmetry of L-shape. As far as we know, no efficient method exists for embedding regular graphs on double-loop networks.

Meshes and tori networks represent the communication structures of many applications in scientific computations as well as the topologies of many large-scale interconnection networks [90]. The issue of embedding meshes and tori networks has gained considerable attention in the area of parallel processing, which has been discussed in Chapter 1. However, the embedding for meshes and tori on double-loop networks was not well studied, although meshes, tori and double-loop networks have all been widely studied and used in a large number of parallel algorithms, originally designed on meshes and tori, can be applied to double-loop networks. Since meshes and tori have the same node degree with double-loop networks, it is of great interest to find how meshes and tori can be embedded on double-loop networks from the topological point of view. Therefore, the problem of embedding meshes and tori on double-loop networks has both practical and theoretical significance. In [50], simple and snake-like embedding of meshes and tori networks onto degree-four chordal rings, which is equivalent to a special case of double-loop networks, i.e. $DL(N; 1, s)$, was designed. However, the embedding method is limited and the performance is not satisfactory because the average dilation becomes prohibitively large with the increase of the system size. In this chapter, we devise a novel tessellation technique to study the problem of embedding meshes and tori on double-loop networks. The key contributions of this work are summarized as follows.

(1) We propose a novel tessellation approach to partition the geometric plane of

double-loop networks into a set of parallelogram shaped tiles, called P-shape.

(2) We construct P-shape for $DL(N; 1, s)$, and improve the previous scheme [50] on $DL(N; 1, s)$.

(3) We further extend the construction of P-shape to the general case of $DL(N; s_1, s_2)$. To the best of our knowledge, this is the first result for embedding meshes and tori on $DL(N; s_1, s_2)$.

(4) We evaluate the embedding metrics of dilation, average dilation and congestion, and derive the conditions for achieving optimal or near-optimal embeddings of meshes and tori on double-loop networks.

2.2 Preliminaries

2.2.1 Double-loop Networks

$DL(N; 1, s)$ has N nodes numbered from 0 to $N-1$, and $2N$ links with each node i connected to $i+1 \pmod N$ and $i+s \pmod N$, where $i = 0, 1, ..., N-1$. For $DL(N; s_1, s_2)$, each node i connected to $i+s_1 \pmod N$ and $i+s_2 \pmod N$, where s_1 and s_2 are called steps of double-loop network, and the links $i \rightarrow i+s_1 \pmod N$ and $i \rightarrow i+s_2 \pmod N$ are called s_1-link and s_2-link respectively, where $s_1 \neq s_2$ and $s_1, s_2 \leq N/2$. It is well known that $DL(N; s_1, s_2)$ is strongly connected if and only if $gcd(N, s_1, s_2) = 1$, where gcd denotes the greatest common divisor.

Double-loop networks can be visualized in a geometric manner [51]. With each node occupying a unit square on the plane, the nodes horizontally next to its left side and right side square are $i-s_1 \pmod N$ and $i+s_1 \pmod N$ respectively, and vertically next to its lower side and upper side square are $i-s_2 \pmod N$ and $i+s_2 \pmod N$ respectively, as shown in Figure 2.1.

For a given $DL(N; s_1, s_2)$, Cheng and Hwang [32] proposed an $O(\log N)$ algorithm to compute an L-shape tile, which periodically tessellates the geometrical plane of $DL(N; s_1, s_2)$. L-shape has been intensively studied to compute the diameter, and to find a shortest path for any two nodes for double-loop networks [27][28]. Figure 2.2

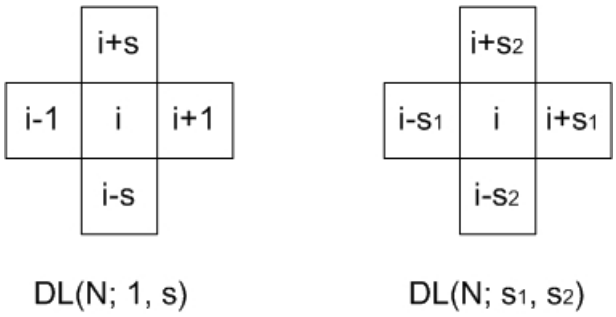

Figure 2.1: Geometric representation of i and its neighbors for $DL(N;1,s)$ and $DL(N;s_1,s_2)$

shows an example of $DL(16;1,3)$ and its L-shape tiles.

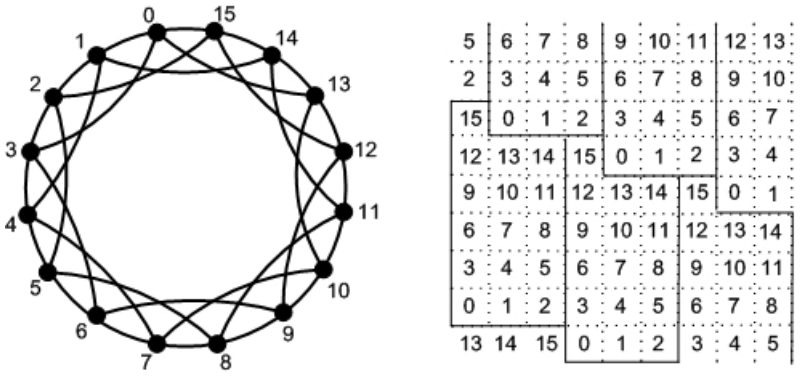

Figure 2.2: $DL(16;1,3)$ and its L-shape

2.2.2 Meshes and Tori

Let $M(m_1,m_2)$ and $T(m_1,m_2)$ represent an $m_1 \times m_2$ mesh and torus respectively with m_1 columns numbered from 0 to m_1-1, and m_2 rows numbered from 0 to m_2-1. Assume the node on the pth row and qth column is identified by (p,q), where $0 \le p \le m_2-1$ and $0 \le q \le m_1-1$. In this chapter, we assume $N = m_1 \times m_2$, and node (p,q) has index $p \times m_1 + q$. Let $e[(p,q),(p',q')]$ denote the edge which connects nodes (p,q) and (p',q').

For $M(m_1,m_2)$, the set of row edges can be denoted by $R = \{e[(p,q),(p,q+1)]|0 \le p \le m_2-1, 0 \le q \le m_1-2\}$, and the set of column edges by $C = \{e[(p,q),(p+1,q)]|0 \le p \le m_2-2, 0 \le q \le m_1-1\}$.

$T(m_1, m_2)$ can be obtained from $M(m_1, m_2)$ by adding the wrap-around edges of row around edge set, $R^a = \{e[(p, m_1 - 1), (p, 0)] | 0 \leq p \leq m_2 - 1\}$, and column around edge set $C^a = \{e[(m_2 - 1, q), (0, q)] | 0 \leq q \leq m_1 - 1\}$.

We denote the dilation for row edges on $M(m_1, m_2)$ embedded on double-loop networks by $Dil(e_r)$, where $e_r \in R$, and dilation of column edges by $Dil(e_c)$, where $e_c \in C$. So, average dilation for embedding $M(m_1, m_2)$ on double-loop networks, denoted by $ADil(M(m_1, m_2), DL)$, can be calculated by: $ADil(M(m_1, m_2), DL) = \frac{\sum_{e_r \in R} Dil(e_r) + \sum_{e_c \in C} Dil(e_c)}{2m_1 m_2 - m_1 - m_2}$. Similarly, the average dilation for embedding $T(m_1, m_2)$ on $DL(N; s_1, s_2)$ can be calculated by: $ADil(T(m_1, m_2), DL) = \frac{\sum_{e_r \in R \cup R^a} Dil(e_r) + \sum_{e_c \in C \cup C^a} Dil(e_c)}{2m_1 m_2}$.

2.3 Construction of P-shape on Double-loop Networks

2.3.1 Motivation for Construction of P-shape

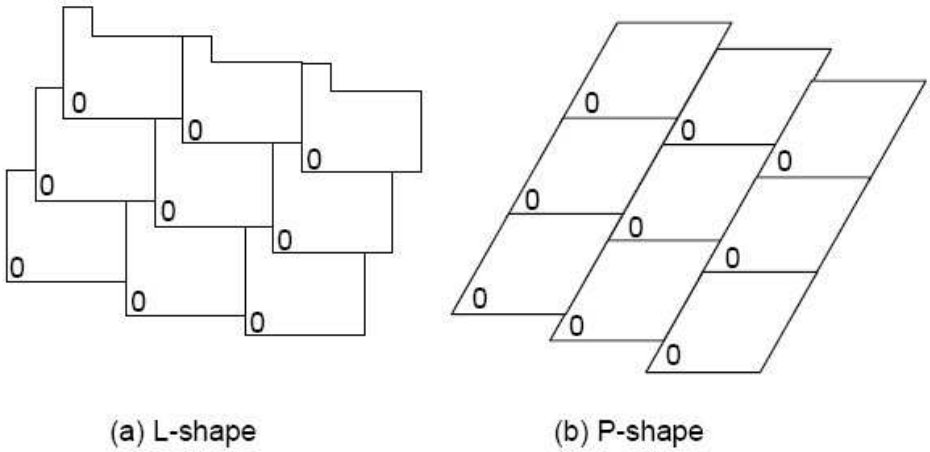

Figure 2.3: Tessellations of the geometrical plane using L-shape and P-shape

As $M(m_1, m_2)$ can be divided into m_2 arrays with m_1 nodes in each array, the key of embedding $M(m_1, m_2)$ is to find the efficient way of embedding a group of arrays on double-loop networks. Due to the asymmetry and uniqueness (defined by the double-loop network) of L-shape shown in Figure 2.3 (a), it is difficult to embed a given size

($m_1 \times m_2$) mesh/torus to L-shape because of the difficulties of decomposing m_2 segments with m_1 consecutive nodes on each segment within the area of L-shape. Therefore, we need to look for a new construction of double-loop networks that can enable this embedding. For this purpose, we propose a novel tessellation approach by finding a set of parallelogram tiles, called *P-shape*, each being composed of m_2 segments with m_1 consecutive nodes on each segment. As illustrated in Figure 2.3 (b), P-shape is centrosymmetric and periodically tessellates the geometric plane of double-loop networks.

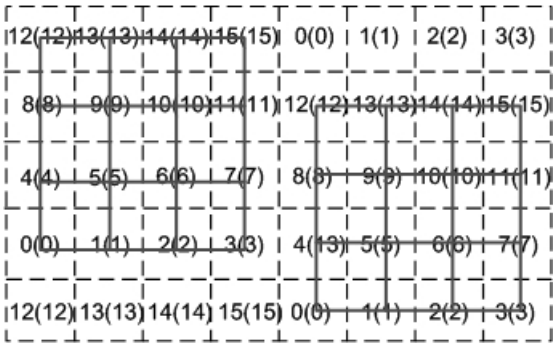

Figure 2.4: Embedding of $M(4,4)$ on $DL(16;1,4)$.

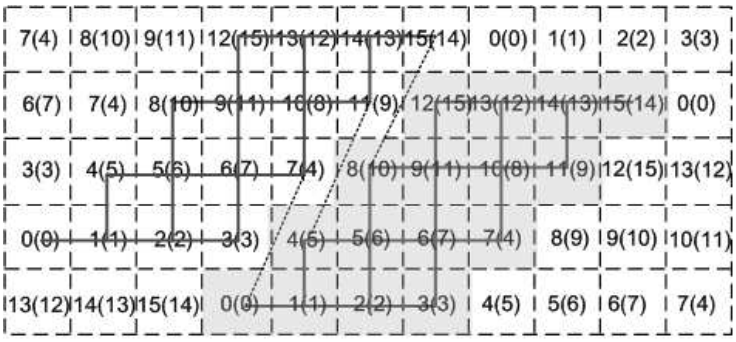

Figure 2.5: Embedding of $M(4,4)$ on $DL(16;1,3)$ in parallelogram tiles

To illustrate the construction of P-shape, we first give 3 simple examples of embedding $M(4,4)$ on $DL(16;1,4)$, $DL(16;1,5)$ and $DL(16;1,3)$ in the following. Figure 2.4 shows that $M(4,4)$ can be embedded on $DL(16;1,4)$ perfectly with dilation 1 and congestion 1 by simply embedding the nodes of $M(4,4)$ in row major indexing onto the nodes of $DL(16;1,4)$ with the same index. However, it can be easily proven that there is no dilation 1 embedding of $M(4,4)$ on $DL(16;1,3)$ or $DL(16;1,5)$. As shown in Fig-

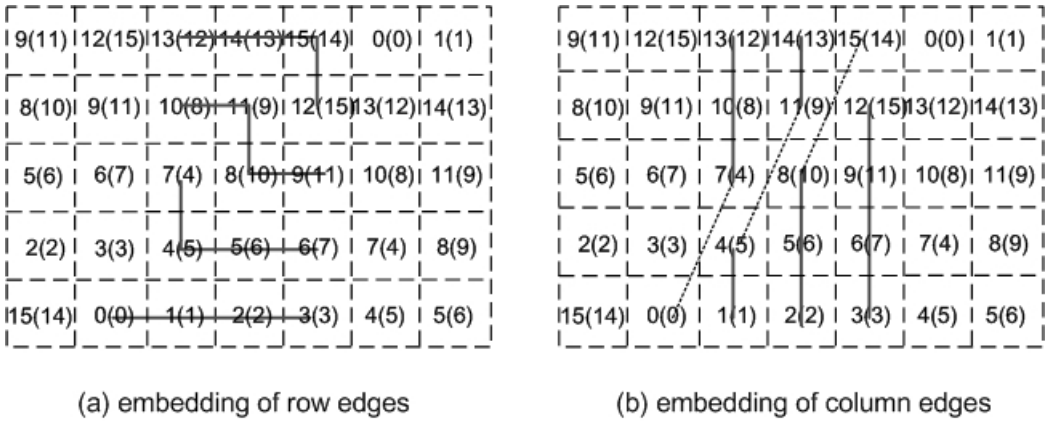

Figure 2.6: Embedding for row and column edges of $M(4,4)$ on $DL(16;1,3)$

ure 2.5, there exists a parallelogram shape tile, which is composed of 4 disjoint arrays with 4 horizontally consecutive nodes of $DL(16;1,3)$ on each array. In addition, the upper side neighbor array shifts one node square distance *right* to its lower side neighbor array. By embedding the nodes of $M(4,4)$ (indicated in the brackets) on $DL(16;1,3)$ within the parallelogram area, a one-to-one mapping can be constructed. By adjusting the positions for the nodes of $M(4,4)$ on the arrays of $DL(16;1,3)$, 3 column edges on each column and at least 2 row edges on each row have dilation of 1, as shown in Figure 2.6 (grid edges crossed by solid lines). Similarly, a one-to-one embedding from $M(4,4)$ to a parallelogram shape tile on $DL(16;1,5)$ can be constructed with upper side neighbor array shifts one node square distance *left* to its lower side neighbor array, as shown in Figure 2.7. By this embedding, 3 row edges on each row and at least 2 column edges on each column have dilation of 1, as shown in Figure 2.8.

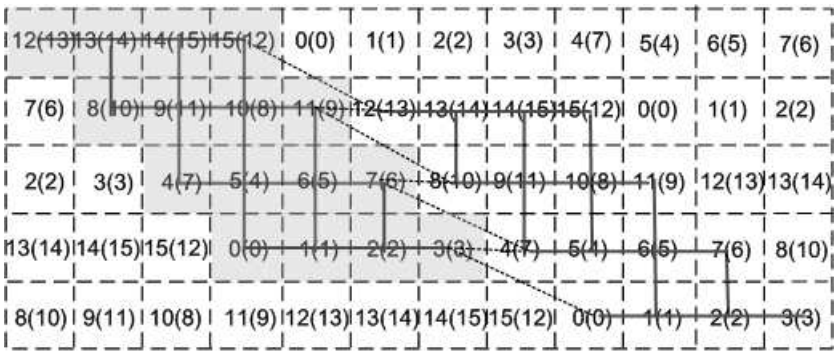

Figure 2.7: Embedding of $M(4,4)$ on $DL(16;1,5)$ in parallelogram tiles.

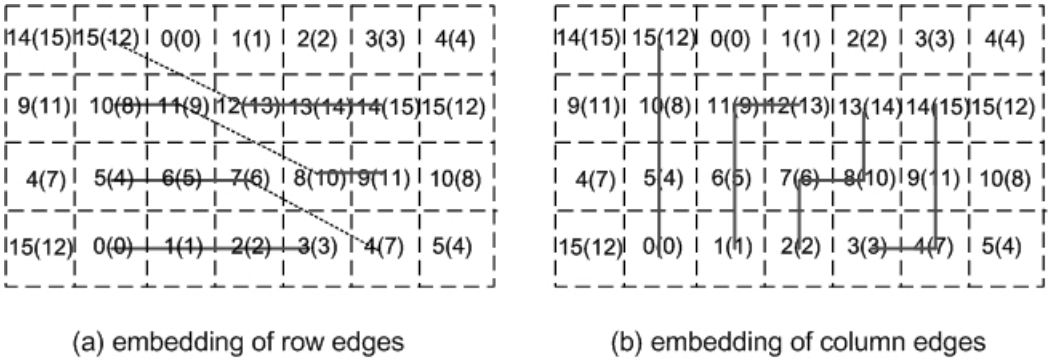

Figure 2.8: Embedding for row and column edges of $M(4,4)$ on $DL(16;1,5)$.

The common idea of these 3 examples is to construct a one-to-one mapping from the nodes of $M(4,4)$ to the nodes of double-loop networks in parallelogram tiles in a way that a large number of the neighboring nodes of meshes are embedded on the neighboring nodes of double-loop networks, and a large number of edges have dilation 1. Our task is to find such a parallelogram shape tile, which we call *P-shape* on a given double-loop networks for embedding a given mesh or torus, so that the efficient embedding can be constructed.

2.3.2 Parameters of P-shape for Double-loop Networks

To construct P-shape on the geometric plane of double-loop networks, the following properties must be satisfied:

1) Each node of double-loop networks only appears once on P-shape.

2) The same P-shape copies periodically tessellate the geometric plane of double-loop networks.

We first introduce the following important parameters for the construction of P-shape.

2.3.2.1 Base m_1 and Height m_2

We define P-shape of double-loop networks to be composed of m_2 disjoint horizontal segments numbered from 0 to m_2-1 from bottom to top with m_1 nodes on each segment, where the *i*th segment is called *tier* i. We call m_1 and m_2 *base* and *height* of P-shape

respectively. Let (i, j) denote the jth $(0 \leq j \leq m_2)-1$ node on the ith $(0 \leq i \leq m_1)-1$ tier, and $I(i, j)$ denote node index of double-loop networks located on (i, j) of P-shape. Without loss of generality, we assume node 0 of double-loop networks is located on $(0, 0)$ of P-shape.

2.3.2.2 Shift τ

We assume the $(i + 1)$th tier shifts horizontally from the ith tier by τ nodes distance, which we call *shift* of P-shape. Define $\tau > 0$ if the $(i + 1)$th tier shift to the right side of the ith tier, $\tau < 0$ if to the left side, and $\tau = 0$ without shift. In addition, we assume $|\tau| < m_1$. As shown in Figure 2.4, 2.5 and 2.7, $\tau = 0, 1, -1$ for P-shape of $M(4, 4)$ embedded on $DL(16; 1, 4)$, $DL(16; 1, 3)$, and $DL(16; 1, 5)$ respectively. It is easy to see that node (i, j) can connect node $(i + 1, j)$ by passing through τ horizontal links, and 1 vertical link. Alternatively, if node (i, j) and node $(i + 1, j')$ are connected by a vertical link on a P-shape, $j' = j - \tau$, where $0 \leq i \leq m_2 - 2$, $\tau \leq j \leq m_1 - 1$ when $\tau \geq 0$, and $0 \leq j \leq m_1 - \tau - 1$ when $\tau < 0$.

2.3.2.3 Copy Distance h

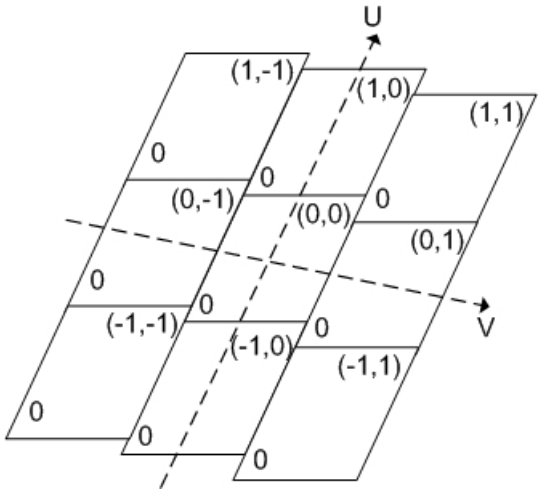

Figure 2.9: Tessellation of the plane using P-shape and the lattice points occupied by node 0

Due to the circular property of double-loop networks, the same copies of P-shape

appear periodically on the tessellation plane of double-loop networks. The distance between the neighbor P-shape copies is an important characteristic for the partition of tessellation plane. As shown in Figure 2.9, the same copy of P-shape appears periodically along two dimensions of $\overrightarrow{U}$ and $\overrightarrow{V}$ in the geometric plane of double-loop networks. We assume the upside and right are positive directions. Assign label $(0, 0)$ to one P-shape copy, and label (u, v) to the copy which is u copy distance along $\overrightarrow{U}$ direction and v copy distance along $\overrightarrow{V}$ direction, where u and v are integers. It is easy to see that the vertical geometric distance between the neighbor copy along the $\overrightarrow{U}$ direction is height m_2, and horizontal geometric link distance is τm_1. We define the vertical geometric link distance between the neighbor copy of the $\overrightarrow{U}$ direction is h, where $-\frac{m_2}{2} < h \leq \frac{m_2}{2}$. Assume $h < 0$ if the right neighbor copy is located on the upper side of its left copy, $h > 0$ if on the lower side of its left copy, and $h = 0$ if on the same horizontal level.

Figure 2.10 shows four scenarios for different τ and h. As P-shape can be determined by geometric parameters of m_1, m_2, τ and h, we denote P-shape by $Pshape(m_1, m_2, \tau, h)$ for simplicity.

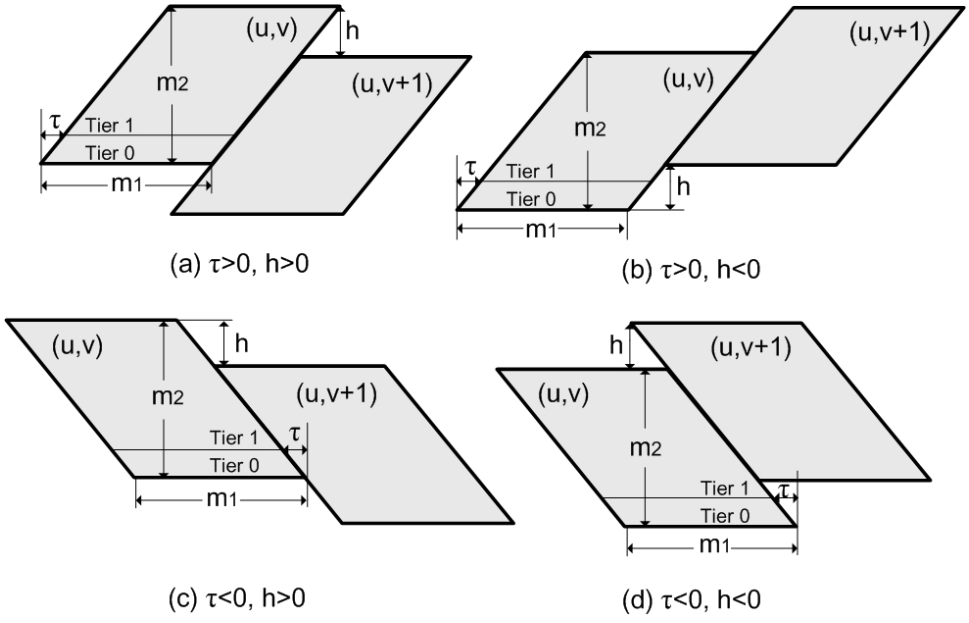

Figure 2.10: $Pshape(m_1, m_2, \tau, h)$

2.3.3 Node Distance

Let $X_{u,v}((i',j'),(i,j))$ and $Y_{u,v}((i',j'),(i,j))$ denote the geometric horizontal and vertical distance of node (i',j') on copy (u,v) and node (i,j) on copy $(0,0)$. By the definitions of shift τ and copy distance h, the geometric distance between node (i',j') on copy (u,v) and node (i,j) on copy $(0,0)$, denoted by $XY_{u,v}((i',j'),(i,j))$, can be calculated by the following lemma.

Lemma 2. $XY_{u,v}((i,j),(i',j')) = X_{u,v}((i',j'),(i,j)) + Y_{u,v}((i',j'),(i,j))$, *where* $X_{u,v}((i',j'),(i,j)) = |j'-j+(i'-i+um_2)\tau+v(m_1-\tau h)|$, *and* $Y_{u,v}((i',j'),(i,j)) = |i'-i+um_2-vh|$.

Proof. It is easy to see the geometric horizontal and vertical distance between node (i',j') on copy (u,v) and node (i,j) on copy $(0,v)$ are $X_u((i,j),(i',j')) = j'-j+(i'-i+um_2)\tau$, and $Y_u((i,j),(i',j')) = i'-i+um_2$ respectively. The geometric horizontal and vertical distance distance between node (i',j') on copy (u,v) and node (i,j) on copy $(u,0)$ are $X_v((i,j),(i',j')) = j'-j+(i'-i)\tau+v(m_1-\tau h)$ and $Y_v((i,j),(i',j')) = i'-i-vh$ respectively. So, $XY_{u,v}((i,j),(i',j')) = X_{u,v}((i',j'),(i,j)) + Y_{u,v}((i',j'),(i,j)) = |X_u((i,j),(i',j)) + X_v((i',j),(i',j'))| + |Y_u((i,j),(i',j))+Y_v((i',j),(i',j'))| = |j'-j+(i'-i+um_2)\tau+v(m_1-\tau h)|+|(i'-i)+um_2-vh|$. □

By Lemma 2, the shortest distance between node $I(i,j)$ and $I(i',j')$ on double-loop networks, denoted by $Dist(I(i,j),I(i',j'))$, can be obtained in the following lemma.

Lemma 3. $Dist(I(i,j),I(i',j')) = min_{u,v\in Z} XY_{u,v}((i,j),(i',j'))$.

2.4 Embedding of Meshes on P-shape of $DL(N;1,s)$

We first introduce the properties of $Pshape(m_1,m_2,\tau,h)$ for $DL(N;1,s)$, and then design the embedding scheme, P-shape embedding, for meshes on $Pshape(m_1,m_2,\tau,h)$. By P-shape embedding, the embedding metrics including expansion, dilation, average dilation and congestion are evaluated. Furthermore, we discuss the results in different cases.

2.4.1 $Pshape(m_1, m_2, \tau, h)$ for $DL(N; 1, s)$

Property 1. *$Pshape(m_1, m_2, \tau, h)$ for $DL(N; 1, s)$ satisfies $\tau = km_1 - s$, where $k = \lfloor s/m_1 \rfloor$ or $\lceil s/m_1 \rceil$.*

Proof. By Lemma 2, the geometric vertical and horizontal distance between node (i, j) on P-shape copy (u, v) and copy $(u+1, v)$ is m_2 and τm_2 respectively. So, $I(i, j)+(\tau \times 1 + s) \times m_2 \pmod N = I(i, j)$. Thus $(\tau + s) \times m_2 = kN$, where k is an integer. As $N = m_1 m_2$, $\tau + s = km_1$. So, $\tau = km_1 - s$. As $|\tau| < m_1$, $\lfloor s/m_1 \rfloor \leq k \leq \lceil s/m_1 \rceil$. □

By Property 1, the following corollaries can be obtained.

Corollary 1. *Let $s = \alpha m_1 + \beta$, where $\alpha = \lfloor s/m_1 \rfloor$ and $0 < \beta < m_1$. $Pshape(m_1, m_2, \tau, h)$ for $DL(N; 1, s)$ satisfies,*

(1) if $m_1 | s$, $\tau = 0$ ($k = s/m_1$).

(2) if $m_1 \nmid s$, $\tau = -\beta < 0$ ($k = \alpha$) or $\tau = m_1 - \beta > 0$ ($k = \alpha + 1$).

Corollary 2. *For $Pshape(m_1, m_2, \tau, h)$ on $DL(N; 1, s)$, $I(i, j) = ikm_1 + j \pmod N$, where $0 \leq i \leq m_2 - 1, 0 \leq j \leq m_1 - 1$.*

Proof. According to our assumption, $I(0, 0) = 0$. As node $(0, 0)$ can reach node (i, j) on one P-shape by passing through s-links vertically for i times and 1-links horizontally for $i\tau + j$ times, $I(i, j) = 0 + is + i\tau + j \pmod N = is + i(km_1 - s) + j \pmod N = ikm_1 + j \pmod N$. □

Property 2. *$Pshape(m_1, m_2, \tau, h)$ for $DL(N; 1, s)$ exists if and only if $gcd(k, m_2) = 1$.*

Proof. Necessity: Prove that if $gcd(k, m_2) \neq 1$, there exists node of $DL(N; 1, s)$ which appears more than once on one P-shape copy. Suppose that $gcd(k, m_2) = \delta \neq 1$ such that $k = a\delta$ and $m_2 = b\delta$. By Corollary 2, $I(i, j) = ikm_1 + j \pmod N = ia\delta m_1 + j \pmod N$. Assume $i \geq b$, and $i = i_1 + i_2 b$, where $0 \leq i_1 \leq b - 1$ and $1 \leq i_2 \leq \delta - 1$. Thus, $I(i, j) = (i_1 + i_2 b)a\delta m_1 + j \pmod N = i_1 km_1 + i_2 am_2 m_1 + j \pmod N = i_1 km_1 + i_2 aN + j \pmod N = i_1 km_1 + j \pmod N = I(i_1, j)$. So, $I(i, j) = I(i_1, j)$ and $i \neq i_1$ contradicting the fact that each node of $DL(N; 1, s)$ only appears once on one P-shape copy.

Sufficiency: Prove that if $gcd(k, m_2) = 1$, each node on $DL(N; 1, s)$ must appear once on P-shape. For $\forall(i, j)$ and $\forall(i', j')$ on a P-shape, $i \neq i'$ or $j \neq j'$. As $0 \leq i, i' \leq m_2 - 1$ and $0 \leq j, j' \leq m_1 - 1$, $|i - i'| < m_2$ and $|j - j'| < m_1$. If $gcd(k, m_2) = 1$, $m_2 \nmid (i-i')k$, and $N \nmid (i-i')km_1$. So, $N \nmid (i-i')km_1+(j-j')$. As $I(i, j)-I(i', j') = (j - j') + (i - i')km_1 \pmod N \neq 0$, $I(i, j) \neq I(i', j')$. □

Property 3. *For $Pshape(m_1, m_2, \tau, h)$ of $DL(N; 1, s)$, $|h|$ is the smallest integer satisfying $h = \frac{tm_2+1}{k}$, where t is an integer and $-\frac{m_2}{2} < h \leq \frac{m_2}{2}$.*

Proof. By Lemma 2, the geometric vertical and horizontal distance between node (i, j) on P-shape copy (u, v) and node (i, j) on copy $(u, v + 1)$ are $-h$ and $m_1 - \tau h$ respectively. So, $I(i, j) + m_1 - \tau h - hs \pmod N = I(i, j)$. Thus $khm_1 - m_1 = tN$, where t is an integer. So, $h = \frac{tm_2+1}{k}$. Suppose that there exist integers h, t and δ such that $h = \frac{tm_2+1}{k}$ and $(\delta - 1)m_2 + m_2/2 < h \leq \delta m_2 + m_2/2$. So there must be integers h' and t' such that $h' = h - \delta m_2 = \frac{(t-\delta k)m_2+1}{k} = \frac{t'm_2+1}{k}$ and $-\frac{m_2}{2} < h' \leq \frac{m_2}{2}$. □

2.4.2 Node Mapping Function

Assume f_τ is a function of one-to-one mapping from $M(m_1, m_2)$ to $Pshape(m_1, m_2, \tau, h)$.

$f_\tau : (p, q) \rightarrow (p, q - \tau p \pmod{m_1})$, where $0 \leq p \leq m_2 - 1, 0 \leq q \leq m_1 - 1$.

Mapping function f_τ have the following characteristics:

1) *First Row Consecutive Characteristic*: Nodes $(0, q)$ on row 0 of meshes are embedded on node $(0, q)$ on tier 0 of P-shape.

2) *Row Consecutive Characteristic*: Nodes on the pth row of meshes are embedded on the pth tier of P-shape. Row neighboring nodes (p, q) and $(p, q+1)$ $(0 \leq q \leq m_1-2)$ are embedded on neighboring nodes connected by a horizontal link on the pth tier if $q+1-\tau p \pmod{m_1} \neq 0$, or embedded on (p, m_1-1) and $(p, 0)$ respectively on the pth tier if $q + 1 - \tau p \pmod{m_1} = 0$. We define node set $RCZ = \{(i, j)|0 \leq j \leq m_1 - 2\}$, called *Row Consecutive Zone (RCZ)*, as shown in Figure 2.11. If (p, q) is embedded on *RCZ*, the row neighboring nodes (p, q) and $(p, q + 1)$ are embedded on neighboring nodes connected by a horizontal link on the pth tier. Assume $R = \bar{R} \cup \hat{R}$, where $\bar{R} =$

$\{e[(p,q),(p,q+1))|f_\tau(p,q) \in RCZ\}$, and $\hat{R} = \{e[(p,q),(p,q+1))|f_\tau(p,q) \in \overline{RCZ}\}$. It is easy to calculate that $|\hat{R}| = (m_2-1)(1-\frac{gcd(m_1,\tau)}{m_1})$ and $|\bar{R}| = m_1 m_2 + \frac{m_2 gcd(m_1,\tau)}{m_1} - \frac{gcd(m_1,\tau)}{m_1} + 1$.

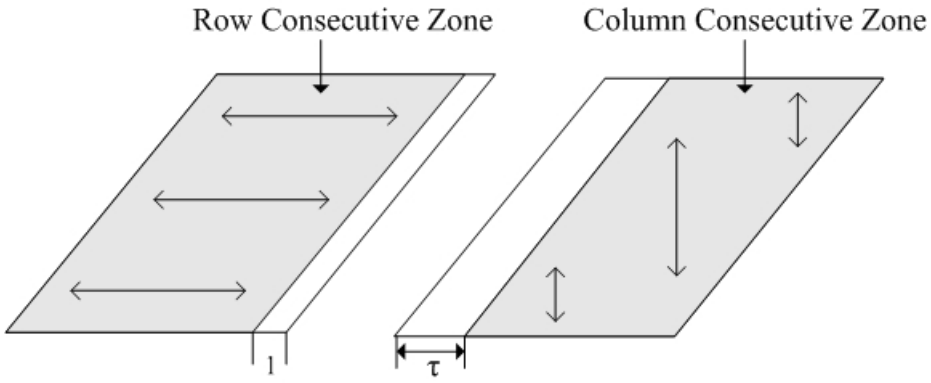

Figure 2.11: Row and Column Consecutive Zone

3) *Column Consecutive Characteristic*: Node on the pth row and qth column of meshes are embedded on node $q-\tau p \pmod{m_1}$ of the pth tier of P-shape. The column neighboring nodes (p,q) and $(p+1,q)$ $(0 \le p \le m_2-2)$ are embedded on the neighboring nodes connected by a vertical link if $\tau \le q-\tau p \pmod{N} \le m_1 - 1(\tau > 0)$ or $0 \le q-\tau p \pmod{N} \le m_1 - \tau - 1(\tau < 0)$. We define node set $CCZ = \{(i,j)|\tau \le j \le m_1 - 1\}$ if $\tau \ge 0$, or $CCZ = \{(i,j)|0 \le j \le m_1 - \tau - 1\}$ if $\tau < 0$, called *Column Consecutive Zone*, as shown in Figure 2.11. If (p,q) is embedded on *CCZ*, column neighboring nodes (p,q) and $(p+1,q)$ are embedded on neighboring nodes connected by a vertical link. Assume $C = \bar{C} \cup \hat{C}$, where $\bar{C} = \{e[(p,q),(p,q+1)]|f_\tau(p,q) \in CCZ\}$, and $\hat{C} = \{e[(p,q),(p+1,q)]|f_\tau(p,q) \in \overline{CCZ}\}$. Thus $|\hat{C}| = |\tau|(m_2-1)$ and $|\bar{C}| = (m_1-\tau)(m_2-1)$.

We call such an embedding *P-shape embedding*, which ensures that nodes on the same row of meshes are embedded on the same tier. Moreover, nodes connected by a horizontal link between the neighboring tiers are column neighboring nodes of meshes.

2.4.3 Expansion, Dilation and Congestion

2.4.3.1 Expansion

According to our assumption, the number of nodes in $M(m_1, m_2)$ is equal to that in double-loop networks. That is, $N = m_1 m_2$. So, expansion for embedding $M(m_1, m_2)$ on N-node double-loop networks is 1.

2.4.3.2 Dilation and Average Dilation

Dilation of an edge is the distance in $DL(N; 1, s)$ between the nodes that host the two neighboring nodes of $M(m_1, m_2)$. By P-shape embedding, $Dil(e_r) = Dist(f_\tau(p, q + 1), f_\tau(p, q)) = Dist((p, q + 1 - \tau p \pmod N), (p, q - \tau p \pmod N))$, and $Dil(e_c) = Dist(f_\tau(p + 1, q), f_\tau(p, q)) = Dist((p + 1, q - \tau(p + 1) \pmod N), (p, q - \tau p \pmod N))$. Let $\bar{e_r}$, $\bar{e_c}$, $\hat{e_r}$ and $\hat{e_c}$ denote the edges in $\bar{R}$, $\bar{C}$, $\hat{R}$ and $\hat{C}$ respectively. The dilations of the edges for embedding $M(m_1, m_2)$ on $Pshape(m_1, m_2, \tau, h)$ can be obtained in the following theorems.

Theorem 1. $Dil(\bar{e_r}) = Dil(\bar{e_c}) = 1$.

Proof. As $q - \tau p \pmod{m_1} \neq 0$, by Lemma 3, $Dil(\bar{e_r}) = min_{u,v \in Z} |um_2 - vh| + |1 + um_2\tau + v(m_1 - \tau h)| = 1$ when $u = v = 0$. Similarly, $Dil(\bar{e_c}) = min_{u,v \in Z} |1 + um_2 - vh| + |um_2\tau + v(m_1 - \tau h)| = 1$. □

Theorem 2. $Dil(\hat{e_r}) = min_{u,v \in Z} r(u, v)$ *and* $Dil(\hat{e_c}) = min_{u,v \in Z} c(u, v)$, *where* $r(u, v) = |um_2 - vh| + |m_1 - 1 + um_2\tau + v(m_1 - \tau h)|$ *and* $c(u, v) = |1 + um_2 - vh| + |m_1 + um_2\tau + v(m_1 - \tau h)|$.

Proof. As $q - \tau p \pmod{m_1} = 0$, $Dil(\hat{e_c}) = Dist(f_\tau(p, q), f_\tau(p, q + 1)) = Dist((p, m_1 - 1), (p, 0) = min_{u,v \in Z}(|um_2 - vh| + |m_1 - 1 + um_2\tau + v(m_1 - \tau h)|)$ by Lemma 3. Similarly, it can be calculated that $Dil(\hat{e_c}) = min_{u,v \in Z}(|1 + um_2 - vh| + |m_1 + um_2\tau + v(m_1 - \tau h)|)$. □

By Theorem 1 and 2, the follow corollaries can be obtained. Corollary 3 proves that a large number of edges on meshes can achieve dilation 1 by P-shape embedding.

Corollary 4 gives the upper bound for the edge dilation of row and column edges on meshes embedded on double-loop networks by P-shape embedding. The conditions for obtaining optimal embedding for $M(m_1, m_2)$ on $DL(N; s_1, s_2)$ are derived by Corollary 5.

Corollary 3. *By P-shape embedding of $M(m_1, m_2)$ on $Pshape(m_1, m_2, \tau, h)$, $\frac{m_1-|\tau|}{m_1}$ fraction of column edges and at least $\frac{m_1-2}{m_1-1}$ fraction of row edges have dilation 1. The fraction of the edges on $M(m_1, m_2)$ with dilation 1 by P-shape embedding is at least $1 - \frac{(|\tau|+1)m_2-|\tau|}{2m_1m_2-m_1-m_2}$, which increases with the decrease of $|\tau|$.*

Proof. According to the row and column consecutive characteristics, $\frac{|\bar{C}|}{|C|} = \frac{(m_1-|\tau|)(m_2-1)}{m_1(m_2-1)} = \frac{m_1-|\tau|}{m_1}$ and $\frac{|\bar{R}|}{|R|} > \frac{m_2(m_1-2)}{m_2(m_1-1)} = \frac{m_1-2}{m_1-1}$. So, $\frac{|\bar{C}|+|\bar{R}|}{|C|+|R|} > \frac{(m_1-|\tau|)(m_2-1)+m_2(m_1-2)}{2m_1m_2-m_1-m_2} = 1 - \frac{(|\tau|+1)m_2-|\tau|}{2m_1m_2-m_1-m_2}$. □

Corollary 4. *$Dil(\hat{e_r}) \leq m_1 - 1$, and $Dil(\hat{e_c}) \leq m_1 + 1$. In the worst case, the average dilation is approximately $\frac{3+|\tau|}{2}$.*

Proof. By Theorem 2, $Dil(\hat{e_r}) \leq r(0,0) = m_1 - 1$, and $Dil(\hat{e_c}) \leq c(0,0) = m_1 + 1$.

So, $ADil(M(m_1, m_2), DL) = \frac{|\bar{R}|+|\hat{R}|\times\min r(u,v)+|\bar{C}|+|\hat{C}|\times\min c(u,v)}{2m_1m_2-m_1-m_2}$

$= 1 + \frac{(m_2-1)((1-\frac{gcd(m_1,\tau)}{m_1})(\min r(u,v)-1)+|\tau|(\min c(u,v)-1))}{2m_1m_2-m_1-m_2}$

$\leq 1 + \frac{(m_2-1)((1-\frac{gcd(m_1,\tau)}{m_1})(m_1-2)+|\tau|m_1)}{2m_1m_2-m_1-m_2}$

$< 1 + \frac{(m_2-1)(m_1-2+|\tau|m_1)}{2m_1m_2-m_1-m_2}$

$= 1 + \frac{(1+|\tau|)m_1m_2-(1+|\tau|)m_1-2(m_2-1)}{2m_1m_2-m_1-m_2}$

$\approx \frac{3+|\tau|}{2}$. □

Corollary 5. *If $m_1|s$ and $gcd(\frac{s}{m_1}, m_2) = 1$, P-shape embedding for $M(m_1, m_2)$ on $DL(N; 1, s)$ is optimal with dilation 1 and congestion 1.*

Proof. By Corollary 1, if $m_1|s$, $\tau = 0$ and $k = \frac{s}{m_1}$. According to Property 2, P-shape exists if and only if $gcd(\frac{s}{m_1}, m_2) = 1$. By P-shape embedding, $f = (p, q)$. That is, node (p, q) of $M(m_1, m_2)$ is embedded on node (p, q) of P-shape. As $\tau = 0$, there is no shift between the neighboring tiers. It is easy to see each P-shape copy is a rectangular shaped tile when $\tau = 0$, which can host $M(m_1, m_2)$ perfectly. Therefore, dilation and

congestion for all edges of $M(m_1, m_2)$ on $DL(N; s_1, s_2)$ are 1. In this case, P-shape embedding is optimal, which preserves adjacency [80]. □

2.4.3.3 Congestion

Congestion of an edge is the number of the edges in $M(m_1, m_2)$ embedded on one edge in $DL(N; 1, s)$. We assume the routing path of $\hat{e_r}$ is from copy (0,0) to copy (u, v) first

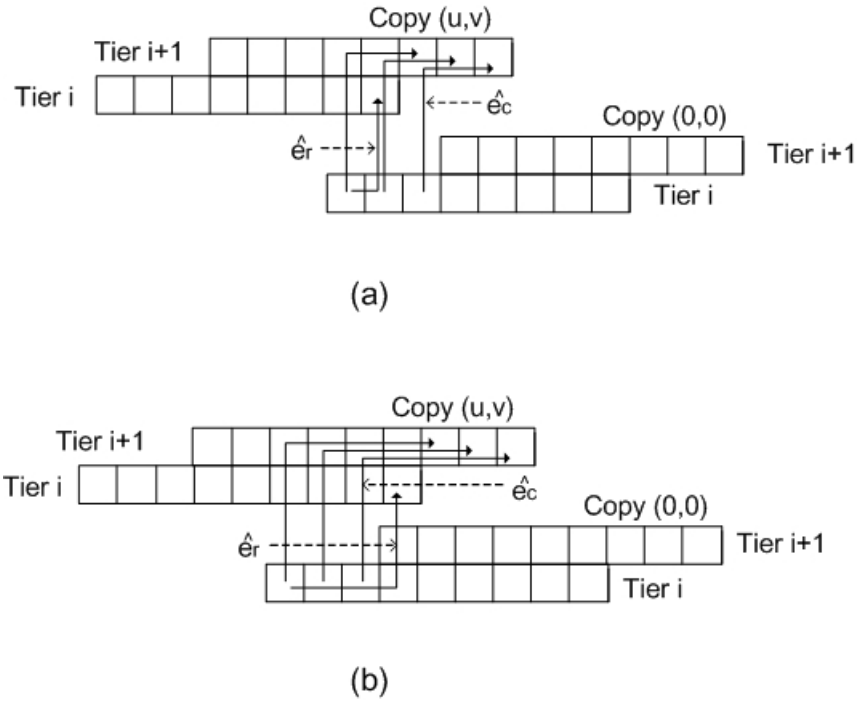

Figure 2.12: (a) $X(\hat{e_c}) < \tau$ and (b) $Y(\hat{e_c}) > \tau$

passing through $X(\hat{e_r})$ horizontal links, and then through $Y(\hat{e_r})$ vertical links; and $\hat{e_c}$ first passing through $Y(\hat{e_c})$ vertical links, and then through $X(\hat{e_c})$ horizontal links, as shown in Figure 2.12. By P-shape embedding, edge congestion of the vertical links and horizontal links, denoted by $Cong(l_v)$ and $Cong(l_h)$ respectively, can be calculated by the following theorem.

Theorem 3. $Cong(l_v) = \lceil \frac{Y(\hat{e_c})+Y(\hat{e_r})-1}{m_1/\tau} \rceil + 1$ *and* $Cong(l_h) = \lfloor \frac{X(\hat{e_c})+X(\hat{e_r})}{m_1} \rfloor + \min(\tau, X(\hat{e_r})) + 1$.

Proof. As each vertical link, connecting the neighboring tiers of P-shape, hosts one column edge of meshes, these vertical links have congestion of at least 1. In addition,

the number of edges in $e_c \in \hat{C}$ and $e_r \in \hat{R}$ passing through the vertical links can be calculated by $\lceil \frac{Y(\hat{e_c})+Y(\hat{e_r})-1}{m_1/\tau} \rceil$. So, $Cong(l_v) = \lceil \frac{Y(\hat{e_c})+Y(\hat{e_r})-1}{m_1/\tau} \rceil + 1$. Similarly, each horizontal link, connecting the neighboring nodes in each tiers of P-shape, has congestion of at least 1. As shown in Figure 2.12, the maximum number of edges in $e_c \in \hat{C}$ passing through the horizontal links is $X(\hat{e_c})$ if $X(\hat{e_c}) < \tau$, and τ if $X(\hat{e_c}) \geq \tau$. So, $Cong(l_h) = \lfloor \frac{X(\hat{e_c})+X(\hat{e_r})}{m_1} \rfloor + \min(\tau, X(\hat{e_r})) + 1$. □

Corollary 6. *By P-shape embedding, edge congestion of the vertical links is in the range of* $[1, 2\tau]$*, and edge congestion of the horizontal links is in the range of* $[1, \tau + 2]$.

Proof. It is easy to prove from the fact that $1 \leq Y(\hat{e_c}) + Y(\hat{e_r}) < 2m_1$ and $0 \leq X(\hat{e_c}) + X(\hat{e_r}) < 2m_1$. □

2.4.4 Case Analysis

2.4.4.1 $s < m_1$

Theorem 4. *P-shape*$(m_1, m_2, m_1 - s, 1)$ *exists if* $s < m_1$.

Proof. If $s < m_1$, $k = 1$ by Property 1. As $gcd(1, m_2) = 1$, P-shape exists by Property 2. So, $\tau = m_1 - s$. By Property 3, $h = 1$. □

Theorem 5. *If* $s < m_1$,

$Dil(\hat{e_r}) \leq \min(\rho_1 + \rho_2, \rho_1 - \rho_2 + s + 1) \leq \frac{m_1-1}{s} + \frac{s+1}{2}$ *, where* $\rho_1 = \frac{m_1-1}{s}$ *and* $\rho_2 = m_1 - 1 \pmod{s}$*, and*

$Dil(\hat{e_c}) \leq \min(\gamma_1 + \gamma_2 + 1, \gamma_1 - \gamma_2 + s + 2) \leq \frac{m_1}{s} + \frac{s+1}{2} + 1$ *, where* $\gamma_1 = \frac{m_1}{s}$ *and* $\gamma_2 = m_1 \pmod{s}$.

Proof. By Theorem 2 and Theorem 4, $Dil(\hat{e_r}) = min_{u,v \in Z} r(u, v)$, where $r(u, v) = |um_2 - v| + |m_1 - 1 + um_2\tau + vs|$. $Dil(\hat{e_r}) \leq min_{v \in Z} r(0, v) = min_{v \in Z} |v| + |m_1 - 1 + vs|$. If $s|(m_1 - 1)$, $Dil(e_r) \leq \frac{m_1-1}{s}$. If $s \nmid (m_1 - 1)$, assume $m_1 - 1 = \rho_1 s + \rho_2$, where $\rho_1 = \frac{m_1-1}{s}$ and $\rho_2 = m_1 - 1 \pmod{s}$. It can be proven that $Dil(\hat{e_r}) \leq \min(\rho_1 + \rho_2, \rho_1 - \rho_2 + s + 1) \leq \frac{m_1-1}{s} + \frac{s+1}{2}$.

Similarly, $Dil(\hat{e_c}) = min_{u,v \in Z} |1 + um_2 - v| + |m_1 + um_2\tau + vs|$. $Dil(\hat{e_c}) \leq min_{v \in Z} c(0, v) = min_{v \in Z} |1 - v| + |m_1 + vs|$. If $s|m_1$, $Dil(\hat{e_c}) \leq \frac{m_1}{s} + 1$. If $s \nmid m_1$,

assume $m_1 = \gamma_1 s + \gamma_2$, where $\gamma_1 = \frac{m_1}{s}$ and $\gamma_2 = m_1 \pmod s$. It can be proven that $Dil(e_c) \leq \min(\gamma_1 + \gamma_2 + 1, \gamma_1 - \gamma_2 + s + 2) \leq \frac{m_1}{s} + \frac{s+1}{2} + 1$. □

Corollary 7. *If $s < m_1$, $Dil(\hat{e_r}) \approx \frac{m_1}{s}$ and $Dil(\hat{e_c}) \approx \frac{m_1 - 1}{s}$. P-shape embedding is near optimal when s is near m_1.*

2.4.4.2 $s > m_1$

Theorem 6. *If $s > m_1$,*

$$Dil(\hat{e_c}) \leq \begin{cases} \frac{(m_1-1)|\Delta|}{d} + \frac{\Delta+|h|}{2}, \text{ if } \Delta \geq 0, \\ \frac{-(m_1-1)|h|}{\Delta} + \frac{\Delta-|h|}{2}, \text{ if } \Delta < 0, \end{cases}$$

and

$$Dil(\hat{e_r}) \leq \begin{cases} \frac{m_1|h|}{\Delta} + \frac{m_1-\tau h+|h|}{2}, \text{ if } \Delta \geq 0, \\ \frac{m_1|h|}{\Delta} + \frac{m_1-\tau h+|h|}{2}, \text{ if } \Delta < 0, \end{cases}$$

where $\Delta = m_1 - \tau h$.

Proof. By Theorem 2, $Dil(e_r) \leq min_{v \in Z} r(0, v) = min_{v \in Z} |vh| + |m_1 - 1 + v(m_1 - \tau h)|$, and $Dil(e_c) \leq min_{v \in Z} c(0, v) = min_{v \in Z} |1 - vh| + |m_1 + v(m_1 - \tau h)|$. It can be proven similarly with Theorem 5. □

Corollary 8. *$Dil(\hat{e_r}) \approx |\frac{(m_1-1)h}{\Delta}|$ and $Dil(\hat{e_c}) \approx |\frac{m_1 h}{\Delta}|$. P-shape embedding is near optimal when $|\Delta|$ is near $m_1|h|$.*

It can be seen from the above discussion, the embedding performance of P-shape embedding depends heavily on the parameters of P-shape. Table 2.1 shows an example for embedding $M(8, 16)$ embedded on $DL(8 \times 16; 1, s)$, where $2 \leq s \leq 9$.

2.5 Embedding of Tori on P-shape of $DL(N; 1, s)$

As $T(m_1, m_2)$ can be obtained from $M(m_1, m_2)$ by adding wrap-around edges of R^a and C^a, we study the embedding of edges in R^a and C^a on P-shape(m_1, m_2, τ, h).

s	τ	h	$Dil(\hat{e_r})$	$Dil(\hat{e_c})$	$Adil$	$Cong(l_v)$	$Cong(l_h)$
2	6	1	4	5	2.7	7	2
3	5	1	3	5	2.4	5	3
4	4	1	3	3	1.5	4	2
5	3	1	3	5	1.7	2	4
6	2	1	2	4	1.4	2	3
7	1	1	1	3	1.1	2	2
8	0	1	$-$	$-$	1	1	1
9	-1	1	3	1	1.1	2	2

Table 2.1: $M(8, 16)$ embedded on $DL(8 \times 16; 1, s)(2 \leq s \leq 9)$

By P-shape embedding, node mapping function f_τ also ensures the neighboring nodes $(p, m_1 - 1)$ and $(p, 0)$ on tori, where $0 \leq p \leq m_2 - 1$, connected by row edge $e_r^a \in R^a$, are embedded on neighboring nodes of the pth tier if $f_\tau(p, m_1 - 1) \in CCZ$, or embedded on $(p, m_1 - 1)$ and $(p, 0)$ respectively on the pth tier if $f_\tau(p, m_1 - 1) \in \overline{CCZ}$. We denote $R^a = \bar{R}^a \cup \hat{R}^a$, where $\bar{R}^a = \{e[(p, m_1 - 1), (p, 0))|f_\tau(p, m_1 - 1) \in RCZ\}$, and $\hat{R}^a = \{e[(p, m_1 - 1), (p, 0))|f_\tau(p, m_1 - 1) \in \overline{RCZ}\}$. Thus $|\bar{R} \cup \bar{R}^a| = m_1 m_2 - m_2$, $|\hat{R} \cup \hat{R}^a| = m_2$. We denote $C^a = \bar{C}^a \cup \hat{C}^a$, where $\bar{C}^a = \{e[(m_2 - 1, q), (0, q))|f_\tau(m_2 - 1, q) \in CCZ\}$, and $\hat{R}^a = \{e[(p, m_1 - 1), (i, 0))|f_\tau(m_2 - 1, q) \in \overline{CCZ}\}$. $|\bar{C} \cup \bar{C}^a| = m_1 m_2 - |\tau| m_2$, and $|\hat{C} \cup \hat{C}^a| = |\tau| m_2$.

Theorem 7. *$Dil(\bar{e_r^a}) = 1$ and $Dil(\hat{e_r^a}) = min_{u,v \in Z} r(u, v)$.*

Proof. By P-shape embedding, $Dist(f_\tau(p, m_1 - 1), f_\tau(p, 0)) = Dist((p, m_1 - 1 - \tau p \pmod{m_1}), (p, 0 - \tau p \pmod{m_1}))$. If $\tau p \pmod{m_1} \neq 0$, $Dist(f_\tau(p, m_1 - 1), f_\tau(p, 0)) = 1$. If $\tau p \pmod{m_1} = 0$, $Dist(f_\tau(p, m_1 - 1), f_\tau(p, 0)) = Dist((p, m_1 - 1), (p, 0)) = min_{u,v \in Z} r(u, v)$ calculated by the same way for $Dil(e_r)$ on $M(m_1, m_2)$. □

Theorem 8. *If $\tau m_2 \pmod{m_1} = 0$, $Dil(\bar{e_c^a}) = 1$ and $Dil(\hat{e_c^a}) = min_{u,v \in Z} c(u, v)$.*

Proof. By P-shape embedding, nodes $(m_2 - 1, q)$ and $(0, q)$, connected by round column edges on $T(m_1, m_2)$, are embedded on $(m_2 - 1, q - \tau m_2 + \tau \pmod{m_1})$ and $(0, q)$ respectively. By Lemma 2, $Dist(f_\tau(m_2 - 1, q), f_\tau(0, q)) = min_{u,v \in Z} |1 + (u - 1)m_2 - vh| + |-\varepsilon m_1 + u m_2 \tau + v(m_1 - \tau h)|$, where $q - \tau m_2 + \tau \pmod{m_1} = q - \tau m_2 + \tau - \varepsilon m_1$.

If $\tau m_2 \pmod{m_1} = 0$, $q + \tau \pmod{m_1} = q - \tau m_2 + \tau - \varepsilon m_1$. If $0 \leq q \leq m_1 - \tau - 1 (\tau > 0)$ or $-\tau \leq q \leq m_1 - 1 (\tau < 0)$, $\varepsilon m_1 = -\tau m_2$ and $Dist(f_\tau(m_2 -$

$1, q), f_\tau(0, q)) = 1$. Otherwise, $Dist(f_\tau(m_2 - 1, q), f_\tau(0, q)) = min_{u,v \in Z} c(u, v)$ calculated by the same way for $Dil(e_c)$ on $M(m_1, m_2)$. □

Theorem 9. *If* $\tau m_2 \pmod{m_1} = 0$*, the average dilation is no more than* $\frac{3+|\tau|}{2} - \frac{1}{m_1}$ *for embedding* $T(m_1, m_2)$ *on* $DL(N; 1, s)$.

Proof. By Theorem 8, $ADil(T(m_1, m_2), DL) = \frac{|\bar{R} \cup \bar{R^a}| + |\hat{R} \cup \hat{R^a}| \times \min r(u,v) + |\bar{C} \cup \bar{C^a}| + |\hat{C} \cup \hat{R^a}| \times \min c(u,v)}{2m_1 m_2} \leq 1 + \frac{(1+|\tau|)m_2 m_1 - 2m_2}{2m_1 m_2} = \frac{3+|\tau|}{2} - \frac{1}{m_1}$. □

If $\tau m_2 \pmod{m_1} \neq 0$, $Dil(e[(m_2 - 1, q), (0, q)]) = min_{u,v \in Z} c'(u, v)$, where $c'(u, v) = |1 + (u - 1)m_2 - vh| + | - \varepsilon m_1 + u m_2 \tau + v(m_1 - \tau h)|$ and $q - \tau m_2 + \tau \pmod{m_1} = q - \tau m_2 + \tau - \varepsilon m_1$.

Corollary 9. *By P-shape embedding for* $T(m_1, m_2)$*,* $\frac{m_1 - 1}{m_1}$ *fraction of row edges and at least* $\frac{(m_1 - |\tau|)(m_2 - 1)}{m_1 m_2}$ *fraction of column edges have dilation 1. The fraction of the edges on* $T(m_1, m_2)$ *with dilation 1 by P-shape embedding is at least* $1 - \frac{m_1 + (|\tau| + 1)m_2 - |\tau|}{2m_1 m_2}$*, which increases with the decrease of* $|\tau|$.

Proof. For $T(m_1, m_2)$, $\frac{|\bar{C}|}{|C| + |C^a|} > \frac{(m_1 - |\tau|)(m_2 - 1)}{m_1 m_2}$ and $\frac{|\bar{R}| + |\bar{R^a}|}{|R| + |R^a|} = \frac{m_2(m_1 - 1)}{m_2 m_1} = \frac{m_1 - 1}{m_1}$. So, $\frac{|\bar{C}| + |\bar{R}| + |\bar{R^a}|}{|C| + |R| + |C^a| + |R^a|} > \frac{(m_1 - |\tau|)(m_2 - 1) + m_2(m_1 - 1)}{2m_1 m_2} = 1 - \frac{m_1 + (|\tau| + 1)m_2 - |\tau|}{2m_1 m_2}$. □

Corollary 10. *If* $\tau = 0$*,* $Dil(e_c^a) = 1$ *and* $Dil(e_r^a) = \min(|h| + 1, m_1 - 1)$*. If* $\tau = 0$ *and* $h = 1$*, P-shape embedding for* $T(m_1, m_2)$ *on* $DL(N; 1, s)$ *is optimal with* $Dil(e_c^a) = 1$ *and* $Dil(e_r^a) = 2$.

Proof. If $\tau = 0$, it is easy to obtain by Lemma 2. It can be proven there is no dilation 1 embedding for tori embedded on double-loop networks. □

Corollary 11. *For embedding* $T(m_1, m_2)$ *on* $DL(N; 1, s)$ *with* $|\tau| = 1$*, the average dilation is* $1 + \frac{1}{m_1}$*, which is near optimal with the increasing of* m_1.

2.6 Construction of P-shape for $DL(N; s_1, s_2)$

For $DL(N; 1, s)$, the difference between the horizontal neighboring nodes on the tessellation plane is 1. That is, node index is consecutive on each tier of P-shape.

For the sake of simplicity, we assume s_1 is the horizontal difference on the tessellation plane of $DL(N; s_1, s_2)$. Our designed P-shape for $DL(N; 1, s)$ can be extended to $DL(N; s_1, s_2)$. Since the parameters of $DL(N; s_1, s_2)$ is more flexible than $DL(N; 1, s)$, the construction of P-shape for $DL(N; s_1, s_2)$ is much more difficult.

2.6.1 $Pshape(m_1, m_2, \tau, h)$ for $DL(N; s_1, s_2)$

Property 4. *$Pshape(m_1, m_2, \tau, h)$ for $DL(N; s_1, s_2)$ satisfies $\tau = \frac{(Km_2+k)m_1-s_2}{s_1}$, where k and K are integers.($\lceil -s_1 + s_2/m_1 \pmod{m_2} \rceil < k < \lfloor s_1 + s_2/m_1 \pmod{m_2} \rfloor$, $\lceil \frac{-s_1m_1+s_2-km_1}{N} \rceil < K < \lfloor \frac{s_1m_1+s_2-km_1}{N} \rfloor$.)*

Proof. Similar with the proof for P-shape of $DL(N; 1, s)$, $x + (\tau \times s_1 + s_2) \times m_2 \pmod{N} = x$, where $x (0 \leq x \leq N-1)$. So, $\tau s_1 + s_2 \pmod{N} = km_1$. As $-m_1s_1+s_2 \pmod{N} < \tau s_1+s_2 < m_1s_1+s_2 \pmod{N}$, $\lceil -s_1+s_2/m_1 \pmod{m_2} \rceil < k < \lfloor s_1 + s_2/m_1 \pmod{m_2} \rfloor$. Assume $\tau s_1 + s_2 = KN + km_1$, $\tau = \frac{(Km_2+k)m_1-s_2}{s_1}$, where $\lceil \frac{-s_1m_1+s_2-km_1}{N} \rceil < K < \lfloor \frac{s_1m_1+s_2-km_1}{N} \rfloor$. □

By Lemma 4, τ can be calculated by the following *Algorithm 1*.

Algorithm 1: $Pshape(m_1, m_2, \tau, h)$ on $DL(N; s_1, s_2)$

For $k = \lceil -s_1 + \frac{s_2}{m_1 \pmod{m_2}} \rceil$ to $\lfloor s_1 + \frac{s_2}{m_1 \pmod{m_2}} \rfloor$
  For $K = \lceil \frac{-s_1m_1+s_2-km_1}{N} \rceil$ to $\lfloor \frac{s_1m_1+s_2-km_1}{N} \rfloor$
    $\tau = \frac{(Km_2+k)m_1-s_2}{s_1}$;
    If τ is an integer, break.

The time complexity of this algorithm is $O(m_2 \times \frac{2m_1s_1}{N}) = O(s_1)$.

Corollary 12. *For $Pshape(m_1, m_2, \tau, h)$ on $DL(N; s_1, s_2)$, $I(i, j) = ikm_1 + js_1 \pmod{N}$, where $0 \leq i \leq m_2 - 1, 0 \leq j \leq m_1 - 1$.*

Property 5. *For $Pshape(m_1, m_2, \tau, h)$ of $DL(N; s_1, s_2)$, left copy distance $|h|$ is the smallest integer satisfying $h = \frac{tm_2+s_1}{k}$, where t is an integer and $-\frac{m_2}{2} < h \leq \frac{m_2}{2}$.*

Property 6. *$Pshape(m_1, m_2, \tau, h)$ for $DL(N; s_1, s_2)$ exists if and only if $gcd(k, m_2) = 1$ and $gcd(m_1, s_1) = 1$.*

Proof. The proof for the condition of $gcd(k, m_2) = 1$ is similar with Property 2. *Necessity:* As the horizontal difference is s_1, there are $\frac{N}{gcd(N,s_1)}$ nodes , $i, i + s_1, i + 2s_1, ..., i + \frac{N}{gcd(N,s_1)}s_1$ where $0 \leq i \leq gcd(N, s_1)$, periodically appeared on the plane of $DL(N; s_1, s_2)$. To construct $Pshape(m_1, m_2, \tau, h)$, $\frac{N}{gcd(N,s_1)}$ should be an integer which can be divided by m_1. If $gcd(s_1, m_1) = 1$, $\frac{N}{gcd(N,s_1)} = \frac{N}{gcd(m_2,s_1)}$, which must be an integer. It can be proved that $\tau = \frac{(Km_2+k)m_1-s_2}{s_1}$ exist if $gcd(m_1, s_1) \neq 1$. *Sufficiency:* Prove that if $gcd(m_1, s_1) = 1$, each node on $DL(N; s_1, s_2)$ must appear once on one P-shape. For $\forall(i, j)$ and $\forall(i', j')$ on a P-shape, $i \neq i'$ or $j \neq j'$. As $0 \leq i, i' \leq m_2 - 1$ and $0 \leq j, j' \leq m_1 - 1$, $|i - i'| < m_2$ and $|j - j'| < m_1$. If $gcd(m_1, s_1) = 1$, $m_1 \nmid (j - j')s_1$. As $N \nmid (i - i')km_1$, $N \nmid (i - i')km_1 + (j - j')s_1$. So $I(i, j) - I(i', j') = (j - j') + (i - i')km_1 \pmod N \neq 0$, and $I(i, j) \neq I(i', j')$. □

Theorem 10. *If $m_1|s_2$, $gcd(\frac{s_2}{m_1}, m_2) = 1$ and $gcd(s_1, m_1) = 1$, P-shape embedding for $M(m_1, m_2)$ on $DL(N; s_1, s_2)$ is optimal with dilation 1 and congestion 1.*

It can be seen that the edge dilation, average dilation and congestion for embedding $M(m_1, m_2)$ and $T(m_1, m_2)$ on $Pshape(m_1, m_2, \tau, h)$ for $DL(N; s_1, s_2)$ are the same for embedding $M(m_1, m_2)$ and $T(m_1, m_2)$ on $Pshape(m_1, m_2, \tau, h)$ for $DL(N; 1, s)$. That is, the embedding performance depends on the parameters of P-shape, once P-shape is constructed on double-loop networks.

2.6.2 $Pshape(m_1, m_2, \tau, g \cdot h)$ for $DL(N; s_1, s_2)$ if $gcd(s_1, m_1) \neq 1$

By Property 6, the condition of the construction of P-shape is $gcd(s_1, m_1) = 1$. If $gcd(s_1, m_1) > 1$ and $gcd(s_1, N)|m_2$, we construct $Pshape(m_1, m_2, \tau, g \cdot h)$ for $DL(N; s_1, s_2)$ as follows, where $d = gcd(s_1, m_1)$, $g = gcd(s_1, N)$.

1) Construct $Pshape(m_1, m_2/g, \tau, h)$ for $DL(N/g; s_1/d, s_2)$.

2) Construct sub-$Pshape(m_1, m_2/g, 0, h)$ in each tier of $Pshape(m_1, g, \tau, h)$.

Figure 2.13 shows $Pshape(4, 6, 1, h)$ for $DL(24; 2, 3)$, which can be constructed from $Pshape(4, 3, 1, 1)$ for $DL(12; 1, 3)$ with sub-$Pshape(4, 2, 0, h)$ in each tier of $Pshape(4, 3, 1, 1)$, since $gcd(1, 2) = 2$.

16	18	20	22	0	2	4	6	8	10	12
13	15	17	19	21	23	1	3	5	7	9
10	12	14	16	18	20	22	0	2	4	6
7	9	11	13	15	17	19	21	23	1	3
4	6	8	10	12	14	16	18	20	22	0
1	3	5	7	9	11	13	15	17	19	21
22	0	2	4	6	8	10	12	14	16	18
19	21	23	1	3	5	7	9	11	13	15
16	18	20	22	0	2	4	6	8	10	12
13	15	17	19	21	23	1	3	5	7	9

Figure 2.13: $Pshape(4, 6, 1, 1, 2)$ for $DL(24; 2, 3)$

Accordingly, node mapping function $f_{\tau/g}$ for $M(m_1, m_2)$ on $Pshape(m_1, m_2, \tau, g \cdot h)$ can be extended as,

$f_{\tau/g} : (p, q) \rightarrow (p, q - \tau p/g \pmod{m_1})$, where $0 \leq p \leq m_2 - 1, 0 \leq q \leq m_1 - 1$.

Mapping function $f_{\tau/g}$ have the following characteristics:

2) *Row Consecutive Characteristic*: The row neighboring nodes (p, q) and $(p, q+1)$ $(0 \leq q \leq m_1 - 2)$ on meshes are embedded on neighboring nodes connected by a horizontal link of the pth tier of P-shape if $q + 1 - \tau p/g \pmod{m_1} \neq 0$, or embedded on $(p, 0)$ and $(p, m_1 - 1)$ of P-shape respectively if $q + 1 - \tau p/g \pmod{m_1} = 0$. We denote $R = \bar{R} \cup \hat{R}$, where $\bar{R} = \{e[(p, q), (p, q + 1))|q + 1 - \tau p/g \pmod{m_1} \neq 0\}$, and $\hat{R} = \{e[(p, q), (p, q + 1))|q + 1 - \tau p/g \pmod{m_1} = 0\}$. 3) *Column Consecutive Characteristic*: The column neighboring nodes (p, q) and $(p+1, q)$ $(0 \leq p \leq m_2-2)$ on meshes are embedded on the neighboring nodes connected by a vertical link between the neighbor subtiers if $p \pmod{g} < g - 1$, or between the neighbor tiers if $p \pmod{g} = g - 1$ and $\tau \leq q - \tau p/g \pmod{N} \leq m_1 - 1(\tau > 0)$ or $0 \leq q - \tau p \pmod{N} \leq m_1 - \tau - 1(\tau < 0)$. We denote $C = \bar{C}'_1 \cup \bar{C}'_2 \cup \hat{C}'$, where

$\bar{C}'_1 = \{e[(p, q), (p, q + 1))|p \pmod{g} < g - 1\}$,

$\bar{C}'_2 = \{e[(p, q), (p, q + 1))|p \pmod{g} = g - 1$ and $\tau \leq q - \tau p/g \pmod{N} \leq m_1 - 1(\tau > 0)$ $(0 \leq q - \tau p/g \pmod{N} \leq m_1 + \tau - 1(\tau < 0))\}$,

$\hat{C'} = \{e[(p,q),(p+1,q))|p \pmod g = g-1$ and $0 \leq q - \tau p/g \pmod N \leq \tau - 1(\tau > 0)$ $(m_1 + \tau \leq q - \tau p/g \pmod N \leq m_1 - 1(\tau < 0))\}$.

The following theorem can be similarly obtained.

Theorem 11. $Dil(\bar{e_r}) = Dil(\bar{e_c}) = 1$, $Dil(\hat{e_r}) = \min_{u,v \in Z} r_g(u,v)$ ***and*** $Dil(\hat{e_c}) = \min_{u,v \in Z} c_g(u,v)$, ***where*** $r_g(u,v) = |um_2 - vhg| + |m_1 - 1 + um_2\tau + v(m_1 - \tau h)|$ ***and*** $c_g(u,v) = |1 + um_2 - vhg| + |m_1 + um_2\tau + v(m_1 - \tau h)|$.

If $gcd(s_1, m_1) = d > 1$ and $gcd(s_1, N) \nmid m_2$, P-shape can be constructed by changing m_2 as base, or changing s_2 as the horizontal step to satisfy $gcd(s_i, N)|m_j$, where $i = 1$ or 2 and $j = 1$ or 2. For example, if $gcd(s_2, m_2) = 1$, $Pshape(m_2, m_1, \tau, h)$ can be constructed on $DL(N; s_2, s_1)$; If $gcd(s_2, m_2) = d > 1$ and $gcd(s_2, N)|m_1$, $Pshape(m_2, m_1, \tau, g \cdot h)$ can be constructed. As $gcd(N, s_1, s_2) = 1$ for $DL(N; s_1, s_2)$, it can be proved that the scenario of $gcd(s_i, N) \nmid m_j$ for both $i = 1, 2$ and $j = 1, 2$ happens with very little chance under strict conditions. Even if this case happens, dummy nodes can be added to satisfy $gcd(s_i, N')|m'_j$, which requires $s_i - 1$ dummy tiers added in the worst case. Since s_i is usually very small compared with the size of the networks in practical, the expansion rate is no larger than $1 + \frac{s_i - 1}{m_j}$, which is near 1.

In summary, P-shape on $DL(N; s_1, s_2)$ can be constructed using the following *Algorithm 2*.

Algorithm 2: P-shape construction for $DL(N; s_1, s_2)$

$d = gcd(s_1, m_1)$, $g = gcd(s_1, N)$.
If $d = 1$
  Calculate τ for $Pshape(m_1, m_2, \tau, h)$ on $DL(N; s_1, s_2)$;
If $d \neq 1$
  If $\frac{m_2}{g}$ is an integer
    Calculate τ for for $Pshape(m_1, \frac{m_2}{g}, \tau, h, g)$ on $DL(\frac{N}{g}; \frac{s_1}{g}, s_2)$;
  If $\frac{m_2}{g}$ is not an integer
    Output("adding dummy nodes").

2.7 Extended P-shape on $DL(N;1,s)$ and $DL(N;s_1,s_2)$

It can be seen from Property 2 and Property 6 that P-shape for $DL(N;1,s)$ or $DL(N;s_1,s_2)$ is constructed on the condition that $gcd(k,m_2)=1$. In this section, we design the extended P-shape, which is not restricted by the condition of $gcd(k,m_2)=1$. To construct the extended P-shape, we fist give the following lemmas.

Lemma 4. *If $s > m_1$ and $m_1 \nmid s$, there exist two and only two, $-m_1 < \tau_1 < 0$ and $0 < \tau_2 < m_1$, satisfying $\tau_1 = k_1 m_1 - s = \lfloor s/m_1 \rfloor m_1 - s < 0$ and $\tau_2 = k_2 m_1 - s = \lceil s/m_1 \rceil m_1 - s > 0$, where $k_2 - k_1 = 1$ and $\tau_2 - \tau_1 = m_1$.*

Lemma 5. *If $m_1 \nmid s_2$, there exist two and only two, $-m_1 < \tau_1 < 0$ and $0 < \tau_2 < m_1$, satisfying $\tau_i = \frac{(K_i m_2 + k_i)m_1 - s_2}{s_1}$, where $k_2 - k_1 = s_1 - (K_2 - K_1)$ and $\tau_2 - \tau_1 = m_1$.*

By Lemma 4 and 5, if $gcd(k_i, m_2) = 1$ ($i = 1$ or 2), $Pshape(m_1, m_2, \tau_i, h)$ can be constructed for $DL(N;1,s)$ or $DL(N;s_1,s_2)$ using only one τ_i. If $gcd(k_1, m_2) \neq 1$ and $gcd(k_2, m_2) \neq 1$, the extended P-shape, denoted by $Pshape(m_1, m_2, \tau_1, \tau_2, h)$, can be constructed using both τ_1 and τ_2 as follows, where $gcd(k_1, m_2) = \kappa$.

1) Construct $Pshape(m_1, m_2/\kappa, \tau_1, h_1)$ for $DL(N/\kappa;1,s)$ or $DL(N/\kappa;s_1,s_2)$.

2) Construct sub-$Pshape(m_1, \kappa, \tau_2, h_2)$ for $DL(m_1\kappa;1,s)$ or $DL(m_1\kappa;s_1,s_2)$ on each tier of P-shape$_1(m_1, m_2/\kappa, \tau_1, h_1)$.

As shown in Figure 2.14, for embedding $M(4 \times 6)$ on $DL(24;1,11)$, it can be calculated that $k_1 = 2$, $\tau_1 = -3$, and $k_2 = 3$, $\tau_2 = 1$. As $gcd(2,6) = 2 \neq 1$ and $gcd(2,6) = 3 \neq 1$, we first construct $Pshape(4,3,-3,h_1)$, and then construct a sub-$Pshape(4,2,1,h_2)$ on each tier of $Pshape(4,3,-3,h_1)$. We denote the horizontal distance between the $(i+1)$th tier and the ith tier is $\tau(i)$, where $1 \leq i \leq m_2 - 1$. For $Pshape(m_1, m_2, \tau_1, \tau_2, h)$, $\tau(i) = \tau_1$ if $i \pmod{\kappa} = 0$, and $\tau(i) = \tau_2$ if $i \pmod{\kappa} \neq 0$. The node mapping function for embedding $M(m_1, m_2)$ or $T(m_1, m_2)$ on $Pshape(m_1, m_2, \tau_1, \tau_2, h)$ can be extended as:

$f_{\tau_i} : (p,q) \rightarrow (p, q - \sum_{i=1}^{p} \tau_i \pmod{m_1})$.

Corollary 13. *The embedding function f_{τ_i} for $Pshape(m_1, m_2, \tau_1, \tau_2, h)$ is equivalent to $f_{\tau_1} : (p,q) \rightarrow (p, q - \tau_1 p \pmod{m_1})$ or $f_{\tau_2} : (p,q) \rightarrow (p, q - \tau_2 p \pmod{m_1})$.*

11	12	13	14	15	16	17	18	19	20	21	22	23
0	1	2	3	4	5	6	7	8	9	10	11	12
13	14	15	16	17	18	19	20	21	22	23	0	1
2	3	4	5	6	7	8	9	10	11	12	13	14
15	16	17	18	19	20	21	22	23	0	1	2	3
4	5	6	7	8	9	10	11	12	13	14	15	16
17	18	19	20	21	22	23	0	1	2	3	4	5
6	7	8	9	10	11	12	13	14	15	16	17	18
19	20	21	22	23	0	1	2	3	4	5	6	7
8	9	10	11	12	13	14	15	16	17	18	19	20

Figure 2.14: Construction of $Pshape(4, 6, -3, , 1, h_2)$ on $DL(24; 1, 11)$

Proof. As $\tau_2 - \tau_1 = m_1$ by Lemma 4, $q - \sum_{i=1}^{i=p} \tau_i \pmod{m_1} = q - \tau_2 p + \frac{p}{\kappa}\tau_2 - \tau_1 \pmod{m_1} = (q - \tau_2 p) \pmod{m_1}$. Similarly, $q - \sum_{i=1}^{i=p} \tau_i \pmod{m_1} = q - \tau_1 p \pmod{m_1}$. □

Based on the construction of the extended P-shape, the edge dilations for extended P-shape embedding can be calculated by the following theorems.

Theorem 12. $Dil(\hat{e_r}) = min_{v \in Z}|m_1 + v\tau_2\kappa| + |v\kappa|$.

Theorem 13. $Dil(\hat{e_c}) = \begin{cases} min_{v \in Z}| - m_1 + v\tau_2\kappa| + |1 + v\kappa|; \textit{ if } p + 1 \pmod{\kappa} = 0; \\ min_{v \in Z}|m_1 + v\tau_2\kappa| + |1 + v\kappa|; \textit{ if } p + 1 \pmod{\kappa} \neq 0. \end{cases}$

2.8 Comparison

2.8.1 P-shape vs. L-shape

The major differences between the traditional L-shape and our proposed P-shape are listed as follows:

(1) L-shape is asymmetric, whereas P-shape is centrosymmetric, thus enabling other regular graphs to be embedded on double-loop networks in a regular and systematic way.

(2) L-shape concerns double-loop network's own properties, whereas P-shape is designed to exploit the relationships between double-loop networks and other regular networks. Therefore, P-shape can act as a bridge between double-loop networks and other regular networks.

(3) For a given double-loop network, there is a unique L-shape, whereas different P-shape constructions can be made on different base lengths for the same double-loop network, thus providing more choices on the construction of P-shape.

These differences show that P-shape is more flexible than L-shape in terms of exploiting the relative performance between double-loop networks and other topologies.

2.8.2 P-shape Embedding vs. Simple and Snake-like Embedding

In [50], the embedding performance of simple and snake-like embedding was studied for meshes and tori on chordal ring of degree four, which is a special class of double-loop networks. Advantages of P-shape embedding compared with simple and snake-like embedding can be demonstrated as follows.

(1) P-shape embedding is more scalable. Simple and snake-like embedding can only be implemented on $DL(N; 1, s)$, and can not be extended to $DL(N; s_1, s_2)$. P-shape embedding can be used on $DL(N; 1, s)$ introduced in Section 2.4 and Section 2.5. Moreover, P-shape embedding can be extended on $DL(N; s_1, s_2)$ shown in Section 2.6. Furthermore, the extended P-shape tessellation approach in Section 2.7 ensures that P-shape embedding always exists on $DL(N; 1, s)$.

(2) P-shape embedding has a larger number of edges with dilation 1 than simple and snake-like embedding. Table 2.2 shows the number of edges with dilation 1 in meshes and tori by simple, snake-like and P-shape embedding. As $0 \leq |\tau| \leq m_1 - 1$, the number of edges with dilation 1 by P-shape embedding is about double of that by simple and snake-like embedding in the best case, and about the same with simple and snake-like embedding in the worst case.

(3) P-shape embedding has more optimal cases than simple and snake-like embedding. For simple embedding, the optimal case for $M(m_1, m_2)$ on $DL(N; 1, s)$ with

N'	$M(m_1 \times m_2)$
Simple	$m_1m_2 - m_2$
Snake-like	$m_1m_2 - 1$
P-shape	$\geq 2m_1m_2 - (\lvert\tau\rvert + 2)m_2 - m_1 + \lvert\tau\rvert$

Table 2.2: Number of edges (N') with dilation 1 in meshes by simple, snake-like and P-shape embedding

dilation 1 and average dilation 1 only happens if and only if $s = m_1$. For snake-like embedding, it is impossible to achieve optimal embedding in any case. It can be seen from Corollary 5 that P-shape embedding for $M(m_1, m_2)$ on $DL(N; 1, s)$ is optimal in a group of cases when $m_1|s$ and $gcd(\frac{s}{m_1}, m_2) = 1$. For example, the dilation and average dilation of embedding $M(4, 15)$ on $DL(4 \times 15; 1, 8)$ are 1 by Corollary 5, whereas the dilation and average dilation of simple embedding for $M(4, 15)$ on $DL(4 \times 15; 1, 8)$ are 4 and 2.96 respectively, and snake-like embedding are 5 and 2.19.

2.9 Conclusion

Due to the topological complexity of double-loop networks, little work has been done on embedding other types of networks on double-loop networks. For the purpose of embedding meshes and tori onto double-loop networks, which is of great significance in both theory and applications for the popularity of these networks and the desirable property of equal node-degree, we proposed a novel tessellation method of P-shape to partition the the geometric plane of double-loop networks, since the traditional L-shape is not symmetric to illustrate the embedding of regular graphs.

Based on the characteristics of P-shape, we designed P-shape embedding, which ensures that a large number of edges in meshes or tori have dilation 1. Furthermore, we evaluated the dilation, average dilation and congestion of P-shape embedding, and derived the conditions for achieving the optimal embedding (dilation 1 and congestion 1) and near optimal embedding (dilation near 1). Our results show that the proposed P-shape is a useful theoretical tool for analyzing the embedding problems on double-loop networks as a bridge between double.

2.10 Application Extensions

Some applications of this work may be extended in the following ways.

2.10.1 Large Meshes

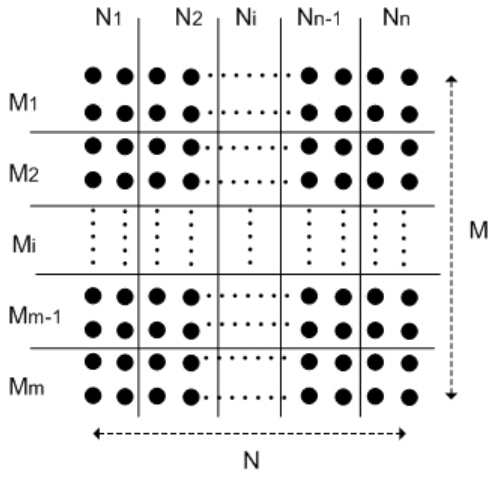

Figure 2.15: Partition of $M \times N$ mesh

According to the definition of P-shape embedding, it is assumed that the number of nodes in meshes is equal to that in double-loop networks. If the number of nodes in meshes is larger than that of double-loop networks, it is easy to partition the meshes into a group of small meshes, such that the number of "super" nodes in the partitioned meshes is equal to that in the double-loop networks by considering each small mesh as a "super" node. In this way, the embedding scheme can be constructed similarly.

For example, given an $M' \times N'$ mesh and an $m \times n$-node double-loop network, where $M' \times N' > m \times n$, the $M' \times N'$ mesh can be partitioned into an $m \times n$ mesh, where $M' = M_1 + M_2 + \ldots M_i \ldots + M_{m-1} + M_m$ and $N' = N_1 + N_2 + \ldots N_i \ldots + N_{n-1} + N_n$, as illustrated in Figure 2.15. In this way, the $M' \times N'$ mesh is partitioned into an $m \times n$ mesh with each "super" node composed of a group of nodes. Thus, the embedding can be easily extended by embedding each "super" node on the node of double-loop networks by P-shape embedding.

2.10.2 Embedding Other Topologies on Double-loop Networks

As mentioned in Chapter 1, a large number of embedding problems on meshes have been studied. It is easy to see that the embedding problems of other topologies on double-loop networks may be solved in two steps by combining two embedding functions illustrated as the following *Algorithm*:

Algorithm *Embedding Topology G_x on Double-loop Network.*

---

(1) *Embedding G_x on mesh*;

/*results obtained by previous results on embedding G_x on mesh*/

(2) *Embedding mesh on double-loop network*;

/*results obtained by our results in this chapter*/

2.10.3 Other Application Extensions

For the future research, the properties of P-shape, which may help to analyze other routing and embedding problems, can be further investigated. One open problem is to extend our methods to the embedding of high dimensional meshes on multi-loop networks $DL(N; s_1, s_2, ..., s_{n-1}, s_n)$, which has a higher degree of technical complexity. Also, if the double-loop networks are connected by optical fibers, the congestion provided by our results can be regarded as the lower bound of the wavelength requirement. However, the advantage of our scheme is small dilation, which represents short communication latency. Due to the complexity of double-loop networks, the embedding schemes which can provide efficient communication bandwidth will be more complex. Furthermore, our proposed technique provides a way for matrix mapping onto double-loop networks, since it is well-known that the mapping of matrix on meshes has been extensively studied in the past years.

Chapter 3

Embedding of Hypercubes on Array-based WDM Optical Networks

In this chapter, we first study routing and wavelength assignment for realizing hypercubes on WDM optical networks including linear arrays and rings with the consideration of communication directions. Specifically, we analyze this problem for both bidirectional and unidirectional hypercubes. For each case, we identify a lower bound on the number of wavelengths required, and design the embedding scheme and wavelength assignment algorithm that uses a provably near-optimal number of wavelengths. In addition, we extend the results to meshes and tori.

3.1 Introduction

Optical communication, in particular, Wavelength Division Multiplexing (WDM) technique, has become a promising technology for many emerging networking and parallel/distributed computing applications because of its huge bandwidth [34][138]. In WDM optical networks, the bandwidth in optical fiber is partitioned into multiple data channels, in which different messages can be transmitted simultaneously using different wavelengths. In general, an optical WDM network consists of routing nodes interconnected by point-to-point fiber links, which can support a certain number of wavelengths. Each wavelength can carry a separate stream of data. To efficiently utilize the bandwidth

resources and to eliminate the high cost and bottleneck caused by optoelectrical conversion and processing at intermediate nodes, end-to-end lightpaths are usually set up between each pair of source-destination nodes. A *connection* or a *lightpath* in a WDM network is an ordered pair of nodes (x, y) corresponding to transmission of a packet from source x to destination y. Routing and wavelength assignment for the connections are subject to the following two constraints [134]:

1. *Wavelength continuity constraint*: a lightpath must use the same wavelength on all the links along its path from source to destination node.

2. *Distinct wavelength constraint*: all lightpaths using the same link (fiber) must be assigned distinct wavelengths.

If there is no wavelength converter facility available in the network, a connection must use the same wavelength throughout its path. Due to the wavelength-continuity constraint, traditional embedding techniques, which pay attention to the congestion of the embedding, are not sufficient to minimize the number of wavelengths required to realize communication patterns on WDM optical networks. The resulting problem is referred to as *Routing and Wavelength Assignment* (RWA) [134], which is a key problem for increasing the efficiency of wavelength-routed all-optical networks. Given a physical network structure and the required connections, the problem of RWA is to select a suitable path and wavelength among many possible choices for each connection so that no two paths sharing a link are assigned the same wavelength. RWA tries to minimize the number of wavelengths to realize a communication requirement by taking into consideration both routing options and wavelength assignment options. There has been a great deal of research on RWA problem for various communications, such as all-to-all and multicast communications, which has been extensively discussed in Chapter 1.

Hypercube has become one of the most popular communication patterns shared by a large number of computational problems [80]. However, the number of connections for each node is a logarithmic function of the total number of nodes. Therefore, hypercube networks is not a good candidate for very large scale due to the port limitations. Since WDM divides the bandwidth of an optical fiber into multiple wavelength channels, physical topologies for realizing hypercube connections can be significantly simplified

by realizing the connections of hypercube through different channels concurrently on WDM optical networks. As optical technology can provide for parallel computing systems with an enormous amount of bandwidth and low latency, the existing results on hypercube can be incorporated into the optical networks by taking advantages of the parallel transmission characteristic of optical communication. As mentioned in Chapter 1, hypercubes realized on optical networks have attracted a lot of attentions. In [20][120][122], hypercube on WDM partitioned optical passive star networks was studied. In [91], a solution for embedding a virtual unidirectional incomplete hypercube into optical networks was presented. In [132], wavelength assignments for hypercube communications on mesh-like optical networks were studied. However, the results obtained in [132] were based on traditional standard embedding scheme. As mentioned in [132], optimal node numbering (and its RWA) is a much more complex problem. Different from the traditional standard embedding used in [132], we provide the lower bounds of wavelengths irrespective of different node numbering. In addition, those results in [132] are only applicable for realizing bidirectional hypercubes on bidirectional networks.

Due to the lack of bidirectional electrical/optical converters, unidirectional topologies are often used to reduce the hardware cost. We study routing and wavelength assignments for both bidirectional and unidirectional hypercubes on a class of optical WDM networks including linear arrays, rings, meshes and tori with the consideration of communication directions. Moreover, we discuss the above problems for rings and tori with both bidirectional and unidirectional cases. We identify lower bounds on the numbers of wavelengths required for hypercubes on the optical networks, and develop the embedding schemes and wavelength assignment algorithms.

The main differences between our work and that in [132] are summarized as follows.

1. Different with the traditional embedding scheme used in [132], we derive the lower bounds on the number of wavelengths for realizing bidirectional hypercube on WDM optical networks irrespective of embedding schemes.

2. By taking advantage of the freedom of the embedding, we design a simple embedding scheme and wavelength assignment for realizing bidirectional hypercube

on WDM bidirectional rings, which reduce the wavelength requirement in [132].

3. The study in [132] is based on bidirectional hypercube realized on bidirectional networks. As the unidirectional hypercube can save wavelength resource compared to the bidirectional case, we further derive the results for unidirectional hypercubes. Moreover, we discuss the problem on unidirectional rings and tori which can save network resource compared to the bidirectional networks.

3.2 Bidirectional Hypercube and Unidirectional Hypercube

Assume the number of nodes in hypercube communication is $N = 2^n$. Two nodes are connected in hypercube if and only if their binary representations differ by exactly 1 bit. A connection in hypercube is called a *dimensional i connection* [80] if it connects two nodes that differ in the *i*th bit position.

For bidirectional hypercube, two nodes of *x* and *y*, whose binary representations differ by the *i*th bit position, are connected by two dimensional *i* connections of (x, y) and (y, x). We define H_n^b as bidirectional hypercube communications, and $DIM_{n,i}^b$, where $0 \leq i \leq n-1$, as the set of all the corresponding dimensional *i* connections. That is,

$H_n^b = \bigcup_{i=0}^{n-1} DIM_{n,i}^b$, $DIM_{n,i}^b = \{(j, j+2^i), (j+2^i, j) | j \ mod \ 2^{i+1} < 2^i\}$.

For H_n^b, there are $n \times 2^n = N \log N$ connections and 2^n connections in $DIM_{n,i}^b$ for each $i (0 \leq i \leq n-1)$.

Unidirectional hypercube [33] proposed by Chou and Du preserves most of the nice characteristics of conventional hypercubes such as short diameter, short average distance and efficient routing equivalent to bidirectional hypercube. Many studies [72][122] were based on the unidirectional hypercube proposed in [33]. We denote the unidirectional hypercube by H_n^u. For the communication pattern of H_n^u, each connection is assigned a fixed direction. The port of node j for dimensional i connection is assigned a polarity according to the following function [33]:

$P(i,j) = (-1)^{b_{n-1}+b_{n-2}+...+b_1+b_0+i}$,

where $b_{n-1}b_{n-2}\ldots b_1b_0$ is the binary representation of node j in H_n^u. The direction of each dimensional i connection is from positive port to negative port. H_4^u is shown in Figure 3.1.

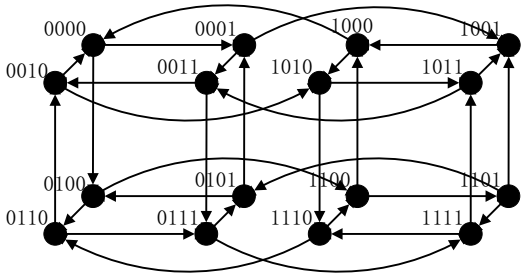

Figure 3.1: 3-D view of unidirectional hypercube ($N = 16$)

H_n^u and the corresponding dimensional *i* connections, denoted by $DIM_{n,i}^u$, are defined as follows,

$H_n^u = \bigcup_{i=0}^{n-1} DIM_{n,i}^u$, $DIM_{n,i}^u = \{(j^+, j^-)|P(i,j^+) = 1, P(i,j^-) = -1, (j^+, j^-) \in DIM_{n,i}^b\}$.

For H_n^u, there are $n \times 2^{n-1} = (N \log N)/2$ connections and 2^{n-1} connections in $DIM_{n,i}^u$ for each $0 \leq i \leq n-1$.

The congestion of embedding hypercube on linear array, denoted by $Cong(H_n, L_n)$, is the minimum over all embedding schemes of the maximum number of hypercube edges that pass any edge of the linear array, which can be obtained by the following lemma [14].

Lemma 6. $Cong(H_n, L_n) = \begin{cases} (2N-2)/3, & \textit{if n is even;} \\ (2N-1)/3, & \textit{if n is odd.} \end{cases}$

3.3 Hypercubes on WDM Linear Arrays

In this section, the WDM linear arrays are referred to bidirectional WDM linear arrays denoted by L_n^b.

3.3.1 Bidirectional Hypercubes on Linear Arrays

3.3.1.1 Lower Bound

In [132], the results were derived based on the traditional embedding scheme which is to embed the ith node of hypercube onto the ith node of the networks. We show that the following lower bound on the number of wavelengths holds irrespective of embedding schemes.

Lemma 7. *The number of wavelengths required to realize bidirectional hypercube communications on bidirectional linear arrays is no less than* $\lfloor 2N/3 \rfloor$. *That is, for* $\forall e$, $\lambda_e(H_n^b, L_n^b) \geq \lfloor 2N/3 \rfloor$.

Proof. According to the definition of congestion, no matter what the embedding scheme is used, there exists such a cut on a bidirectional linear array that partitions the nodes of L_n^b into two sets, S_1 and S_2, such that at least $Cong(H_n, L_n)$ connections in H_n^b originating at nodes in S_1 and terminating at nodes in S_2, and $Cong(H_n, L_n)$ connections in H_n^b originating at nodes in S_2 and terminating at nodes in S_1. Since there is 1 link connecting from S_1 to S_2 and 1 link from S_2 to S_1, each of these 2 links must be used at least $Cong(H_n, L_n)$ times, regardless of the embedding and routing schemes used. By Lemma 1 and Lemma 6, the number of wavelengths required, for $\forall e$, satisfies $\lambda_e(H_n^b, L_n^b) \geq \lfloor 2N/3 \rfloor$. □

3.3.1.2 Wavelength Assignment Algorithm

By Lemma 10, it is easy to see the result for realizing bidirectional hypercube by traditional embedding derived in [132] can achieve the optimal number of wavelengths among all embeddings. Similar with the idea used in [132] on traditional embedding scheme, we provide a proof and wavelength assignment algorithm, which are simpler.

Theorem 14. *The number of wavelengths required to realize bidirectional hypercube communications on bidirectional linear arrays is* $\lfloor 2N/3 \rfloor$.

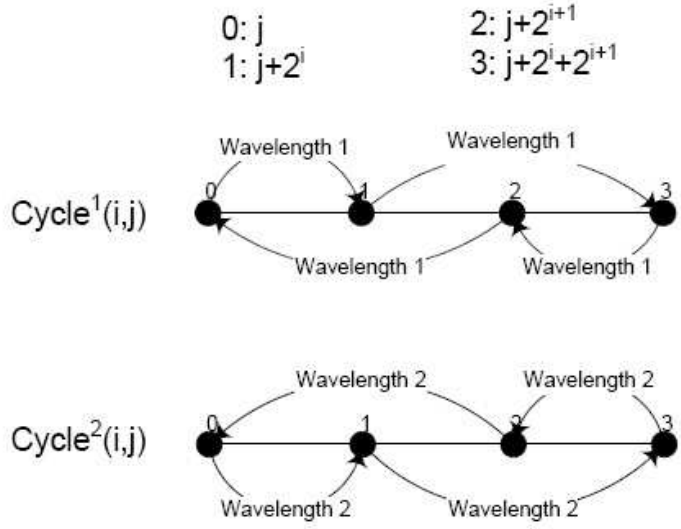

Figure 3.2: $Cycle^1(i,j)$ using wavelength 1 and $Cycle^2(i,j)$ using wavelength 2

Proof. Assume the nodes of L_n^b are numbered from 0 to $N-1$ from left to right. Embed the *i*th node of H_n^b on the *i*th node of L_n^b. Let j, $j+2^i$, $j+2^{i+1}$, $j+2^i+2^{i+1}$ be the four nodes forming a 2-dimensional sub-cube H_2 with eight connections in dimensions i and $i+1$. As illustrated in Figure 3.2, four of the connections $(j, j+2^i), (j+2^i, j+2^i+2^{i+1}), (j+2^i+2^{i+1}, j+2^{i+1})$ and $(j+2^{i+1}, j)$ (forming a clockwise cycle denoted by $Cycle^1(i,j)$) can be realized by one wavelength and the other four connections, $(j, j+2^{i+1}), (j+2^{i+1}, j+2^i+2^{i+1}), (j+2^i+2^{i+1}, j+2^i)$ and $(j+2^i, j)$ denoted by $Cycle^2(i,j)$, in the opposite direction can be realized by another wavelength. For each $i (0 \leq i \leq n-2)$, the connections in $DIM_{n,i}^b \cup DIM_{n,i+1}^b$ are routed on 2^{n-i-2} disjoint subarrays. Since the wavelengths can be reused between subarrays, the total number of wavelengths required to realize the connections in $DIM_{n,i}^b \cup DIM_{n,i+1}^b$ is $(2 \times 2^n/4)/2^{n-i-2} = 2^{i+1}$. For n is even, $\lambda(H_n^b, L_n^b) = \lambda(\bigcup_{i=0}^{n-1} DIM_{n,i}^b, L_n^b) = \lambda(\bigcup_{i=0,2,4,..n-2}(DIM_{n,i}^b \cup DIM_{b,i+1}^b), L_n^b) = 2^1 + 2^3 + 2^5 + \ldots + 2^{n-1} = 2N/3 - 2/3$. For n is odd, $\lambda(H_n^b, L_n^b) = \lambda(\bigcup_{i=0}^{n-1} DIM_{n,i}^b, L_n^b) = \lambda(\bigcup_{i=1,3,5,\ldots,n-2}(DIM_{n,i}^b \cup DIM_{n,i+1}^b), L_n^b) + \lambda(DIM_{n,0}^b, L_n^b) = 2^2 + 2^4 + 2^6 + \ldots + 2^{n-1} + 1 = 2N/3 - 1/3$, since one wavelength is sufficient to realize $DIM_{n,0}^b$.

Therefore, there exists a wavelength assignment algorithm described in *Algorithm* 1, which requires $\lfloor 2N/3 \rfloor$ wavelengths. □

Algorithm 1: $Assign\_H_n^b\_L_n^b$

(1) For $i = n - 2$ downto 0 step 2

(2) for $k = 0$ to $2^{n-i-2} - 1$

(3) for $j = k \cdot 2^{i+2}$ to $k \cdot 2^{i+2} + 2^{i+1}$

(4) assign one wavelength unused to $Cycle^1(i, j)$

(5) assign another one wavelength unused to $Cycle^2(i, j)$

/*assign wavelengths for $DIM_{n,i}^b \cup DIM_{n,i+1}^b$*/

(6) If $i = -1$ /*if n is odd*/

(7) assign one wavelength to $DIM_{n,0}^b$

3.3.2 Unidirectional Hypercubes on Linear Arrays

Figure 3.3 illustrates the 2-D representation for H_4^u showed in Figure 3.1.

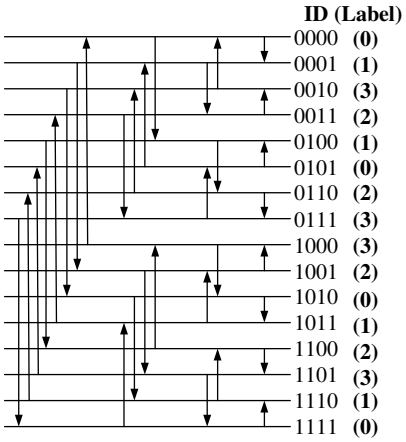

Figure 3.3: 2-D view of unidirectional hypercube ($N = 16$)

3.3.2.1 Lower Bound

Lemma 8. *The number of wavelengths required to realize unidirectional hypercube communications on bidirectional linear arrays is no less than* $\lfloor N/3 \rfloor$ *if* n *is even and* $\lceil N/3 \rceil$ *if* n *is odd. That is, for* $\forall e$, $\lambda_e(H_n^u, L_n^b) \geq \begin{cases} \lfloor N/3 \rfloor, & \text{if n is even;} \\ \lceil N/3 \rceil, & \text{if n is odd.} \end{cases}$

Proof. No matter what the embedding scheme is used, there exists such a cut on a bidirectional linear array that partitions the nodes of L_n^b into two sets, S_1 and S_2, such that at least $Cong(H_n, L_n)$ connections in H_n^u either originating at nodes in S_1 and terminating at nodes in S_2, or originating at nodes in S_2 and terminating at nodes in S_1. Since there is 1 link connecting from S_1 to S_2 and 1 link from S_2 to S_1, one of the 2 links must be used at least $\lceil Cong(H_n, L_n)/2 \rceil$ times, regardless of the embedding and routing schemes used. By Lemma 1 and Lemma 6, the number of wavelengths required, for $\forall e$, satisfies $\lambda_e(H_n^u, L_n^b) \geq \begin{cases} \lfloor N/3 \rfloor & \text{if } n \text{ is even;} \\ \lceil N/3 \rceil & \text{if } n \text{ is odd.} \end{cases}$ □

3.3.2.2 Wavelength Assignment Algorithm

Property 7. *For the connections of $DIM_{n,i}^u \cup DIM_{n,j}^u$ in H_n^u, any nodes are embedded in a cycle of length four if and only if $i + j$ is odd [33].*

Property 8. *For H_n^u, the connections in $DIM_{n,i}^u \cup DIM_{n,i+1}^u$ consist of $N/4$ cycles of length four, for each $0 \leq i \leq n-2$.*

Proof. By Property 7, all the connections in $DIM_{n,i}^u$ and $DIM_{n,i+1}^u$ are embedded in a cycle of length four, since $i+(i+1) = 2i+1$ is always odd. For each $0 \leq j \leq N-1$, if $P(i,j) = 1$, then $P(i, j+2^i) = -1$, $P(i+1, j+2^i) = 1$, $P(i+1, j+2^i+2^{i+1}) = -1$, $P(i, j+2^i+2^{i+1}) = 1$, $P(i, j+2^{i+1}) = -1$, $P(i+1, j+2^{i+1}) = 1$ and $P(i+1, j) = -1$. Thus, connections of $(j, j+2^i), (j+2^i, j+2^i+2^{i+1}), (j+2^i+2^{i+1}, j+2^{i+1})$ and $(j+2^{i+1}, j)$ can form one directed cycle. Similarly, if $P(i,j) = -1, (j, j+2^{i+1}), (j+2^{i+1}, j+2^i+2^{i+1}), (j+2^i+2^{i+1}, j+2^i)$ and $(j+2^i, j)$ can form one cycle. Thus, there are $N/4$ such cycles of length four in $DIM_{n,i}^u \cup DIM_{n,i+1}^u$. □

Theorem 15. *The number of wavelengths required to realize unidirectional hypercube communications on bidirectional linear arrays is $\lfloor N/3 \rfloor$ if* n *is even and $\lceil N/3 \rceil$ if* n *is odd.*

Proof. Embed the *i*th node of H_n^u on the *i*th node of L_n^b. According to Property 8, $DIM_{n,i}^u \cup DIM_{i+1}^u$ consists of $N/4$ cycles. For the four connections of each cycle, two

connections are routed from left to right and the other two are from right to left. In addition, the two connections in the same direction do not share any link of L_n^b. Thus, the same wavelength can be realized to each cycle. For each i, $DIM_{n,i}^u \cup DIM_{n,i+1}^u$ are routed on 2^{n-i-2} disjoint subarrays and the cycles on each subarray with 2^{i+2} nodes do not share any links with the cycles on the other subarray. Therefore, the number of wavelengths required to realize $DIM_{n,i}^u \cup DIM_{n,i+1}^u$ is 2^i. For n is even, $\lambda(H_n^u, L_n^b) = \lambda(\bigcup_{i=0}^{n-1} DIM_{n,i}^u, L_n^b) = \lambda(\bigcup_{i=0,2,4,\ldots,n-2}(DIM_{n,i}^u \cup DIM_{n,i+1}^u), L_n^b) = 2^0+2^2+2^4+\ldots+2^{n-2} = N/3-1/3$. For n is odd, $\lambda(H_n^u, L_n^b) = \lambda(\bigcup_{i=0}^{n-1} DIM_{n,i}^u, L_n^b) = \lambda(\bigcup_{i=1,3,5,\ldots,n-2}(DIM_{n,i}^u \cup DIM_{u,i-1}^u), L_n^b) + \lambda(DIM_{n,0}^u, L_n^b) = 2^1 + 2^3 + 2^5 + \ldots + 2^{n-2} + 1 = N/3 + 1/3$, since one wavelength is sufficient to realize $DIM_{n,0}^u$.

Therefore, there exists a wavelength assignment algorithm described in *Algorithm* 2, which requires $\lfloor N/3 \rfloor$ wavelengths if n is even and $\lceil N/3 \rceil$ if n is odd. □

The wavelength assignment algorithms for bidirectional hypercube communications and unidirectional hypercube communications on linear arrays, which achieve the lower bounds with respect to the number of wavelengths, are optimal by embedding the ith node of hypercube on the ith node of linear arrays.

Algorithm 2: Assignment_H_n^u_L_n^b

(1) For $i = n-2$ downto 0 step 2
(2) for $k = 0$ to $2^{n-i-2}-1$
(3) for $j = k \cdot 2^{i+2}$ to $k \cdot 2^{i+2} + 2^i$
(4) if $P(i,j) = 1$
(5) assign one wavelength unused from λ^1 to $Cycle^1(i,j)$
(6) else
(7) assign one wavelength unused from λ^2 to $Cycle^2(i,j)$
/*assign wavelengths for $DIM_{n,i}^u \cup DIM_{n,i+1}^u$*/
(8) If $i = -1$ /*if n is odd*/
(9) assign one wavelength to $DIM_{n,0}^u$

3.4 Hypercubes on WDM Rings

For bidirectional rings, there are two possible paths for a connection between any two nodes: clockwise or counter-clockwise. We denote the bidirectional ring by R_n^b with N nodes numbered from 0 to $N-1$ clockwise.

For unidirectional ring, the path for a connection between any two nodes is unique. Without loss of generality, we assume the direction of unidirectional ring is clockwise. We denote the unidirectional ring by R_n^u with N nodes numbered from 0 to $N-1$ clockwise.

3.4.1 Bidirectional Hypercubes on Bidirectional Rings

3.4.1.1 Lower Bound

By Lemma 1, the number of wavelengths required to realize H_n^b on R_n^b is no less than the congestion of embedding H_n^b on R_n^b, regardless of which embedding scheme e is used. That is,

Lemma 9. $\lambda_e(H_n^b, R_n^b) \geq Cong(H_n^b, R_n^b)$.

One lower bound for the number of wavelengths required to realize H_n^b on R_n^b is derived in the following lemma.

Lemma 10. *The number of wavelengths required to realize bidirectional hypercube communications on bidirectional rings is no less than* $\lfloor N/3 \rfloor$ *if* n *is even and* $\lceil N/3 \rceil$ *if* n *is odd. That is, for* $\forall e$, $\lambda_e(H_n^b, R_n^b) \geq \begin{cases} \lfloor N/3 \rfloor, & \textit{if n is even;} \\ \lceil N/3 \rceil, & \textit{if n is odd.} \end{cases}$

Proof. Irrespective to what the embedding scheme is used, there exists such a cut on a bidirectional ring that partitions the nodes of R_n^b into two sets, S_1 and S_2, such that at least $Cong(H_n, L_n)$ connections in H_n^b originate at nodes in S_1 and terminate at nodes in S_2. Since there are 2 links connecting from S_1 to S_2, one of these 2 links must be used at least $\lceil Cong(H_n, L_n)/2 \rceil$ times, regardless of the embedding and routing schemes

used. Symmetrically, at least $Cong(H_n, L_n)$ connections in H_n^b originate at nodes in S_2 and terminate at nodes in S_1. Since there are also 2 links connecting from S_2 to S_1, one of these 2 links must be used at least $\lceil Cong(H_n, L_n)/2 \rceil$ times. By Lemma 6 and Lemma 9 , the number of wavelengths required to realize H_n^b on R_n^b, for $\forall e$, satisfies $\lambda_e(H_n^b, R_n^b) \geq Cong(H_n^b, R_n^b) \geq \lceil Cong(H_n, L_n)/2 \rceil = \begin{cases} \lfloor N/3 \rfloor, & \text{if } n \text{ is even;} \\ \lceil N/3 \rceil, & \text{if } n \text{ is odd.} \end{cases}$ □

3.4.1.2 Wavelength Assignment Algorithm

We propose the embedding scheme of H_n^b on R_n^b as follows.

Assume η is a function of one-to-one mapping from the node of H_n^b to the node of R_n^b. Define

$$\eta(i) = \begin{cases} i, \text{if } 0 \leq i \leq N/2 - 1; \\ 3N/2 - 1 - i, \text{if } N/2 \leq i \leq N - 1. \end{cases}$$

In other words, by the embedding η, the nodes of H_n^b from 0 to $N/2 - 1$ are mapped onto the nodes of R_n^b from 0 to $N/2 - 1$ in ascending order one by one, and the nodes of H_n^b from $N/2$ to $N - 1$ onto the nodes of R_n^b from $N - 1$ to $N/2$ in descending order one by one. We assume all the connections are routed by the shortest path.

Theorem 16. *By the embedding scheme of η, the number of wavelengths required to realize bidirectional hypercube communications on bidirectional rings is $\lfloor 5N/12 \rfloor$. That is, $\lambda_\eta(H_n^b, R_n^b) = \lfloor 5N/12 \rfloor$.*

Proof. By embedding scheme of η, connections in $H_n^b - DIM_{n,n-1}^b - DIM_{n,n-2}^b$ embedded on R_n^b can be regarded as four H_{n-2}^b embedded on four bidirectional linear arrays with 2^{n-2} nodes, denoted by $Subarray_i (i = 0, 1, 2, 3)$, as illustrated in Figure 3.4. Since $Subarray_0$, $Subarray_1$, $Subarray_2$ and $Subarray_3$ are disjoint and the connections in each subarray do not share links with the connections in other subarrays by the shortest path, wavelengths can be reused and the same set of wavelengths can be assigned to each subarray. By Theorem 14, the number of wavelengths required for each subarray with 2^{n-2} nodes is $\lfloor N/6 \rfloor$.

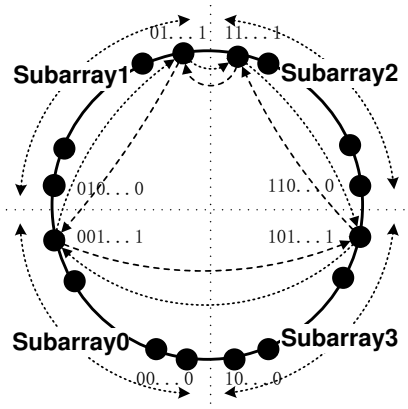

Figure 3.4: H_n^b embedded on R_n^b by embedding scheme of η

For the connections in $DIM_{n,n-1}^b \cup DIM_{n,n-2}^b$, $(i, i+2^{n-2}), (i+2^{n-2}, i+2^{n-2}+2^{n-1}), (i+2^{n-2}+2^{n-1}, i+2^{n-1}), (i+2^{n-1}, i)$ do not share any links on the ring by the shortest path and can be realized using one wavelength λ_i, for each $0 \leq i \leq 2^{n-2}-1$. Since connections of $(i, i+2^{n-1}), (i+2^{n-1}, i+2^{n-2}+2^{n-1}), (i+2^{n-2}+2^{n-1}, i+2^{n-2}), (i+2^{n-2}, i)$ are routed in the opposite direction, the same wavelength λ_i can be assigned to these connections. So, $N/4$ wavelengths are required to realize the connections in $DIM_{n,n-1}^b \cup DIM_{n,n-2}^b$.

Therefore, the number of wavelengths required to realize H_n^b on R_n^b is $\lfloor N/6 \rfloor + N/4 = \lfloor 5N/12 \rfloor$ by the embedding scheme of η using wavelength assignment of *Algorithm* 3. □

By taking advantage of the freedom of the mapping, this result of $\lfloor 5N/12 \rfloor$ can reduce the wavelength requirement $(\lfloor 7N/12 \rfloor)$ in [132]. In addition, it is equal to the conjecture for congestion of hypercube embedded on cycle in [48]. If the conjecture is held, our scheme is optimal.

Algorithm 3: $Assign\_H_n^b\_R_n^b(n > 2)$

(1) For $i = 0, 1, 2, 3$

(2) apply $Assign\_H_{n-2}^b\_L_{n-2}^b(n > 0)$ for $Subarray_i$

/*apply Theorem 14 using the same set of wavelengths for each i*/

(3) For $i = 1$ to 2^{n-2}

(4) assign λ_i to connections of $(i, i + 2^{n-2}), (i + 2^{n-2}, i + 2^{n-2} + 2^{n-1}), (i + 2^{n-2} + 2^{n-1}, i + 2^{n-1}),(i + 2^{n-1}, i)$

(5) assign λ_i to connections of $(i, i+2^{n-1}), (i+2^{n-1}, i+2^{n-2}+2^{n-1}),(i+2^{n-2} + 2^{n-1}, i + 2^{n-2}),(i + 2^{n-2}, i)$

/*assign wavelengths for $DIM_{n,n-1}^b \cup DIM_{n,n-2}^b$*/

The congestion of embedding hypercube on cycle has been studied as the problem of cyclic cutwidth for hypercube [48]. As far as we know, the problem of cyclic cutwidth for hypercube is still an open problem [48][116]. The best lower bound known for the cyclic cutwidth for hypercube, denoted by $ccw(Q_n)$ in [48], is $ccw \geq \frac{1}{2}lcw(Q_n)$. $lcw(Q_n)$ is referred to cutwith of hypercube which is equal to congestion of hypercube on linear array. Although the cyclic cutwidth hypercube has not been discovered, a conjecture, $ccw(Q_n) = \lfloor 5N/12 \rfloor$, has been made in [48]. So far as has been tested, this conjecture has been held [4][21][75]. In [132], the number of wavelengths required is $\lfloor 7N/12 \rfloor$ for realizing H_n^b on R_n^b. Our embedding scheme is very simple, and the wavelength assignment algorithm for H_n^b realized on R_n^b outperforms the previous result in [132]. In addition, the number of wavelengths achieves the lower bound with respect to the conjecture for the cyclic cutwidth of hypercube.

3.4.2 Unidirectional Hypercubes on Bidirectional Rings

3.4.2.1 Lower Bound

Lemma 11. *The number of wavelengths required to realize unidirectional hypercube communications on bidirectional rings is no less than* $\lceil N/6 \rceil$. *That is, for* $\forall e, \lambda_e(H_n^u, R_n^b) \geq \lceil N/6 \rceil$.

Proof. No matter what embedding scheme is used, there exists such a cut on a bidirectional ring that partitions the nodes of R_n^b into two sets, S_1 and S_2, such that at least $Cong(H_n, L_n)$ connections in H_n^u either originating at nodes in S_1 and terminating at nodes in S_2, or originating at nodes in S_2 and terminating at nodes in S_1. Since there are 2 links connecting from S_1 to S_2 and 2 links from S_2 to S_1, one of the 4 links must be used at least $\lceil Cong(H_n, L_n)/4 \rceil$ times, regardless of the embedding and routing schemes used. Therefore, the congestion of embedding H_n^u on R_n^b is no less than $\lceil Cong(H_n, L_n)/4 \rceil$. Using the result of Lemma 6, $Cong(H_n^u, R_n^b) \geq \lceil Cong(H_n, L_n)/4 \rceil = \lceil N/6 \rceil$. By Lemma 1, the number of wavelengths required to realize H_n^u on R_n^b, for $\forall e$, satisfies $\lambda_e(H_n^u, R_n^b) \geq Cong(H_n^u, R_n^b) \geq \lceil N/6 \rceil$. □

3.4.2.2 Wavelength Assignment Algorithm

Theorem 17. *By the embedding scheme of η, the number of wavelengths required to realize unidirectional hypercube communications on bidirectional rings is $\lfloor 5N/24 \rfloor$ if n is even and $\lceil 5N/24 \rceil$ if n is odd.*

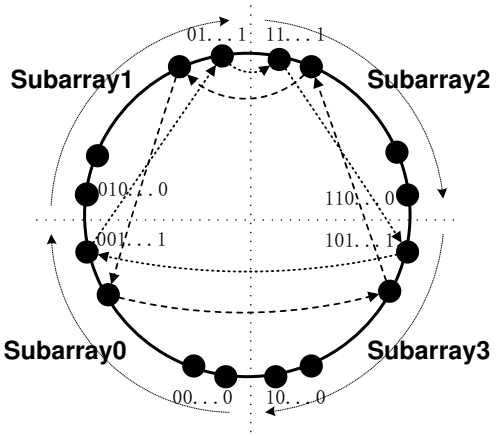

Figure 3.5: H_n^u embedded on R_n^b by η

Proof. Similar with the proof of Theorem 16, connections in $H_n^u - DIM_{n,n-1}^u - DIM_{n,n-2}^u$ embedded on R_n^b by embedding scheme η can be regarded as four H_{n-2}^u embedded on four bidirectional linear arrays of 2^{n-2} nodes, denoted by $Subarray_i (i =$

$0, 1, 2, 3)$, as illustrated in Figure 3.5. By Theorem 15, the number of wavelengths required for each subarray is $\lfloor N/12 \rfloor$ if n is even and $\lceil N/12 \rceil$ if n is odd.

By Property 8, all the connections in $DIM^u_{n,n-1} \cup DIM^u_{n,n-2}$ form $N/4$ cycles of length four. If $P(n-2, j) = 1$, connections of $(j, j+2^{n-2}), (j+2^{n-2}, j+2^{n-2}+2^{n-1}), (j+2^{n-2}+2^{n-1}, j+2^{n-1}), (j+2^{n-1}, j)$ do not share any links on R^b_n by the embedding scheme of η and can be realized clockwise using one wavelength. If $P(n-2, j) = -1$, connections of $(j, j+2^{n-1}), (j+2^{n-1}, j+2^{n-2}+2^{n-1}), (j+2^{n-2}+2^{n-1}, j+2^{n-2}), (j+2^{n-2}, j)$ can be realized counter-clockwise using one wavelength. It can be examined that $N/8$ cycles are routed clockwise and $N/8$ cycles are routed counter-clockwise. Thus, $N/8$ wavelengths are sufficient to realize the connections in $DIM^u_{n,n-1} \cup DIM^u_{n,n-2}$.

Therefore, the number of wavelengths required by embedding scheme η to realize H^u_n on R^b_n is $\lfloor N/12 \rfloor + N/8 = \lfloor 5N/24 \rfloor$ if n is even and $\lceil N/12 \rceil + N/8 = \lceil 5N/24 \rceil$ if n is odd. □

Assume $Cycle^1(i, j) = \{(j, j+2^i), (j+2^i, j+2^i+2^{i+1}), (j+2^i+2^{i+1}, j+2^i), (j+2^i, j)\}$ and $Cycle^2(i, j) = \{(j, j+2^{i+1}), (j+2^{i+1}, j+2^i+2^{i+1}), (j+2^i+2^{i+1}, j+2^i), (j+2^i, j)\}$. Thus, $Cycle^1(n-2, j)$ is the set of connections in $DIM^u_{n,n-1} \cup DIM^u_{n,n-2}$ routing clockwise and $Cycle^2(n-2, j)$ is that routing counter-clockwise. Let $\lambda^1 = \lambda^2$ be sets of wavelengths. We describe the wavelength assignment algorithm of H^u_n on R^b_n in the following *Algorithm 4*.

Algorithm 4: $Assign\_H^u_n\_R^b_n(n > 2)$

(1) For $i = 0, 1, 2, 3$

(2) apply $Assign\_H^u_{n-2}\_L^b_{n-2}(n > 0)$ for $Subarray_i$

/*apply Theorem 15 using the same set of wavelengths for each i*/

(3) For $j = 1$ to 2^{n-2}

(4) if $P(n-2, j) = 1$

(5) assign one wavelength unused from λ^1 to $Cycle^1(n-2, j)$

(6) else

(7) assign one wavelength unused from λ^2 to $Cycle^2(n-2, j)$

/*assign wavelengths for $DIM^u_{n,n-1} \cup DIM^u_{n,n-2}$*/

3.4.3 Bidirectional Hypercubes on Unidirectional Rings

3.4.3.1 Lower Bound

Lemma 12. *The number of wavelengths required to realize bidirectional hypercube communications on unidirectional rings is no less than* $(N \log N)/2$. *That is,* $\lambda_e(H^b_n, R^u_n) \geq (N \log N)/2$.

Proof. For the bidirectional hypercube communications, if $(x, y) \in H^b_n$, then $(y, x) \in H^b_n$. Since the routing for each connection is unique in a unidirectional ring, each link on R^u_n must be passed through either by (x, y) or by (y, x) at least once. In all, there are $n \times 2^{n-1}$ such connection pairs for H^b_n. No matter what embedding scheme is used to embed the node of H^b_n on R^u_n, each link on R^u_n must be passed through by at least $(N \log N)/2$ connections of H^b_n. So, the congestion in this case is no less than $(N \log N)/2$. By Lemma 1, $\lambda_e(H^b_n, R^u_n) \geq Cong(H^b_n, R^u_n) \geq (N \log N)/2$. □

3.4.3.2 Wavelength Assignment Algorithm

Theorem 18. *The number of wavelengths required to realize bidirectional hypercube communications on unidirectional rings is* $(N \log N)/2$.

Proof. If connection (x, y) is routed in the opposite direction with (y, x) along the ring, these two connections do not share any links and one wavelength can be assigned to

(x, y) and (y, x). Since there are $(N \log N)/2$ such connection pairs in H_n^b, $(N \log N)/2$ wavelengths are sufficient for R_n^u to realize H_n^b. □

Therefore, the necessary and sufficient number of wavelengths for R_n^u to realize H_n^b is $(N \log N)/2$. The wavelength assignment algorithm is described in *Algorithm* 5.

Algorithm 5: $Assign\_H_n^b\_R_n^u (n > 2)$

(1) For $i = 1$ to n
(2) for $j = 0$ to $2^n - 1$
(3) if j *mod* $2^{i+1} < 2^i$
(4) assign wavelength λ_{ij} to $(j, j + 2^i), (j + 2^i, j)$

3.4.4 Unidirectional Hypercubes on Unidirectional Rings

3.4.4.1 Lower Bound

Lemma 13. *The number of wavelengths required to realize unidirectional hypercube communications on unidirectional rings is no less than* $\lfloor \log N/2 \rfloor \times N/4$.

Proof. Since the routing for each connection is unique in R_n^u, each link must be passed through by each cycle at least once. By Property 8, if n is even, $DIM_{n,0}^u \cup DIM_{n,1}^u$, $DIM_{n,2}^u \cup DIM_{n,3}^u$, ... , $DIM_{n,n-2}^u \cup DIM_{n,n-1}^u$ form $\log N/2 \times N/4$ cycles. If n is odd, $DIM_{n,0}^u \cup DIM_{n,1}^u$, $DIM_{n,2}^u \cup DIM_{n,3}^u$,..., $DIM_{n,n-3}^u \cup DIM_{n,n-2}^u$ form $(\log N - 1)/2 \times N/4$ cycles. No matter what embedding scheme is used to embed H_n^u on R_n^u, each link on R_n^u must be passed through by the connections of H_n^u at least $\lfloor \log N/2 \rfloor \times N/4$ times. Thus, $Cong(H_n^u, R_n^u) \geq \lfloor \log N/2 \rfloor \times N/4$. By Lemma 1, for $\forall e$, $\lambda_e(H_n^u, R_n^u) \geq Cong(H_n^u, R_n^u) \geq \lfloor \log N/2 \rfloor \times N/4$. □

3.4.4.2 Wavelength Assignment Algorithm

We design the embedding scheme θ for H_n^u embedded on R_n^u as follows.

Give a label to each node of H_n^u by the following method. Assume the label of node u is l, where $0 \leq l \leq 3$. If a connection is from u to v, then the label for v is $(l + 1)$

mod 4. If the connection is from v to u, then the label for v is $(l-1)$ mod 4. Give label 0 to node 0 initially. It can be proven that each node of H_n^u has a unique label by this method and $N/4$ nodes are assigned to the same label. The label of each node for H_4^u is showed on Figure 3.6.

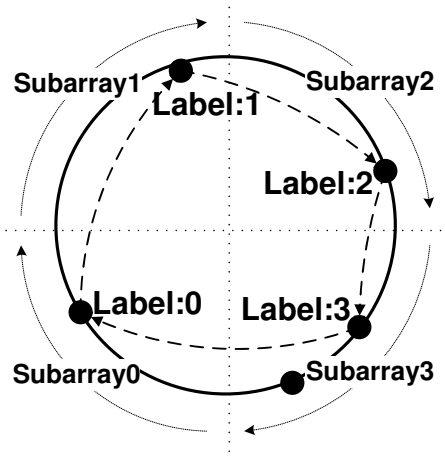

Figure 3.6: Routing of cycle in H_n^u by θ on R_n^u

The embedding scheme for H_n^u embedded on R_n^u is defined as follows. Divide R_n^u into 4 subarrays, denoted by $Subarray_0$, $Subarray_1$, $Subarray_2$ and $Subarray_3$ clockwise, with $N/4$ nodes on each subarray. Embed the $N/4$ nodes with label l onto $Subarray_l$ regardless of what order of these nodes on the subarray. We denote this embedding scheme by θ, which ensures the communication distance of all connections is less than the diameter of the ring.

Theorem 19. *By the embedding scheme θ, the number of wavelengths required to realize unidirectional hypercube communications on unidirectional rings is $\lceil \frac{\log N}{2} \rceil \times N/4$.*

Proof. According to the definition of θ, all the connections are routed from the nodes in $Subarray_l$ to $Subarray_{(l+1)mod4}$. The 4 connections of each cycle are routed along the four nodes labeled by the order of $0, 1, 2, 3$ clockwise. Thus, each of these 4 connections in one cycle does not share links with the other 3 connections as illustrated in Figure 3.6. Therefore, one wavelength can be assigned to the 4 connections in one cycle. If n is even, $N \log N/8$ wavelengths are sufficient to realize the $N \log N/8$ cycles formed by $DIM_{n,0}^u \cup DIM_{n,1}^u$, $DIM_{n,2}^u \cup DIM_{n,3}^u$, ... , $DIM_{n,n-2}^u \cup DIM_{n,n-1}^u$. If n is odd,

$(N-1)\log N/8$ wavelengths are sufficient to realize the $(N-1)\log N/8$ cycles formed by $DIM^u_{n,0} \cup DIM^u_{n,1}$, $DIM^u_{n,2} \cup DIM^u_{n,3}$,..., $DIM^u_{n,n-3} \cup DIM^u_{n,n-2}$. For the connections in $DIM^u_{n,n-1}$, it can be examined that $N/4$ connections are routed from nodes in $Subarray_0$ to $Subarray_1$ and $N/4$ connections are from $Subarray_2$ to $Subarray_3$. Since these two groups of connections do not share any links of the ring with each other, $N/4$ wavelengths are sufficient to realize these connections. So, $NlogN/8 + N/4$ and $(N-1)\log N/8 + N/4$ wavelengths are sufficient to realize H^u_n on R^u_n if n is even and odd respectively.

Therefore, by the embedding scheme θ, the number of wavelengths required to realize H^u_n on R^u_n is $\lceil \frac{\log N}{2} \rceil \times N/4$ using wavelength assignment of *Algorithm 6*. □

Algorithm 6: $Assign\_H^u_n\_R^u_n(n > 2)$

(1) For $i = 0$ to $n-2$, step 2
(2) for $j = 0$ to 2^{n-2}
(3) if $P(i,j) = 1$
(4) assign one wavelength unused from λ^1 to $Cycle^1(i,j)$
(5) else
(6) assign one wavelength unused from λ^2 to $Cycle^2(i,j)$
(7) If $i = n-1$ /*if n is odd*/
(8) for $j = 0$ to 2^{n-1}
(9) if $P(n-1,j) = 1$
(10) assign one wavelength unused from λ^1 to $(j, j+2^{n-1})$
(11) else
(12) assign one wavelength unused from λ^2 to $(j+2^{n-1}, j)$

3.5 Hypercubes on WDM Meshes and Tori

For 2-dimensional meshes or tori with $N = 2^n$ nodes, each row and column must contain a power of two number of nodes. Because hypercube communications can not be realized on unidirectional meshes, we only consider bidirectional meshes in this chap-

ter. We will discuss tori in two cases, since hypercube communications can be realized on both bidirectional tori and unidirectional tori. We denote the 2-dimensional meshes, 2-dimensional bidirectional tori and 2-dimensional unidirectional tori with $N = 2^m \times 2^{n-m}$ nodes by $M^b_{m,n-m}$, $T^b_{m,n-m}$ and $T^u_{m,n-m}$ respectively.

More generally, we denote r-dimensional meshes, r-dimensional bidirectional tori and r-dimensional unidirectional tori with $2^{n_1} \times 2^{n_2} \times ... \times 2^{n_r}$ nodes by $M^b_{n_1,n_2,...,n_r}$, $T^b_{n_1,n_2,...,n_r}$ and $T^u_{n_1,n_2,...,n_r}$ respectively, where $r \geq 2, n_1 + n_2 + \ldots + n_r = n$ and $n_1 \leq n_2 \leq \ldots \leq n_r$.

3.5.1 Bidirectional Hypercubes on WDM Meshes

3.5.1.1 Lower Bound

Lemma 14. $Cong(H^b_n, M^b_{n_1,n_2,...,n_r}) = Cong(H^b_{n_r}, L^b_{n_r})$*[14].*

Lemma 15. *The number of wavelengths required to realize bidirectional hypercube communications on* $2^{n_1} \times 2^{n_2} \times \ldots \times 2^{n_r}$ *meshes is no less than* $\lfloor 2^{n_r+1}/3 \rfloor$.

Proof. By Lemma 6 and Lemma 14, the number of wavelengths required to realize H^b_n on $M^b_{n_1,n_2,...,n_r}$, for $\forall e$, satisfies $\lambda_e(H^b_n, M^b_{n_1,n_2,...,n_r}) \geq Cong(H^b_n, M^b_{n_1,n_2,...,n_r}) = Cong(H^b_{n_r}, L^b_{n_r}) \geq \lfloor 2^{n_r+1}/3 \rfloor$. □

3.5.1.2 Wavelength Assignment

Assume the node of $M^b_{m,n-m}$ on the Pth row and Qth column is identified by (P, Q), where $0 \leq P \leq 2^m - 1$ and $0 \leq Q \leq 2^{n-m} - 1$. For $0 \leq j \leq 2^n - 1$, let $x = j/2^{n-m}$ and $y = j \bmod 2^{n-m}$. Embed the jth node of H^b_n onto node (x, y) of $M^b_{m,n-m}$. Thus, the number of wavelengths required for realizing H^b_n on $M^b_{m,n-m}$ can be obtained by the following theorem.

Theorem 20. *The number of wavelengths required to realize bidirectional hypercube communications on* $2^m \times 2^{n-m}$ *bidirectional meshes is* $\lfloor 2^{\max(m,n-m)+1}/3 \rfloor$.

Proof. As the connections in $\bigcup_{i=0}^{n-m-1} DIM_i^b$ only take place within the nodes on each row by the shortest path, and the connections in $\bigcup_{i=n-m}^{n-1} DIM_i^b$ only take place within the nodes on each column, realizing H_n^b on $M_{m,n-m}^b$ is to realize H_{n-m}^b on L_{n-m}^b in each row and H_m^b on L_m^b in each column, which requires $\lfloor 2^{n-m+1}/3 \rfloor$ wavelengths for each row and $\lfloor 2^{m+1}/3 \rfloor$ for each column respectively by Theorem 14. So the theorem holds. □

Wavelength assignment algorithm of H_n^b on $M_{m,n-m}^b$ is described in *Algorithm 7*.

Algorithm 7: $Assign\_H_n^b\_M_{m,n-m}^b$

(1) For $i = 0$ to 2^{m-1}

(2) apply $Assign\_H_{n-m}^b\_L_{n-m}^b$ for row_i

(3) For $j = 0$ to 2^{n-m-1}

(4) apply $Assign\_H_m^b\_L_m^b$ for $column_j$

We assign the identification of $(x_1, x_2, \ldots, x_r)$ to each node of $M_{n_1,n_2,\ldots,n_r}^b$, where $0 \leq x_1 \leq 2^{n_1}, 0 \leq x_2 \leq 2^{n_2}, \ldots, 0 \leq x_r \leq 2^{n_r}$. Embed the jth node of H_n^b on the node $(x_1, x_2, \ldots, x_r)$ of $M_{n_1,n_2,\ldots,n_r}^b$, where $x_i = (j \bmod 2^{\Sigma_{k=i}^r n_k})/2^{\Sigma_{k=i+1}^r n_k}$ and $1 \leq i \leq r$. Thus, the number of wavelengths required for realizing H_n^b on $M_{n_1,n_2,\ldots,n_r}^b$ can be obtained by the following theorem.

Theorem 21. *The number of wavelengths required to realize bidirectional hypercube communications on* $2^{n_1} \times 2^{n_2} \times \ldots \times 2^{n_r}$ *bidirectional meshes is* $\lfloor 2^{n_r+1}/3 \rfloor$.

Proof. For $1 \leq i \leq r$, as the connections in $\bigcup_{j=\Sigma_{k=1}^{i-1} n_k - 1}^{\Sigma_{k=1}^{i} n_k - 1} DIM_j^b$ only take place within the nodes on the ith dimension of $M_{n_1,n_2,\ldots,n_r}^b$ by the shortest path, realizing H_n^b on $M_{n_1,n_2,\ldots,n_r}^b$ is to realize $H_{n_i}^b$ on $L_{n_i}^b$ on the ith dimension of $M_{n_1,n_2,\ldots,n_r}^b$, which requires $\lfloor 2^{n_i+1}/3 \rfloor$ wavelengths for the ith dimension of $M_{n_1,n_2,\ldots,n_r}^b$ by Theorem 14. The theorem holds because $n_1 \leq n_2 \leq \ldots \leq n_r$. □

Wavelength assignment algorithm of H_n^b on $M_{n_1,n_2,\ldots,n_r}^b$ is described in *Algorithm 8*.

Algorithm 8: $Assign\_H^b_n\_M^b_{n_1,n_2,\ldots,n_r}$

(1) For $i_1 = 0$ to 2^{n-n_1-1}

(2) apply $Assign\_H^b_{n_1}\_L^b_{n_1}$ for Dim_1

(3) For $i_2 = 0$ to 2^{n-n_2-1}

(4) apply $Assign\_H^b_{n_2}\_L^b_{n_2}$ for Dim_2

$\vdots$ $\vdots$

$(2n_r - 1)$ For $i_r = 0$ to 2^{n-n_r-1}

$(2n_r)$ apply Assignment$_H^b_{n_r}_L^b_{n_r}$ for Dim_r

For the case of $n_1 = n_2 ... = n_r = n/r$, the result can be obtained as follows.

Corollary 14. *The number of wavelengths required to realize bidirectional hypercube communications on* $2^{n/r} \times 2^{n/r} \times \ldots \times 2^{n/r}$ *bidirectional meshes is* $\lfloor 2\sqrt[r]{2^n}/3 \rfloor$.

3.5.2 Unidirectional Hypercubes on WDM Meshes

3.5.2.1 Lower Bound

Lemma 16. *The number of wavelengths required to realize unidirectional hypercube communications on* $2^{n_1} \times 2^{n_2} \ldots \times 2^{n_r}$ *meshes is no less than* $\lfloor 2^{n_r}/3 \rfloor$ *if* n_r *is even and* $\lceil 2^{n_r}/3 \rceil$ *if* n_r *is odd.*

Proof. No matter what embedding scheme is used, there exists such a link (x, y) on a bidirectional mesh, such that at least $Cong(H^b_n, M^b_{n_1,n_2,\ldots,n_r})$ connections in H^u_n either passing through in the direction from x to y, or in the direction from y to x. Regardless of which embedding and routing scheme is used, the congestion of embedding H^u_n on $M^b_{n_1,n_2,\ldots,n_r}$ is no less than $\lceil Cong(H^b_n, M^b_{n_1,n_2,\ldots,n_r})/2 \rceil$. By Lemma 6 and Lemma 14, the number of wavelengths required to realize H^u_n on $M^b_{n_1,n_2,\ldots,n_r}$, for $\forall e$, satisfies $\lambda_e(H^u_n, M^b_{n_1,n_2,\ldots,n_r}) \geq Cong(H^u_n, M^b_{n_1,n_2,\ldots,n_r}) \geq \lceil Cong(H^b_n, M^b_{n_1,n_2,\ldots,n_r})/2 \rceil =$ $\lceil Cong(H^b_{n_r}, L^b_{n_r})/2 \rceil \geq \begin{cases} \lfloor 2^{n_r}/3 \rfloor & \text{if } n \text{ is even;} \\ \lceil 2^{n_r}/3 \rceil & \text{if } n \text{ is odd.} \end{cases}$ □

3.5.2.2 Wavelength Assignment

By the same embedding scheme mentioned in the bidirectional case, the results can be obtained as follows.

Theorem 22. *The number of wavelengths required to realize unidirectional hypercube communications on* $2^m \times 2^{n-m}$ *bidirectional meshes is* $\lfloor 2^{\max(m,n-m)}/3 \rfloor$ *if* $\max(m, n-m)$ *is even and* $\lceil 2^{\max(m,n-m)}/3 \rceil$ *if* $\max(m, n-m)$ *is odd.*

Proof. Similar with the proof of Theorem 7, realizing H_n^u on $M_{m,n-m}^b$ is to realize H_{n-m}^u on L_{n-m}^b in each row and H_m^u on L_m^b in each column. By Theorem 15, the number of wavelengths on each row is $\lfloor 2^{n-m}/3 \rfloor$ if $n-m$ is even and $\lceil 2^{n-m}/3 \rceil$ if $n-m$ is odd, and the number of wavelengths on each column is $\lfloor 2^m/3 \rfloor$ if m is even and $\lceil 2^m/3 \rceil$ if m is odd. So the theorem holds. □

Same as the bidirectional case, the above theorem can be easily extended to r-dimensional meshes as follows.

Theorem 23. *The number of wavelengths required to realize unidirectional hypercube communications on* $2^{n_1} \times 2^{n_2} \ldots \times 2^{n_r}$ *bidirectional meshes is* $\lfloor 2^{n_r}/3 \rfloor$ *if* n_r *is even and* $\lceil 2^{n_r}/3 \rceil$ *if* n_r *is odd.*

Corollary 15. *The number of wavelengths required to realize unidirectional hypercube communications on* $2^{n/r} \times 2^{n/r} \times \ldots \times 2^{n/r}$ *bidirectional meshes is* $\lfloor \sqrt[r]{2^n}/3 \rfloor$ *if* n/r *is even and* $\lceil \sqrt[r]{2^n}/3 \rceil$ *if* n/r *is odd.*

3.5.3 Bidirectional Hypercubes on WDM Bidirectional Tori

Since a torus can be considered as a mesh with wraparound links, each dimension of a torus has the similar property with a ring. Same with the way of proving the results for the meshes, the results for realizing H_n^b on tori can be easily obtained as follows by applying the previous results obtained in Section 3.4.

Lemma 17. *The number of wavelengths required to realize bidirectional hypercube communications on* $2^{n_1} \times 2^{n_2} \times ... \times 2^{n_r}$ *bidirectional tori is no less than* $\lfloor 2^{n_r}/3 \rfloor$ *if* n_r *is even and* $\lceil 2^{n_r}/3 \rceil$ *if* n_r *is odd.*

The one-to-one embedding scheme η for H_n^b on $T_{m,n-m}^b$ can be described as follows. Let $x = j/2^{n-m}$ and $y = j \bmod 2^{n-m}$, where $0 \leq x \leq 2^m - 1$ and $0 \leq y \leq 2^{n-m} - 1$. Map the jth node of H_n^b on node (x, y) of $T_{m,n-m}^b$ if $0 \leq x \leq 2^{m-1} - 1$ and $0 \leq y \leq 2^{n-m-1} - 1$, on node $(x, 3 \times 2^{n-m} - 1 - y)$ if $0 \leq x \leq 2^{m-1} - 1$ and $2^{n-m-1} \leq y \leq 2^{n-m} - 1$, on node $(3 \times 2^m - 1 - x, y)$ if $2^{m-1} \leq x \leq 2^m - 1$ and $0 \leq y \leq 2^{n-m-1} - 1$, and on node $(3 \times 2^m - 1 - x, 3 \times 2^{n-m} - 1 - y)$ if $2^{m-1} \leq x \leq 2^m - 1$ and $2^{n-m-1} \leq y \leq 2^{n-m} - 1$. By this embedding scheme, the following result can be obtained.

Theorem 24. *The number of wavelengths required to realize bidirectional hypercube communications on* $2^m \times 2^{n-m}$ *bidirectional tori is* $\lfloor 5 \times 2^{\max(m,n-m)}/12 \rfloor$.

Proof. Realizing H_n^b on $T_{m,n-m}^b$ can be regarded as realizing H_{n-m}^b on R_{n-m}^b in each row and H_m^b on R_m^b in each column. By Theorem 16, the numbers of wavelengths on each row and column are $\lfloor 5 \times 2^{n-m}/12 \rfloor$ and $\lfloor 5 \times 2^m/12 \rfloor$ respectively. So the theorem holds. □

The above theorem can be easily extended to r-dimensional bidirectional tori as follows.

Theorem 25. *The number of wavelengths required to realize bidirectional hypercube communications on* $2^{n_1} \times 2^{n_2} \times ... \times 2^{n_r}$ *bidirectional tori is* $\lfloor 5 \times 2^{n_r}/12 \rfloor$.

Corollary 16. *The number of wavelengths required to realize bidirectional hypercube communications on* $2^{n/r} \times 2^{n/r} \times \ldots \times 2^{n/r}$ *bidirectional tori is* $\lfloor 5\sqrt[r]{2^n}/12 \rfloor$.

For the following cases, the results can be easily obtained by the way similar with the previous results, the proofs are omitted for the sake of simplicity.

3.5.4 Unidirectional Hypercubes on WDM Bidirectional Tori

Lemma 18. *The number of wavelengths required to realize unidirectional hypercube communications on* $2^{n_1} \times 2^{n_2} \times ... \times 2^{n_r}$ *bidirectional tori is no less than* $\lceil 2^{n_r}/6 \rceil$.

Theorem 26. *The number of wavelengths required to realize unidirectional hypercube communications on* $2^m \times 2^{n-m}$ *bidirectional tori is* $\lfloor 5 \times 2^{\max(m,n-m)}/24 \rfloor$ *if* $\max(m, n-m)$ *is even,* $\lceil 5 \times 2^{\max(m,n-m)}/24 \rceil$ *if* $\max(m, n-m)$ *is odd.*

Theorem 27. *The number of wavelengths required to realize unidirectional hypercube communications on* $2^{n_1} \times 2^{n_2} \times ... \times 2^{n_r}$ *bidirectional tori is* $\lfloor 5 \times 2^{n_r}/24 \rfloor$ *if* n_r *is even and* $\lceil 5 \times 2^{n_r}/24 \rceil$ *if* n_r *is odd.*

Corollary 17. *The number of wavelengths required to realize unidirectional hypercube communications on* $2^{n/r} \times 2^{n/r} \times \ldots \times 2^{n/r}$ *bidirectional tori is* $\lfloor 5\sqrt[r]{2^n}/24 \rfloor$ *if* n *is even and* $\lceil 5\sqrt[r]{2^n}/24 \rceil$ *if* n *is odd.*

3.5.5 Bidirectional Hypercubes on WDM Unidirectional Tori

Lemma 19. *The number of wavelengths required to realize bidirectional hypercube communications on* $2^{n_1} \times 2^{n_2} \times ... \times 2^{n_r}$ *unidirectional tori is no less than* $n_r \times 2^{n_r-1}$.

Theorem 28. *The number of wavelengths required to realize bidirectional hypercube communications on* $2^m \times 2^{n-m}$ *unidirectional tori is* $\max(m, n-m) \times 2^{\max(m,n-m)-1}$.

Theorem 29. *The number of wavelengths required to realize unidirectional hypercube communications on* $2^{n_1} \times 2^{n_2} \ldots \times 2^{n_r}$ *unidirectional tori is* $n_r \times 2^{n_r-1}$.

Corollary 18. *The number of wavelengths required to realize bidirectional hypercube communications on* $2^{n/r} \times 2^{n/r} \times \ldots \times 2^{n/r}$ *unidirectional tori is* $n\sqrt[r]{2^n}/2r$.

3.5.6 Unidirectional Hypercubes on WDM Unidirectional Tori

Lemma 20. *The number of wavelengths required to realize unidirectional hypercube communications on* $2^{n_1} \times 2^{n_2} \times ... \times 2^{n_r}$ *unidirectional tori is no less than* $\lfloor n_r/2 \rfloor \times 2^{n_r-2}$.

Theorem 30. *The number of wavelengths required to realize unidirectional hypercube communications on* $2^m \times 2^{n-m}$ *unidirectional tori is* $\lceil \max(m, n-m)/2 \rceil \times 2^{\max(m,n-m)-2}$.

Theorem 31. *The number of wavelengths required to realize unidirectional hypercube communications on* $2^{n_1} \times 2^{n_2} \times ... \times 2^{n_r}$ *unidirectional tori is* $\lceil n_r/2 \rceil \times 2^{n_r-2}$.

Corollary 19. *The number of wavelengths required to realize unidirectional hypercube communications on* $2^{n/r} \times 2^{n/r} \times \ldots \times 2^{n/r}$ *unidirectional tori is* $\lceil n/2r \rceil \times \sqrt[r]{2^n}/4$.

3.6 Comparisons

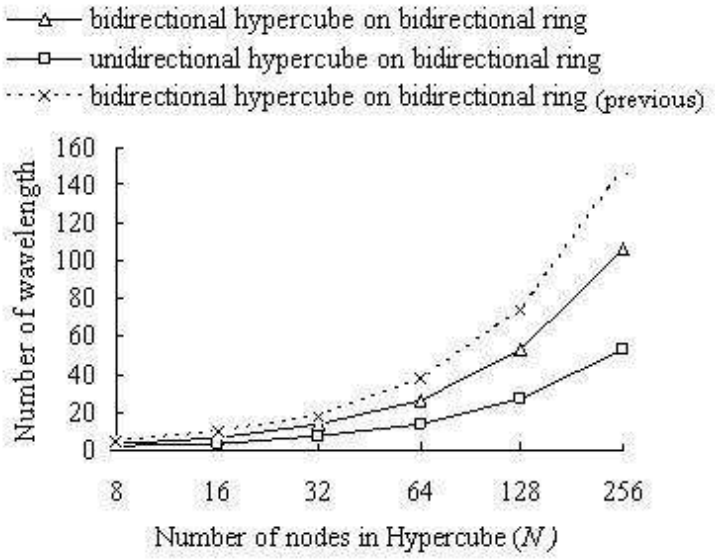

Figure 3.7: Wavelength requirement for H_n^b and H_n^u on R_n^b

Figure 3.7 shows the wavelength requirement for bidirectional hypercubes and unidirectional hypercubes on bidirectional rings when $3 \leq n \leq 8$. As can be seen, our result for bidirectional hypercubes on bidirectional rings outperforms the previous result in [132]. Since the number of connections in bidirectional hypercube is twice of that in unidirectional case, the number of wavelengths required for unidirectional hypercube realized on WDM rings is about half of that for bidirectional case.

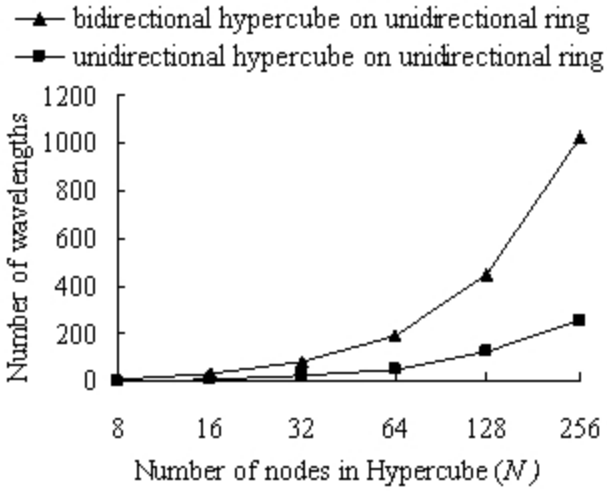

Figure 3.8: Wavelength requirement for H_n^b and H_n^u on R_n^u

Figure 3.8 shows the wavelength requirement for bidirectional hypercubes and unidirectional hypercubes on unidirectional rings when $3 \leq n \leq 8$. The number of wavelengths required for unidirectional hypercube realized on unidirectional rings is about one-fourth of that for bidirectional case.

From Figure 3.7 and Figure 3.8, we can see that the numbers of wavelengths required for hypercubes on optical bidirectional rings are less than those on optical unidirectional rings. However, the bidirectional optical networks require much higher hardware cost than the corresponding unidirectional case.

3.7 Conclusion

In this chapter, we discussed routing and wavelength assignment of bidirectional and unidirectional hypercube communications on a class of WDM optical networks including linear arrays, rings, meshes and tori. For each type of optical networks, we identified a lower bound on the number of wavelengths required, and designed an embedding scheme and wavelength assignment algorithm which uses a provably near-optimal number of wavelengths. In addition, our results for bidirectional hypercube realized on bidirectional rings and meshes improved the known results in [132]. Our results are listed in Table 3.1.

	H_n^b	H_n^u
L_n^b	$\lfloor 2N/3 \rfloor$	$\lfloor N/3 \rfloor$ ($\log N$ is even), $\lceil N/3 \rceil$ ($\log N$ is odd)
R_n^b	$\lfloor 5N/12 \rfloor$	$\lfloor 5N/24 \rfloor$ ($\log N$ is even), $\lceil 5N/24 \rceil$ ($\log N$ is odd)
R_n^u	$(NlogN)/2$	$\lceil logN/2 \rceil \times N/4$
$M_{n_1,n_2,...,n_r}^b$	$\lfloor 2^{n_r+1}/3 \rfloor$	$\lfloor 2^{n_r}/3 \rfloor$ (n_r is even), $\lceil 2^{n_r}/3 \rceil$ (n_r is odd)
$T_{n_1,n_2,...,n_r}^b$	$\lfloor 5 \times 2^{n_r}/12 \rfloor$	$\lfloor 5 \times 2^{n_r}/24 \rfloor$ (n_r is even), $\lceil 5 \times 2^{n_r}/24 \rceil$ (n_r is odd)
$T_{n_1,n_2,...,n_r}^u$	$n_r \times 2^{n_r-1}$	$\lceil n_r/2 \rceil \times 2^{n_r-2}$

Table 3.1: Numbers of wavelengths for directional hypercubes on optical WDM networks

Recently, laboratory experiments have achieved 1000 channels per fiber (NTT Network Innovation Laboratories, NTT Photonics Laboratories). With the results of our work, realizing the 1024-node bidirectional hypercube communication on linear array, bidirectional ring, 32×32 mesh, 32×32 bidirectional tori and 32×32 unidirectional tori requires 682, 426, 21, 13 and 80 wavelengths respectively, and realizing 1024-node unidirectional hypercube communication requires 341, 213, 10, 6 and 24 wavelengths respectively. Considering the number of processors and the capacity of the fiber links in practice, we can select the proper WDM networks to realize hypercube communications according to our results.

Since hypercube communication represents a common communication pattern shared by a large number of computational problems, our results have both theoretical and practical significance which increases with the growth of the popularity of WDM optical networks. In practice, the existing algorithms performed on hypercube architectures can be adapted to WDM optical networks using no more than the wavelengths obtained by our results.

3.8 Application Extensions

Some interesting future research directions are listed as follows.

3.8.1 Realizing All-to-all Communication

It is known that the minimum numbers of wavelengths for realizing all-to-all broadcasting in one-hop of optical routing on rings and the two-dimensional tori of N nodes are $O(N^2)$ and $O(N^{3/2})$ respectively [11]. In multihop WDM optical networks, routing algorithms which realize all-to-all communications in k-hops ($k \geq 2$) by $O(N^{1+1/k})$ wavelengths on rings, $O(N^{1+1/(2k)})$ wavelengths on the 2D tori were proposed in [60]. It is well known that hypercube structure can be used to efficiently simulate all-to-all communication. By performing hypercube communications in $\log N$-hops, it can be anticipated that all-to-all communication can be realized using $O(N)$ wavelengths on WDM optical linear arrays and rings, and $O(N^{1/r})$ wavelengths on r-dimensional meshes and tori. This problem is of great practical interest to be further investigated.

3.8.2 Large Hypercubes

In practical, the number of nodes in hypercube is larger than that of optical networks. In this case, it is easy to partition the hypercube into sub-hypercubes, such that the number of "super" nodes in the partitioned hypercube is equal to that in the optical networks. By partitioning the hypercube, similar embedding schemes and wavelength assignment algorithms can be used.

For example, given a $2^{n'}$ node hypercube and a 2^n node optical networks, where $n' > n$, the $2^{n'}$ node hypercube can be partitioned into a 2^n "super" hypercube, with each "super" node composed of $2^{n'-n}$ nodes. Thus, the embedding can be easily constructed by embedding each "super" node on the node of optical networks by our wavelength assignment algorithms.

3.8.3 Realizing Hypercubic Networks

In the hypercube family, the butterfly networks, cube-connected-cycles, $Beneš$ networks, shuffle-exchange graph, and the de Bruijn graph are the most important and best known networks for variants of hypercube. Other hyercubic networks including the omega networks, the flip networks, the baseline networks, banyan networks and delta

networks also closely related to hypercube in structure. By the embedding technique, these hypercubic networks can also be mapped to optical networks, such that the originally designed algorithms can be incorporated to optical networks by extending our designed wavelength assignment algorithms.

Moreover, it is shown that these hypercubic networks can be used to efficiently simulate a hypercube with the same number of processors, even though they have substantially fewer wires [80]. Since fewer wires are required for most of the hypercubic networks compared with hypercube, the wavelength requirement for these networks can be reduced compared with our obtained results. So, our results provide an upper bound for the wavelength requirement of hypercubic networks.

3.8.4 Other Application Extensions

In this chapter, we consider the single-hop optical networks, since hypercube connections are realized in one hop and there are no wavelength conversions. Actually, the wavelength requirement for realizing hypercube in multi-hop optical networks can not be significantly reduced, since our results are optimal or near-optimal based on the fact that the wavelength requirements are close to the congestion of the embedding. It is of great theoretical and practical interest to investigate the wavelength requirement on other type of future optical networks. In Chapter 4, we further study the embedding problem of realizing hypercubes on chordal ring networks, in order to reduce the wavelength requirement. Moreover, we further study the embedding of dimensional hypercubes on optical networks dimension by dimension in Chapter 5, since all the dimensions are considered in this chapter.

Chapter 4

Embedding Hypercubes on Optical WDM Chordal Rings

In this chapter, we study routing and wavelength assignment for realizing hypercubes on WDM ring networks with additional links, namely chordal rings, to reduce the wavelength requirement. We design the embedding schemes and derive the numbers of wavelengths required on WDM chordal ring networks of both degrees 3 and 4. Based on our proposed embedding schemes, we provide the analysis of chord length with optimal number of wavelengths to realize hypercubes on 3-degree and 4-degree chordal rings. Results show that the wavelength requirement for realizing hypercubes on optical chordal ring networks is significantly lower than that on optical ring networks. In addition, our research also provide solutions for embedding hypercubes on chordal rings from graph embedding theory point of view.

4.1 Introduction

In Chapter 3, we discussed the wavelength requirement for embedding hypercubes on array-based WDM optical networks. Specifically, we improved the results of [132] and extended those to the unidirectional hypercube. However, the numbers of wavelengths required to realize hypercubes on the topologies discussed in [132] and [30] are large if the number of nodes in hypercubes is large. In order to further reduce the number of re-

quired wavelengths, we design the embedding of hypercubes realized on optical chordal ring networks. Chordal ring networks have been intensively studied to efficiently solve a lot of distributed problems [27][128]. In addition, it has been used for both local area computer networks and large area communication networks [74]. As chordal rings have good properties such as low diameter, high connectivity and efficient routing, wavelength routed optical networks with chordal ring topology have been investigated in [55], [52], [53] and [54]. In [97], all-to-all communication realized on 4-degree optical chordal rings was considered. In this chapter, we further provide the results for wavelength requirement of hypercubes on chordal ring networks of degree 3 and degree 4. As described in [3], a chordal ring is basically a ring network, in which each node has an additional link, called a chord. The number of nodes in a chordal ring is assumed to be even, and nodes are indexed as $0, 1, 2, \ldots, N-1$ around the N-node ring. Each even numbered node $i (i = 0, 2, \ldots, N-2)$ is connected to a node $(i + M)$ mod N, where M is the chord length, which is assumed to be positive odd. Thus, the chordal ring consists of a ring of length N formed by the *ring-edges* of $(i, (i+1) \mod N)$, where $0 \leq i \leq N-1$, and of chords formed by the *chord-edges* of $(i, (i+M) \mod N)$ with chord length of M. For 4-degree chordal rings, each node i is connected by a chord of length M to node $(i + M) \mod N$. Note that this implies that there is also a chord from i to $(i - M) \mod N$.

In this chapter, we denote the N-node 3-degree and 4-degree optical chordal rings with chord length of M by $CR(N, M, 3)$ and $CR(N, M, 4)$ respectively. Without loss of generality, we assume $M \leq N - 1$.

4.2 Hypercubes on Chordal Rings of Degree 3

In order to construct the embedding scheme from hypercubes to 3-degree chordal ring, we assume $CR(N, M, 3)$ has $N = 2^n$ nodes with chord length $M = 2^m - 1$. Figure 4.1 shows a 3-degree chordal ring of $CR(32, 7, 3)$. We assume each link in the network is bidirectional and composed of a pair of unidirectional links with one link in each direction. For H_n, if $(x, y) \in H_n$, then $(y, x) \in H_n$. Assuming that these two com-

munications can be realized by two lightpaths in the same path of opposite directions passing through different fiber links, the same wavelength can be assigned to these two lightpaths. In this case, we can ignore the problem of communication directions in H_n and denote the communications in the ith dimension by DIM_n^i.

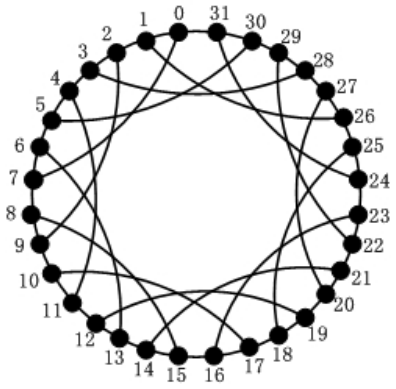

Figure 4.1: $CR(32, 7, 3)$

Our main idea is to find an efficient way of decomposing the chordal rings into a set of array-based subgraphs. In [7], a method for decomposing 3-degree chordal rings is introduced, which will be particularly helpful for the design of our wavelength assignment scheme as follows. As described in [7], a 3-degree chordal ring can be decomposed into a set of $a = \lfloor N/(M+1) \rfloor$ disjoint cycles, denoted by $C_0, \ldots C_{a-1}$, with $M+1$ nodes on each cycle. We call theses cycles *inner cycles*, where

$C_i = \{i(M+1), i(M+1)+1, \ldots, i(M+1)+M\}$.

By this decomposition approach, $CR(N, M, 3)$ consists of 2^{n-m} cycles, labeled from 0 to $2^{n-m}-1$, with 2^m nodes on each cycle. For example, $CR(32, 7, 3)$ as shown in Figure 4.1 can be decomposed into 4 cycles C_0, C_1, C_2, C_3 shown in Figure 4.2. Given a cycle C_i, a node with label $i(M+1)+j$ is said to be the jth node of cycle C_i, where $i = 0, \ldots, 2^{n-m}$ and $j = 0, \ldots, 2^m$. Note that the node 0 of C_i is adjacent to node 1 and m of C_i. Moreover, for each i, $0 \leq i \leq a-1$, cycles C_i and C_{i+1} are connected by $(M+1)/2$ edges. Among these edges, $(M-1)/2$ edges are chord-edges and one edge is ring-edge. It can also be observed that for any even value j, the jth vertex in C_i is adjacent to the $(j-1)$th vertex in C_{i+1} by a chord-edge.

According to this decomposition scheme, $CR(N, M, 3)$ can be decomposed into

2^{n-m} cycles with 2^m nodes on each cycle. For example, $CR(32, 7, 3)$ as shown in Figure 4.1 can be decomposed into 4 inner cycles C_0, C_1, C_2, C_3 shown in Figure 4.2 as follows.

$C_0 = \{0, 1, 2, 3, 4, 5, 6, 7\}$;
$C_1 = \{8, 9, 10, 11, 12, 13, 14, 15\}$;
$C_2 = \{16, 17, 18, 19, 20, 21, 22, 23\}$;
$C_3 = \{24, 25, 26, 27, 28, 29, 30, 31\}$.

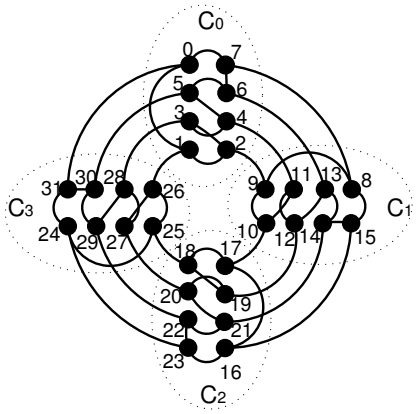

Figure 4.2: Decomposition of $CR(32, 7, 3)$

Base on the decomposition of chordal rings, we assume the jth node of $CR(N, M, 3)$ is identified by (x, y), where $x = j \bmod (M + 1)$ and $y = j/(M + 1)$. In other words, the jth node of $CR(N, M, 3)$ is on the xth node of the yth cycle, where $0 \leq x \leq 2^m - 1$ and $0 \leq y \leq 2^{n-m} - 1$. For the sake of simplicity, we define $a \oplus_i b = (a + b) \bmod 2^i$ and $a \ominus_i b = (a - b) \bmod 2^i$. As the degree of each node (x, y) of $CR(N, M, 3)$ is 3, two edges are connected to each node on cycle C_y, which we call *inner cycle edges*, and the other one is connected to cycle $C_{y \ominus_{n-m} 1}$ or $C_{y \oplus_{n-m} 1}$, which is called *outer cycle edge*. For the connecting of outer cycle edges, the following lemma can be derived.

Lemma 21. *For a given node* (x, y) *on* $CR(N, M, 3)$*, if* $x = 0$*, node* (x, y) *is connected to node* $(M, y \ominus_{n-m} 1)$*; if* $x = M$*,* (x, y) *is connected to* $(0, y \oplus_{n-m} 1)$*. For* $1 \leq x \leq M - 1$*, if* x *is even,* (x, y) *is connected to* $(x \ominus_m 1, y \oplus_{n-m} 1)$*; if* x *is odd,* (x, y) *is*

connected to $(x \oplus_m 1, y \ominus_{n-m} 1)$.

Proof. If $x = 0$, $((y \ominus_{n-m} 1) \times (m+1) + m) \oplus_n 1 = y \times (m+1) + 0$. It can be concluded that (x, y) and $(M, y \ominus_{n-m})$ is connected by a ring-edge. If $x = M$, $((y \oplus_{n-m} 1) \times (m+1) + 0) \oplus_n 1 = y \times (m+1) + m$. Also, (x, y) and $(0, y \oplus_{n-m})$ is connected by a ring-edge. For $1 \leq x \leq m-1$, if x is even, $(y \times (m+1) + x) \oplus_n m = (y \oplus_{n-m} 1) \times (m+1) + x \ominus_m 1$. It can be concluded that (x, y) is connected to $(x \ominus_m 1, y \oplus_{n-m} 1)$ by a chord-edge. Similarly, if x is odd, $(y \ominus_{n-m} 1) \times (m+1) + x \oplus_m 1) \oplus_n m = y \times (m+1) + x$. Also, (x, y) is connected to $(x \ominus_m 1, y \oplus_{n-m} 1)$ by a chord-edge. □

By Lemma 21, for each $x = 1, 3, ..., M-2$, nodes $(x, 0), (x+1, 0), (x, 1), (x+1, 1), (x, 2), (x+1, 2), ..., (x, 2^{n-m}-1)$ and $(x+1, 2^{n-m}-1)$ can be connected node by node into one cycle; Nodes $(0, 0), (M, 0), (0, 1), (M, 1), (0, 2), (M, 2), ..., (0, 2^{n-m}-1)$ and $(M, 2^{n-m}-1)$ can be connected into one cycle. In total, there are $(M+1)/2$ such disjoint 2^{n-m+1}-node cycles, denoted by O_i, which we call *outer cycles* in contrast to the inner cycles. It can be observed that there are some edges which belong to both inner cycles and outer cycles. For these edges, we call them *interconnected edges*. For example, $CR(32, 7, 3)$ as shown in Figure 4.1 can be decomposed into 4 outer cycles O_0, O_1, O_2, O_3 shown in Figure 4.2 as follows.

$O_0 = \{1, 2, 9, 10, 17, 18, 25, 26\}$;
$O_1 = \{3, 4, 11, 12, 19, 20, 27, 28\}$;
$O_2 = \{5, 6, 13, 14, 21, 22, 29, 30\}$;
$O_3 = \{0, 7, 8, 15, 16, 23, 24, 31\}$.

In order to define the embedding scheme of H_n on $CR(n, m)$, we label the jth node of H_n by (X, Y), where $X = j \bmod (M+1)$ and $Y = j/(M+1)$. Embed node (X, Y) of H_n on node $(\eta(X), \eta(Y))$ of $CR(N, M, 3)$. It can be proven by Lemma 21 that two node connected by each connection in H_n must be embedded on either the same inner cycle or the same outer cycle of $CR(N, M, 3)$. Thus, route all the communication lightpaths within the corresponding outer cycles or inner cycles by the shortest path. We

call such an embedding scheme for H_n on $CR(N, M, 3)$ *double cycle embedding*.

For example, node 20 (labeled by $(4, 2)$) of H_5 is embedded on node 29 (labeled by $(7, 3)$) of $CR(5, 3)$, and node 16 (labeled by $(0, 2)$) of H_5 is embedded on node 24 (labeled by $(0, 3)$) of $CR(32, 7, 3)$. It can be seen that hypercube connection of $(16, 20)$ is embedded on the same inner cycle. By double cycle embedding, connection of $(16, 20)$ is routed along the inner cycle of C_3 by the path from node 29 to node 24 on $CR(32, 7, 3)$ passing through nodes 30 and 31 by the shortest path.

By double cycle embedding, the following theorem is held.

Theorem 32. *By double cycle embedding, the number of wavelengths required to realize H_n on $CR(N, M, 3)$ is $\lfloor 5 \times (2^{n-m+1} + 2^m)/12 - 1 \rfloor$.*

Proof: The communications on each of the 2^m-node inner cycle can be regarded as the communications of H_m on 2^m-node ring. So, the number of wavelengths required for inner cycle edges are $\lambda_\eta(H_m, R_m)$. For the communications on the outer cycles, the communications on each outer cycle can be regarded as the communications of two H_{n-m} overlapped on the 2^{n-m+1}-node outer cycle, which requires $2\lambda_\eta(H_{n-m}, R_{n-m})$ wavelengths. Therefore, the number of wavelengths required for the interconnected edges is $\lambda_\eta(H_m, R_m) + 2\lambda_\eta(H_{n-m}, R_{n-m})$. By Theorem 16, the theorem is held.

It can be easily to see that the number of wavelengths for realizing a given hypercube on chordal ring decreases with the increasing of chord length first, and then increase after it reaches a minimum value. The following theorem shows the minimum value of the wavelengths required on the chordal ring the corresponding chord length by our embedding scheme for a given hypercube.

Theorem 33. *By double cycle embedding, the minimum number of wavelengths to realize H_n on N-node chordal ring is $\lfloor 5 \times \sqrt{2N}/6 - 1 \rfloor$ when $m = (n + 1)/2$ if n is odd, and $\lfloor 5 \times \sqrt{N}/4 - 1 \rfloor$ when $m = n/2$ or $m = n/2 + 1$ if n is even.*

Proof. As $\lfloor 5 \times (2^{n-m+1} + 2^m)/12 - 1 \rfloor \geq \lfloor 5 \times 2 \times \sqrt{2^{n-m+1} \times 2^m}/12 - 1 \rfloor = \lfloor 5 \times \sqrt{2^{n+1}}/6 - 1 \rfloor = \lfloor 5 \times \sqrt{2N}/6 - 1 \rfloor$, the minimum value can be obtained if and only if $2^{n-m+1} = 2^m$. For n is odd, the minimum number can be achieved if $m = (n + 1)/2$.

The minimum number for n is even, $\lfloor 5 \times \sqrt{N}/4 - 1 \rfloor$, can be obtained when $m = n/2$ or $m = n/2 + 1$. □

For the convenience of the comparisons given in the following section, we call such chordal rings *optimal 3-degree chordal rings*, with respect to our scheme, which can realize the hypercubes with the minimum numbers of wavelengths.

4.3 Hypercubes on Chordal Rings of Degree 4

We consider embedding H_n into $CR(N, M, 4)$ in two cases: 1) $M = 2^m$ and 2) $M = 2^m - 1$.

4.3.1 Symmetric Embedding

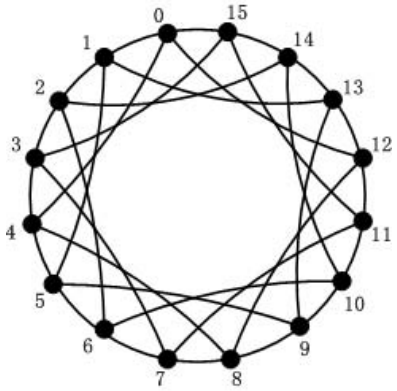

Figure 4.3: $CR(16, 4, 4)$

$CR(2^n, 2^m, 4)$ can be decomposed into a set of 2^m disjoint 2^{n-m}-node cycles, $R_0^c, \ldots R_{2^m-1}^c$, which we call *chord-cycles*, since these chord-cycles are all connected by chord-edges. We define the set of chord-cycles R^c as follows.

$R^c = \{R_i^c(V_i^c, E_i^c) | i = 0, 1, ..., 2^m - 1\}$;

$V_i^c = \{i + k \times 2^m | k = 0, 1, ..., 2^{n-m} - 1\}$;

$E_i^c = \{(v, (v + 2^m) \bmod 2^n) | v \in V_i\}$.

V_i^c and E_i^c are the set of nodes and edges in chord-cycle of R_i^c respectively.

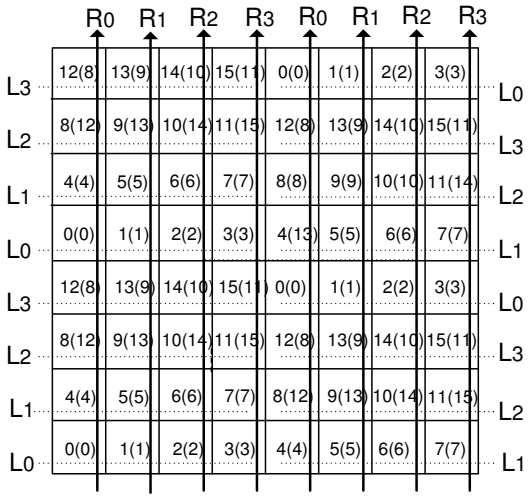

Figure 4.4: Geometrical representation for $CR(16, 4, 4)$

$CR(2^n, 2^m, 4)$ can also be decomposed into a set of 2^m disjoint 2^{n-m}-node linear arrays, $L_0^r, \ldots, L_{2^{n-m}-1}^r$, which we call *ring-lines*, since these ring-lines are all connected by ring-edges in $CR(2^n, 2^m, 4)$. We define the set of ring-lines L^r as follows.

$L^r = \{L_i^r(V_i^r, E_i^r)|i = 0, 1, ..., 2^{n-m} - 1\}$;

$V_i^r = \{i \times 2^m + k|k = 0, 1, ..., 2^m - 1\}$;

$E_i^r = \{(v, v + 1)|v \in\ V_i$ and $v \neq (i + 1) \times 2^m - 1\}$.

V_i^r and E_i^r are the set of nodes and edges in ring-line of L_i^r respectively. It should be noted that R_i^c and L_j^r are edge-disjoint for each i and j. For example, $CR(16, 4, 4)$ shown in Figure 4.3 can be decomposed into the following chord-cycles and ring-lines.

$R_0^c : 0 \rightarrow 4 \rightarrow 8 \rightarrow 12 \rightarrow 0$;

$R_1^c : 1 \rightarrow 5 \rightarrow 9 \rightarrow 13 \rightarrow 1$;

$R_2^c : 2 \rightarrow 6 \rightarrow 10 \rightarrow 14 \rightarrow 2$;

$R_3^c : 3 \rightarrow 7 \rightarrow 11 \rightarrow 15 \rightarrow 3$.

$L_0^r : 0 \rightarrow 1 \rightarrow 2 \rightarrow 3$;

$L_1^r : 4 \rightarrow 5 \rightarrow 6 \rightarrow 7$;

$L_2^r : 8 \rightarrow 9 \rightarrow 10 \rightarrow 11$;

$L_3^r : 12 \rightarrow 13 \rightarrow 14 \rightarrow 15$.

The geometrical representation [18] for $CR(16, 4, 4)$ shown in Figure 4.4 illustrates

the decomposition of $R_0^c, R_1^c, R_2^c, R_3^c$ and $L_0^r, L_1^r, L_2^r, L_3^r$.

Assume j is a node of hypercube and $j \mod 2^m = i$. We define η_{cr} is a function of one-to-one mapping from the node of H_n to the node of $CR(2^n, 2^m, 4)$ as follows.

$\eta_{cr}(i) = 2^m \times \eta(\lfloor i/2^m \rfloor) + i \mod 2^m$

Embed the ith node of H_n onto node $\eta_{cr}(i)$ of $CR(2^n, 2^m, 4)$. It is easy to see that $\eta_{cr}(i) = i$ when $0 \leq i \leq 2^{n-1} - 1$. We call such an embedding *symmetric embedding*. We define the routing scheme as follows. For the connection of (u, v) in H_n, if node u and v are embedded on the same chord-cycle R_i^c, route the connection by the shortest path of R_i^c. If u and v are embedded onto the same ring-line L_j^r, route the connection along the edges of L_j^r. We call such a routing scheme *R-L routing*. In other words, by the symmetric embedding and R-L routing, each connection in H_n must be embedded on either the same chord-cycle or the same ring-line. We define $\lambda_{sym}(H_n, CR(2^n, 2^m, 4))$ as the number of wavelengths required to realize H_n on $CR(2^n, 2^m, 4)$ by the symmetric embedding and R-L routing scheme.

Theorem 34. *By the symmetric embedding and R-L routing scheme, the number of wavelengths required to realize hypercubes on 2^n-node 4-degree chordal rings with chord length of 2^m is $max(\lfloor 2^{m+1}/3 \rfloor, \lfloor 5 \times 2^{n-m}/12 \rfloor)$. That is,*

$$\lambda_{sym}(H_n, CR(2^n, 2^m, 4)) = \begin{cases} \lfloor 5 \times 2^{n-m-2}/3 \rfloor, \textit{if } m < n/2; \\ \lfloor 2^{m+1}/3 \rfloor, \textit{if } m \geq n/2. \end{cases}$$

Proof: For the dimensional k connection of (u, v) in DIM_n^k, $v = u + 2^k$ if $u \mod 2^{k+1} < 2^k$. By the symmetric embedding, node u and node v are embedded in the same L_i^r if $k < m$, and u and v are in the same R_j^c if $k \geq m$. By the R-L routing scheme, communications in $\cup_{k=0}^{m-1} DIM_n^k$ routed within the corresponding L_i^r can be regarded as H_m realizing on linear array of L_m, and communications in $\cup_{k=m}^{n-1} DIM_n^k$ within the corresponding R_j^c can be regarded as H_{n-m} realizing on ring of R_{n-m} by $\eta(\lfloor i/2^m \rfloor)$. By Theorem 16 and Theorem 14, the theorem is held.

It can be seen from Theorem 34 that $\lambda_{sym}(H_n, CR(2^n, 2^m, 4))$ decreases with the increasing of m when $m < n/2$, and increases with the increasing of m when $m \geq n/2$. We derive the results of the minimum of $\lambda_{sym}(H_n, CR(2^n, 2^m, 4))$ in the following theorem.

Theorem 35. *By the symmetric embedding and R-L routing scheme, the minimum number of wavelengths to realize H_n on N-node chordal ring is $\lfloor 2\sqrt{N}/3 \rfloor$ when $m = n/2$ if n is even with chord length of $\sqrt{N}$, and $\lfloor 5 \times \sqrt{2N}/12 \rfloor$ when $m = (n-1)/2$ if n is odd with chord length of $\sqrt{N/2}$.*

Proof: If n is even, $\lambda_{sym}(H_n, CR(2^n, 2^{n/2-1}, 4)) = \lfloor 5 \times 2^{n/2-1}/3 \rfloor = \lfloor 5\sqrt{N}/6 \rfloor$ and $\lambda_{sym}(H_n, CR(2^n, 2^{n/2}, 4)) = \lfloor 2^{n/2+1}/3 \rfloor = \lfloor 2\sqrt{N}/3 \rfloor$. So, $\lambda_{sym}(H_n, CR(2^n, 2^{n/2}, 4)) < \lambda_{sym}(H_n, CR(2^n, 2^{n/2-1}, 4))$. Therefore, the minimum number of wavelengths, $\lfloor 2\sqrt{N}/3 \rfloor$, is obtained when $m = n/2$. If n is odd, $\lambda_{sym}(H_n, CR(2^n, 2^{(n-1)/2}, 4)) = \lfloor 5 \times 2^{(n+1)/2}/12 \rfloor = \lfloor 5\sqrt{2N}/12 \rfloor$ and $\lambda_{sym}(H_n, CR(2^n, 2^{(n+1)/2}, 4)) = \lfloor 2^{(n+1)/2+1}/3 \rfloor = \lfloor 2\sqrt{2N}/3 \rfloor$. Thus, $\lambda_{sym}(H_n, CR(2^n, 2^{(n-1)/2}, 4)) < \lambda_{sym}(H_n, CR(2^n, 2^{(n+1)/2}, 4))$. So, the minimum number of wavelengths, $\lfloor 5\sqrt{2N}/12 \rfloor$, is obtained when $m = (n-1)/2$.

Theorem 34 and Theorem 35 show the results for symmetric embedding with chord length of 2^m, which is always even. In the following, we analyze cyclic permutation embedding with odd chord length of $2^m - 1$.

4.3.2 Cyclic Permutation Embedding

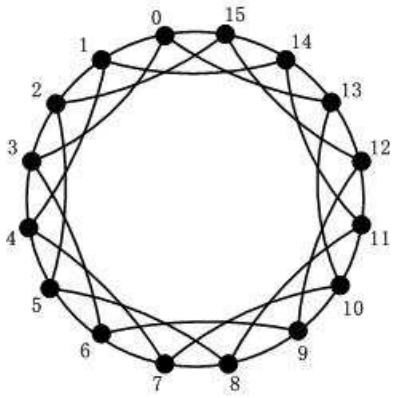

Figure 4.5: $CR(16, 3, 4)$

$CR(2^n, 2^m - 1, 4)$ can be decomposed into a set of 2^{n-m} disjoint 2^m-node cycles, $R^{rc}_0, \ldots R^{rc}_{2^{n-m}-1}$, which we call *ring-chord-cycles*, since these ring-chord-cycles are

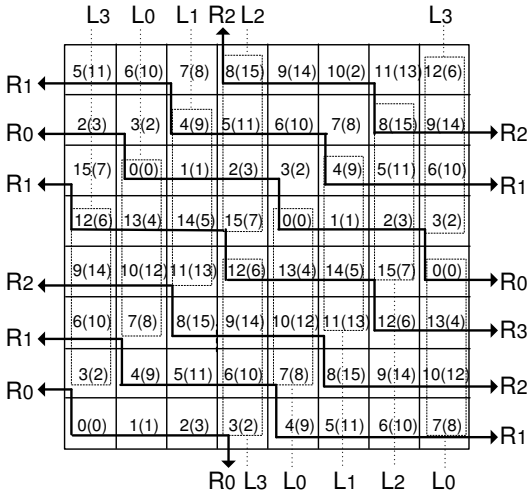

Figure 4.6: Geometrical representation for $CR(16, 3, 4)$

connected by $2^m - 1$ ring-edges and 1 chord-edge. We define the set of ring-chord-cycles R^{rc} as follows.

$R^{rc} = \{R_i^{rc}(V_i^{rc}, E_i^{rc})|i = 0, 1, ..., 2^{n-m} - 1\}$;

$V_i^{rc} = \{i \times 2^m + k|k = 0, 1, ..., 2^m - 1\}$;

$E_i^{rc} = \{(v, v+1)|v \in V_i \text{ and } v \neq (i+1) \times 2^m - 1\} \bigcup \{(v, v - 2^m + 1)|v = (i+1) \times 2^m - 1\}$.

$CR(2^n, 2^m - 1, 4)$ can also be decomposed into a set of 2^m disjoint 2^{n-m}-node linear arrays, $L_0^r, \ldots, L_{2^m-1}^r$, which we call *chord-lines*, since these ring-lines are all connected by chord-edges of $CR(2^n, 2^m - 1, 4)$. We define the set of chord-lines L^c as follows.

$L^c = \{L_i^c(V_i^c, E_i^c)|i = 0, 1, ..., 2^m - 1\}$;

$V_i^c = \{(i \times 2^m - k \times (2^m - 1)) \mod 2^n | k = 0, 1, ..., 2^{n-m} - 1\}$;

$E_i^c = \{(v, (v + 2^m - 1) \mod 2^n) | v \in V_i \text{ and } v \neq i \times 2^m\}$.

For example, $CR(16, 3, 4)$ shown in Figure 4.5 can be decomposed into the following ring-chord-cycles and ring-lines.

$R_0^{rc} : 0 \rightarrow 1 \rightarrow 2 \rightarrow 3 \rightarrow 0$

$R_1^{rc} : 4 \rightarrow 5 \rightarrow 6 \rightarrow 7 \rightarrow 4$;

$R_2^{rc} : 8 \rightarrow 9 \rightarrow 10 \rightarrow 11 \rightarrow 8$;

$R_3^{rc} : 12 \rightarrow 13 \rightarrow 14 \rightarrow 15 \rightarrow 12$;

$L_0^r : 0 \rightarrow 13 \rightarrow 10 \rightarrow 7$;

$L_1^r : 4 \rightarrow 1 \rightarrow 14 \rightarrow 11$;

$L_2^r : 8 \rightarrow 5 \rightarrow 2 \rightarrow 15$;

$L_3^r : 12 \rightarrow 9 \rightarrow 6 \rightarrow 3$.

The geometrical representation for $CR(16, 3, 4)$ shown in Figure 4.6 illustrates the decomposition of $R_0^{rc}, R_1^{rc}, R_2^{rc}, R_3^{rc}$ and $L_0^c, L_1^c, L_2^c, L_3^c$. It should be noted that R_i^{rc} and L_j^c are edge-disjoint for each i and j.

We define the 1-1 mapping from the elements of reversal node order [31] X_n for V_{H_n} to the elements of ordered nodes on linear array V_{L_n} as a permutation over V_{L_n} with 2^n elements. In [31], the definition of X_n is based on the definition of Gray Code [80]. The cyclic permutation P_t from X_n to V_{L_n} with offset t can be written as:

$P_t(X_n[i]) = V_{L_n}[i + t]$ for $i = 0, 1, ..., 2^n - 1$, and

$P_t(X_n[i]) = V_{L_n}[i + t - 2^n]$ for $i = 2^n - t + 1, 2^n - t + 2, ..., 2^n - 1$.

Wavelength requirement by cyclic permutation P_t can be derived in the following lemma, and the proof is omitted.

Lemma 22. *The maximum number of wavelengths required to realizing 2^n-node hypercubes on 2^n-node optical linear arrays by cyclic permutation P_t with offset $t \in \{1, ..., 2^n - 1\}$ is $2 \times \lfloor 5N/12 \rfloor$.*

Based on cyclic permutation P_t, we propose cyclic permutation embedding scheme for the nodes of H_n on the nodes of $CR(2^n, 2^m - 1, 4)$ as follows. Assume θ is a function of one-to-one mapping from the node of H_n to the node of $CR(2^n, 2^m - 1, 4)$. Let $\delta_1(i) = X_{n-m}[\lfloor i/2^m \rfloor]$ and $\delta_2(i) = \eta(i \mod 2^m)$. Define

$$\theta(i) = 2^n - 2^m \times \delta_1(i) + (\delta_1(i) + \delta_2(i)) \mod 2^m.$$

We call such an embedding *cyclic permutation embedding*. For example, the nodes i of H_4 are embedded on the nodes $\theta(i)$ of $CR(16, 3, 4)$ as follows: $\theta(0) = 0$, $\theta(1) = 1$, $\theta(2) = 3$, $\theta(3) = 2$, $\theta(4) = 13$, $\theta(5) = 14$, $\theta(6) = 12$, $\theta(7) = 15$, $\theta(8) = 7$, $\theta(9) = 4$, $\theta(10) = 6$, $\theta(11) = 5$, $\theta(12) = 10$, $\theta(13) = 11$, $\theta(14) = 9$ and $\theta(15) = 8$. (The numbers

in the brackets of Figure 4.5 represent the nodes of H_4.) By cyclic permutation embedding, each node pair connected by one hypercube edge must be embedded on either the same ring-chord-cycle or the same chord-line. We define $\lambda_{cp}(H_n, CR(2^n, 2^m, 4))$ as the number of wavelengths required to realize H_n on $CR(2^n, 2^m - 1, 4)$ by the cyclic permutation embedding and R-L routing scheme.

Theorem 36. *By cyclic permutation embedding and R-L routing scheme, the number of wavelengths required to realize hypercubes on 2^n-node chordal rings of 4-degree with chord length of $2^m - 1$ is $max(\lfloor 5 \times 2^{n-m+1}/12 \rfloor, \lfloor 5 \times 2^m/12 \rfloor)$. That is, $\lambda_{cp}(H_n, CR(2^n, 2^m - 1, 4))$=* $\begin{cases} 2 \times \lfloor 5 \times 2^{n-m}/12 \rfloor, \textit{if } m \leq \frac{n+1}{2}; \\ \lfloor 5 \times 2^m/12 \rfloor, \textit{if } m > \frac{n+1}{2}. \end{cases}$

Proof: Communications in $\cup_{k=0}^{m-1} DIM_n^k$ routed within the corresponding R_i^{rc} can be regarded as H_m realizing on ring of R_m by $\eta(\lfloor i/2^{n-m} \rfloor)$, and communications in $\cup_{k=m}^{n-1} DIM_n^k$ routed within the corresponding L_j^c can be regarded as H_{n-m} realizing on linear array of L_{n-m} by cyclic permutation mapping P_j with offset j. By Lemma 21 and Lemma 22, the theorem holds.

Similar with the proof of Theorem 35, the following Theorem can be obtained.

Theorem 37. *By cyclic permutation embedding and R-L routing scheme, the minimum number of wavelengths to realize H_n on N-node chordal ring is $2 \times \lfloor 5\sqrt{N}/12 \rfloor$ when $m = n/2$ or $m = n/2 + 1$ if n is even with chord length of $\sqrt{N} - 1$ or $2\sqrt{N} - 1$, and $\lfloor 5\sqrt{2N}/12 \rfloor$ when $m = (n+1)/2$ if n is odd with chord length of $\sqrt{2N} - 1$.*

4.4 Comparisons

Figure 4.7 shows the wavelength requirement for realizing H_9, H_{10} and H_{11} on 512-node 3-degree chordal ring, 1024-node 3-degree chordal ring and 2048-node 3-degree chordal ring respectively, with different chord length $2^m - 1$ ($m = 2, 3, \ldots, n-1$). It can be seen that the number of wavelengths for realizing H_9 on 512-node 3-degree chordal ring achieves its minimum value when its chord length equals 31. For realizing H_{10} on 1024-node 3-degree chordal ring, the minimum value is achieved when the chord

length equals 31 or 63. It reaches the minimum for H_{11} realized on 2048-node 3-degree chordal when the chord length equals 63.

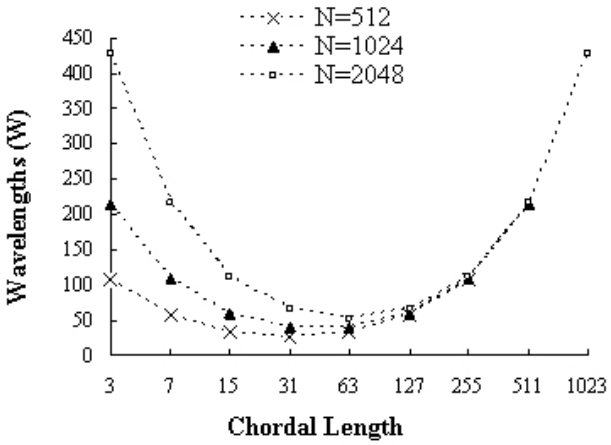

Figure 4.7: Wavelengths for 3-degree chordal ring with different chord length

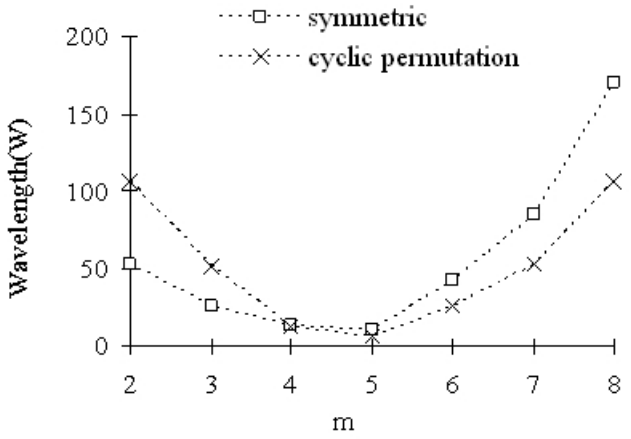

Figure 4.8: Two embedding schemes for H_9

Figure 4.8 shows the wavelength requirement for H_9 realized on 4-degree chordal rings with different chord lengths by symmetric embedding and cyclic permutation embedding. By Theorem 34 and Theorem 36, it can be concluded that cyclic permutation embedding outperforms symmetric embedding when $m > (n+1)/2$, and symmetric embedding outperforms cyclic permutation embedding when $m \leq (n+1)/2$. The results of the two embedding schemes on 4-degree chordal rings are shown in Table 4.1. Table 4.2 shows the wavelength requirement for realizing H_n on rings, 3-degree chordal

	Scheme 1	Scheme 2
chord length	2^m	$2^m - 1$
embedding	symmetric	cyclic permutation
$\lambda(m < \frac{n}{2})$	$\lfloor 5 \times 2^{n-m-2}/3 \rfloor$	$2 \times \lfloor 5 \times 2^{n-m}/12 \rfloor$
$\lambda(m = \frac{n}{2})$	$\lfloor 2^{n/2+1}/3 \rfloor$	$2 \times \lfloor 5 \times 2^{n/2}/12 \rfloor$
$\lambda(m = \frac{n+1}{2})$	$\lfloor 2^{(n+3)/2}/3 \rfloor$	$2 \times \lfloor 5 \times 2^{(n+1)/2}/12 \rfloor$
$\lambda_{min}(m > \frac{n+1}{2})$	$\lfloor 2^{m+1}/3 \rfloor$	$\lfloor 5 \times 2^m/12 \rfloor$
λ_{min} (n is even)	$\lfloor 2\sqrt{N}/3 \rfloor$	$2 \times \lfloor 5\sqrt{N}/12 \rfloor$
M_{min}(n is even)	$\sqrt{N}$	$\sqrt{N}-1, 2\sqrt{N}-1$
m_{min}(n is even)	$n/2$	$n/2, n/2+1$
λ_{min}(n is odd)	$\lfloor 5\sqrt{2N}/12 \rfloor$	$\lfloor 5\sqrt{2N}/12 \rfloor$
M_{min}(n is odd)	$\sqrt{N}/2$	$\sqrt{2N}-1$
m_{min}(n is odd)	$(n-1)/2$	$(n+1)/2$

Table 4.1: Hypercubes embedded onto optical 4-degree chordal rings

N	8	16	32	64	128	256	512	1024
Ring	3	6	13	26	53	106	213	426
$CR(N, M, 3)$	3	5	6	10	13	20	26	40
$CR(N, M, 4)$	1	2	3	5	6	10	13	21

Table 4.2: Wavelengths for realizing H_n on rings, 3-degree and 4-degree chordal rings

rings and 4-degree chordal rings when $3 \leq n \leq 10$. As can be seen, the numbers of wavelengths for realizing hypercubes on 3-degree and 4-degree chordal rings are much less than that on rings, since the wavelength requirement for ring is $O(N)$ and that on chordal ring is $O(\sqrt{N})$. It can also be observed that the number of wavelengths for realizing hypercubes on 4-degree chordal rings is about half of that on 3-degree chordal rings, although the wavelength requirements for N-node 3-degree chordal rings and 4-degree chordal have the same complexity of $O(\sqrt{N})$.

4.5 Conclusion

In this chapter, we discussed routing and wavelength assignment of hypercubes on 3-degree and 4-degree optical chordal ring networks. We proposed embedding schemes for analyzing the numbers of wavelengths required to realize hypercubes on chordal ring of degree 3 and degree 4 with different chord length. Based on our embedding

schemes, the numbers of wavelengths required were derived and the analysis for the minimum number of wavelengths was also provided. The wavelength requirement for realizing hypercube on WDM chordal ring networks is $O(\sqrt{N})$, which is much less than the requirement of $O(N)$ on WDM ring networks. Our embedding approaches also have theoretical significance of providing solutions for hypercubes embedded on chordal rings, which is a graph embedding problem in graph theory.

4.6 Application Extensions

4.6.1 Embedding Hypercubes on Chordal Rings of Degree n

In this chapter, the wavelength requirements for embedding hypercubes on chord ring networks of degrees 3 and 4 are considered. The embedding schemes designed in this chapter provide solutions for embedding hypercubes on chordal ring graphs of degree 3 and degree 4. It can be seen that the embedding complexity is increased with the increasing of the degree of chordal ring graphs. One open problem is to find the solution for embedding hypercubes on n-degree chordal ring graphs.

4.6.2 Realizing All-to-all Communication on Chordal Rings

In [97], all-to-all communication realized on 4-degree optical chordal rings was considered. As far as we know, there is no results for studying all-to-all communication on 3-degree optical chordal rings. As mentioned in Chapter 1 and Chapter 3, hypercube can provide an efficient way to simulate all-to-all communication. By combining our results in this chapter, one interesting future work can be considered to solve the problem of realizing all-to-all communication on 3-degree chord ring networks.

Chapter 5

Lattice Embedding for Parallel FFT (Dimensional Hypercube) on WDM Linear Array

In Chapter 3 and Chapter 4, the embedding schemes designed for hypercubes on optical architectures are based on the consideration of all hypercube dimensions. In this chapter, we design an embedding scheme for realizing parallel FFT communication pattern, defined as dimensional hypercube, on linear arrays by considering the hypercubes dimension by dimension. Based on our proposed embedding scheme, called *lattice embedding*, the number of wavelengths required to realize parallel FFT (dimensional hypercubes) on WDM linear arrays has been significantly reduced compared to the previous results [31][29].

5.1 Introduction

Fast Fourier Transform (FFT) plays an important role in numerous scientific and technical applications. While the application fields of FFT are growing rapidly, the amount of data to be transformed is also increasing tremendously. Hence, there has been a great interest in implementing FFT on parallel computers and some parallel computers have been specially designed to perform FFT computations [80].

FFT developed by Cooley and Tukey in the mid-60s is a method of computing the discrete Fourier transform which reduces the number of operations for an *N*-point complex vector from $O(N^2)$ to $O(Nlog_2N)$. The data-flow graph induced by an *N*-point FFT computation is usually described by means of the so-called butterfly representation [80]. The butterfly representation of FFT algorithm is a diagram made up of blocks representing identical computational units (butterflies) connected by arrows that show the flow of data between the blocks. Assuming that *N* is the length of the sequence to be transformed (*N* is an integer power of two), then the diagram with $N(log_2N + 1)$ nodes arranged in *N* rows and $log_2N + 1$ columns is made of log_2N stages of $N/2$ butterflies each.

Generally, FFT is implemented stage by stage, i.e. any stage of calculation cannot proceed until all the results of its previous stage have been completed. In this chapter, we consider one dimensional data sequence of size $N = 2^n$. If each data is assigned a binary representation, the communications during the ith $(1 \leq i \leq n)$ stage of the butterfly must take place between the nodes whose binary representations differ in the ith bit. If the butterfly representation is viewed as a process graph, i.e. each row of the butterfly is implemented by a process and each arrow by a communication channel, it is apparent that the butterfly communication pattern can map onto a WDM hypercube perfectly those links connecting the nodes having an address that differs by only one bit at each stage. However, if a WDM hypercube is used, only the ith dimensional links are occupied with one wavelength during the *i*th stage whereas other $(n-1) \times 2^{n-1}$ links are vacant during this stage, which may lead to wasting of wavelength channels. As we know, a connection in the hypercube is called a dimensional *i* connection [80] if it connects two nodes that differ in the *i*th bit position, where $1 \leq i \leq n$. In a network of size 2^n, the set DIM_i is defined as the set of all dimension *i* connections and H_n is defined as the hypercube which contains all connections. That is, $H_n = \bigcup_{i=1}^{n} DIM_i$ and $DIM_i = \{(j, j + (-1)^{\lfloor j/2^{n-i} \rfloor} \times 2^{n-i}) | 0 \leq j \leq 2^n - 1\}$. With input data distributed on processors, the set of all communications during *n* stages of parallel FFT is equivalent to H_n, and the set of communications during the *i*th stage is equivalent to DIM_i. Clearly, parallel FFT has a regular communication pattern which we call *dimensional hypercube*

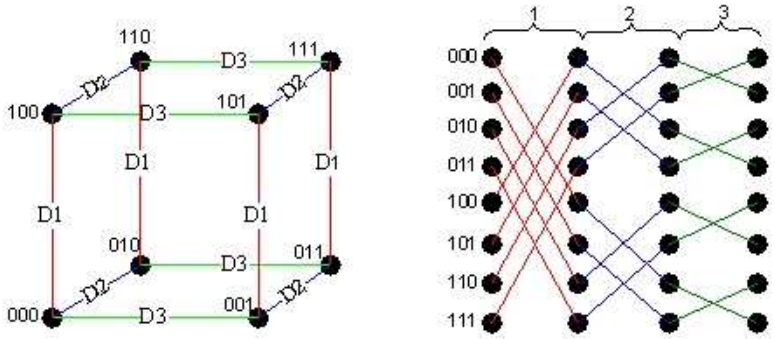

Figure 5.1: FFT_3

denoted by $FFT_n (n \geq 2)$. Figure 5.1 shows a simple example of FFT_3. For FFT_n, if $(x, y) \in FFT_n$, then $(y, x) \in FFT_n$. Assuming that these two communications can be realized by two lightpaths in the same path of opposite directions passing through different fiber links, the same wavelength can be assigned to these two lightpaths. In this case, we can ignore the problem of communication directions in FFT_n.

Since the *n* stages of parallel FFT should be implemented stage by stage, the number of wavelengths required to realize FFT_n on optical WDM networks is the maximum number among the wavelengths required by the *n* stages. That is, $\lambda_e(FFT_n, line) = \max_{1 \leq i \leq n} \big(\lambda_e(DIM_i, line)\big)$.

It should be noted that dimensional hypercube (FFT_n) is not equivalent to hypercube (H_n), since the number of wavelengths required to realize FFT_n on the WDM optical networks is not equal to that required to realize H_n. Different from the embedding schemes for all hypercube dimensions designed in Chapters 3 and 4, the objective of wavelength assignment for embedding dimensional hypercube is to embed each dimension of hypercube, such that the maximum wavelength requirement of dimensional *i* connections, for $1 \leq i \leq n$, is minimized. In other words, this problem arising from the wavelength assignment of FFT_n, which focuses on minimizing the wavelength requirement of each dimensional connections, is different from the embedding of hypercube to minimize wavelength requirement which considers all the connections on hypercube.

In [31], the problem of wavelength assignment for realizing parallel FFT communication pattern on a class of regular optical WDM networks was addressed and two schemes, sequential mapping and shift-reversal mapping, were proposed. In [29], an improved scheme, called cross embedding, was designed. However, the wavelength requirement for realizing parallel FFT communication is $O(N)$ in [31] and [29]. To further reduce the wavelength requirement, we design a new scheme for the wavelength assignment of parallel FFT communication pattern on WDM linear arrays, which requires $O(2^n/\sqrt{n})$ wavelengths for large *n*. Therefore, by lattice embedding, the number of wavelengths required to realize parallel FFT communication pattern on WDM linear arrays significantly improves the known result in [31].

5.2 Lattice Embedding of Parallel FFT on WDM Linear Arrays

5.2.1 Lattice Embedding

We design a new embedding scheme on linear arrays, lattice embedding, which is based on the lattice form of hypercube. Firstly, we introduce the following properties of hypercube in a form of lattice.

Hypercube can be represented in a form of lattice, as shown in Figure 5.2. As we know, for the hypercube with 2^n nodes, each node corresponds to an *n*-bit binary representation, and two nodes are linked with a connection if and only if their binary representations differ in precisely one bit. For the lattice form of 2^n-node hypercube, there are *n*+1 node rows connected by the hypercube connections. If the rows are numbered from top to bottom in ascending order starting from 0, the binary representations of the nodes on the *k*th row, for $0 \leq k \leq n$, have *k* 1s and $n - k$ 0s. In addition, hypercube connections only exist between the nodes on two neighborhood rows. Such a lattice form of hypercube also has the following properties:

Property 9. *Hypercube with* 2^n *nodes can be represented in a form of lattice with* $\binom{n}{k}$ *nodes on the* k*th row for* $0 \leq k \leq n$.

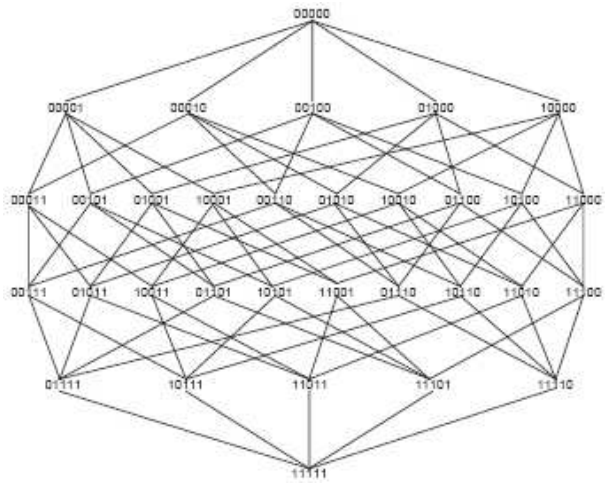

Figure 5.2: H_5 represented as a lattice

Proof. As the number of nodes whose binary representations have *k* 1s among *n* bits is $\binom{n}{k}$, it is easy to know the number of nodes on the *k*th row of the hypercube lattice is $\binom{n}{k}$. □

Property 10. *Hypercube with* 2^n *nodes can be represented in a form of lattice with* $n \times \binom{n-1}{k}$ *connections connecting the nodes of the* k*th row and the (*k+*1)st row, for* $0 \leq k \leq n-1$.

Proof. Since the number of 1s on the *k*th row and (*k*+1)st row are *k* and $k+1$ respectively, node *u* on the *k*th row connects with those nodes on the (*k*+1)st row whose binary representations have *k* 1s on the same positions with *u*. As the number of nodes on the (*k*+1)st row with *k* 1s on the same positions as *u* is $n-k$, each node on the *k*th row has $n-k$ connections with the nodes on the (*k*+1)st row. Therefore, the number of connections between the nodes of the *k*th row and (*k*+1)st row is $(n-k) \times \binom{n}{k} = n \times \binom{n-1}{k}$. □

Property 11. *Hypercube with* 2^n *nodes can be represented in a form of lattice with* $\binom{n-1}{k}$ *dimensional* i *connections, for* $1 \leq i \leq n$*, connecting the nodes of the* k*th row and the* $(k+1)$*th row for* $0 \leq k \leq n-1$.

Proof. If node *u* is on the *k*th row whose *i*th bit is 0, then *u* must connect with one of the nodes on the (*k*+1)st row by dimensional *i* connection. It is easy to know the number of

nodes on the *k*th row, whose binary representations have *k* 1s and *i*th bit is 0, is $\binom{n-1}{k}$. Therefore, the number of dimensional *i* connections, for $1 \leq i \leq n$, connecting the nodes of the *k*th row and the $(k+1)$th row is $\binom{n-1}{k}$. □

It can be seen from the above properties that the number of dimensional *i* connections is identical with each $i(1 \leq i \leq n)$.

Assume that the nodes of WDM linear arrays are numbered from left to right in ascending order starting from 0, and that the links are numbered from left to right starting from 1. Define each node numbering of H_n by a function $\eta : V_{H_n} \mapsto \{0, 1, ..., 2^n - 1\}$ which is a one-to-one mapping from the nodes of H_n to the nodes of an 2^n-node linear array. Let $R(u) = k$ if node *u* is on the *k*th row of hypercube lattice. Embed the nodes of the 2^n-node hypercube lattice from row 0 to row *n* onto the 2^n-node linear array from left to right node by node. That is to say, if $R(u) < R(v)$, then $\eta(u) < \eta(v)$. We call the above embedding way *lattice embedding*. Let $e^n(k) = \sum_{i=0}^{k} \binom{n}{i} = \binom{n}{0} + \binom{n}{1} + \binom{n}{2} + ... + \binom{n}{k}$. By the definition of lattice embedding, the node on the row 0 of hypercube lattice is mapped onto node 0 of the linear array, and nodes on the *k*th row of 2^n-node hypercube lattice, for $1 \leq k \leq n$, are mapped between node $e^n(k-1)$ and node $e^n(k) - 1$ on the 2^n-node linear array. That is to say, if $R(u) = k$, then $e^n(k-1) \leq \eta(u) \leq e^n(k) - 1$.

5.2.2 Wavelength Assignment

Let ω_l^{ij} be the number of wavelengths required by lattice embedding to realize FFT_n on the *j*th link of the linear arrays during the *i*th stage and ω_l^i be the maximum number of wavelengths required among all the links of the linear arrays during the *i*th stage. Therefore, the number of wavelengths required to realize FFT_n by lattice embedding, denoted by ω_l, is

$$\omega_l = \max_{1 \leq i \leq n} \omega_l^i = \max_{1 \leq i \leq n} (\max_{1 \leq j \leq 2^{n-1}} \omega_l^{ij})$$

By lattice embedding, the following results can be obtained.

Theorem 38. *By lattice embedding, the number of wavelengths required to realize* FFT_n *is not less than* $\binom{n-1}{\lfloor (n-1)/2 \rfloor}$.

Proof. By Property 10 and Property 11, all the hypercube connections are only between the nodes of the *k*th row and the $(k+1)$th row with $\binom{n-1}{k}$ dimensional *i* connections, for $0 \leq k \leq n-1$ and $1 \leq i \leq n$. So, the number of dimensional *i* connections passing through link $e^n(k)$ are $\binom{n-1}{k}$. Therefore, the number of wavelengths required to realize FFT_n by lattice embedding satisfies, $\omega_l = \max_{1\leq i\leq n} \omega_l^i$ $= \max_{1\leq i\leq n}(\max_{1\leq j\leq 2^{n-1}} \omega_l^{ij}) \geq \max_{0\leq k\leq n-1} \binom{n-1}{k} = \binom{n-1}{\lfloor (n-1)/2 \rfloor}$. □

Theorem 39. *By lattice embedding, the number of wavelengths required to realize FFT_n is not more than $\binom{n}{\lfloor n/2 \rfloor}$.*

Proof. On the *k*th row of the hypercube lattice for $1 \leq k \leq n-1$, there are $\binom{n-1}{k-1}$ nodes, whose *i*th bit is 1, connecting the nodes on the $(k-1)$th row by dimensional *i* connections and $\binom{n-1}{k}$ nodes, whose *i*th bit is 0, connecting the nodes on the $(k+1)$th row by dimension *i* connections. Therefore, the number of dimensional *i* connections passing thought the links from $e^n(k-1)+1$ to $e^n(k)-1$ is not more than the sum of the maximum number of dimensional *i* connections between the kth row with its two neighborhood rows. Therefore, the number of wavelengths required to realize FFT_n satisfies, $\omega_l = \max_{1\leq i\leq n}(\max_{1\leq j\leq 2^{n-1}} \omega_l^{ij}) \leq \max_{1\leq k\leq n-1}(\binom{n-1}{k} + \binom{n-1}{k-1}) =$ $\max_{1\leq k\leq n-1} \binom{n}{k} = \binom{n}{\lfloor n/2 \rfloor}$. □

As $n! \sim \sqrt{2\pi n}(n/e)^n$ for large *n* according to Stirling's Formula, it can be calculated from Theorem 38 and Theorem 39 that realizing FFT_n requires $O(2^n/\sqrt{n})$ wavelengths for large *n*. It can be concluded that lattice embedding outperforms the known embedding approaches in [31]. The following Theorems show a rough estimation of the number of wavelengths required to realize FFT_n on linear arrays.

Theorem 40. *The minimum number of wavelengths required to realize FFT_n on 2^n-node linear array by lattice embedding is $\binom{n-1}{\lfloor (n-1)/2 \rfloor} + 1$.*

Proof. If $e^n(k-1) \leq j \leq e^n(k)-1$ for some $1 \leq k \leq n-1$, let ω_{l1}^{ij} be the number of dimensional *i* connections between nodes in $U = \{u | e^n(k-1) \leq \eta(u) \leq j-1\}$ and nodes in $U' = \{u' | R(u') = k+1\}$, and ω_{l2}^{ij} be the number of dimensional *i* connections between nodes in $V = \{v | j \leq \eta(v) \leq e^n(k)-1\}$ and nodes in $V' = \{v' | R(v') =$

$k-1\}$. As the connections only take place between the neighborhood rows, the number of dimension *i* connections passing through the *j*th link on the linear array is $\omega_{l1}^{ij} + \omega_{l2}^{ij}$. Define $\eta^{-1}(j)$ as the node of FFT_n which is mapped onto the *j*th node of the linear array. Let $\theta_i(u) = 1$ if the *i*th bit of u is 1 and $\theta_i(\neg u) = 1$ if the *i*th bit of u is 0. From the properties of hypercube lattice, it is easy to know that u connects with a node in $V' = \{v'|R(v') = k-1\}$ by dimensional *i* connection if $\theta_i(u) = 1$, or with a node in $U' = \{u'|R(u') = k+1\}$ by dimensional *i* connection if $\theta_i(\neg u) = 1$. Therefore, $\omega_{l1}^{ij} = \sum_{u=\eta^{-1}(e^n(k-1))}^{\eta^{-1}(j-1)} \theta_i(\neg u)$ and $\omega_{l2}^{ij} = \sum_{u=\eta^{-1}(j)}^{\eta^{-1}(e^n(k)-1)} \theta_i(u)$.

As the number of nodes whose *i*th bit is 0 in $U \bigcup V$ is $\binom{n-1}{k}$, and that in U is ω_{l1}^{ij}, the number of nodes in V whose *i*th bit is 1 can also be calculated by $\omega_{l2}^{ij} = (e^n(k) - j) - (\binom{n-1}{k} - \omega_{l1}^{ij}) = e^n(k) - \binom{n-1}{k} + \omega_{l1}^{ij} - j$.

Therefore, the number of wavelengths required to realize FFT_n on linear arrays can be calculated by the following equation: $\omega_l = \max_{1\le i\le n, 1\le k\le n-1}(\max_{e^n(k-1)\le j\le e^n(k)-1}(\omega_{l1}^{ij} + \omega_{l2}^{ij})) = \max_{1\le i\le n, 1\le k\le n-1}(\max_{e^n(k-1)\le j\le e^n(k)-1}(2\omega_{l1}^{ij} + e^n(k) - \binom{n-1}{k} - j)) = \max_{1\le i\le n, 1\le k\le n-1}(\max_{e^n(k-1)\le j\le e^n(k)-1}(2\omega_{l1}^{ij} + e^n(k) - \binom{n-1}{k} - j))$.

For *n* is even, $\omega_l = \max\{2\sum_{u=\eta^{-1}(e^n(n/2-1))}^{\eta^{-1}(j-1)} \theta_i(\neg u) + e^n(n/2) - \binom{n-1}{n/2} - j : 1 \le i \le n, e^n(n/2-1) \le j \le e^n(n/2) - 1\}$. Since each node has n/2 0s on the $(n/2)$th row, $\sum_{i=1}^{n} \sum_{u=\eta^{-1}(e^n(n/2-1))}^{\eta^{-1}(j-1)} \theta_i(\neg u) = \frac{n}{2} \times (j - e^n(n/2-1))$. So, $\max_{1\le i\le n}(\sum_{u=\eta^{-1}(e^n(n/2-1))}^{\eta^{-1}(j-1)} \theta_i(\neg u)) \ge \lceil \frac{\frac{n}{2}\times(j-e^n(n/2-1))}{n} \rceil$. By the above equations, it can be calculated that $\omega_l \ge \max\{2 \times \lceil \frac{\frac{n}{2}\times(j-e^n(n/2-1))}{n} \rceil + e^n(n/2) - \binom{n-1}{n/2} - j, e^n(n/2-1) \le j \le e^n(n/2) - 1\} = \binom{n-1}{n/2-1} + 1$.

Similarly, it can be calculated that for *n* is odd, $\omega_l \ge \binom{n-1}{(n-1)/2} + 1$. □

From the proof of Theorem 40, it can be observed that the minimum number of wavelengths required by lattice embedding can be achieved if the 0s are distributed as much as evenly among the *n* bits of the number of 0s on the nodes before each node *j* for $e^n(n/2-1) \le j \le e^n(n/2) - 1$.

For *n* is even, the number of 0s of the nodes in $U = \{u|e^n(n/2-1) \le \eta(u) \le e^n(n/2)-1\}$ is $n/2$. If *u* is in U, $\neg u$ must be in U. So, $U = \{u_i \bigvee \neg u_i | 1 \le i \le \binom{n}{n/2}/2\}$. Thus, there are $\binom{n}{n/2}/2$ such node pairs in U. The minimum number of wavelengths re-

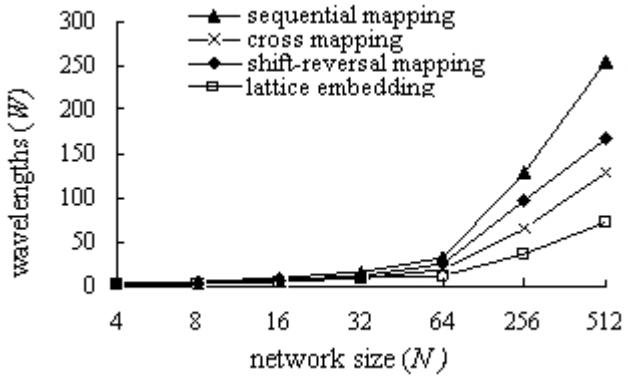

Figure 5.3: Comparisons on the number of wavelengths

quired by lattice embedding can be archived by mapping the nodes in U on the 2^n-node linear array pair by pair. That is to say, the number of wavelengths required is $\binom{n-1}{n/2-1}+1$ if we map $u_1, \neg u_1, u_2, \neg u_2, ..., u_{\binom{n}{n/2}/2}, \neg u_{\binom{n}{n/2}/2}$ onto the node from $e^n(n/2-1)$ to $e^n(n/2)-1$ respectively. For example, the number of wavelengths required to realize FFT_4 on 16-node linear array is 4, if the nodes $0011, 1100, 0101, 1010, 1001, 0110$ on FFT_4 are mapped onto the nodes of $5, 6, 7, 8, 9, 10$ on the 16-node linear array respectively. The minimum number by lattice embedding can be discussed similarly for *n* is odd. For example, if $n = 5$, the nodes of FFT_5 which are mapped onto the nodes of $6, 7, 8, 9, 10, 11, 12, 13, 14, 15$ on the 32-node linear array can be $00011, 01100, 10001, 00110, 11000, 00101, 01010, 10100, 01001, 10010$ respectively.

It can be seen from Figure 5.3 that lattice embedding outperforms the previous embedding approaches to realize parallel FFT communication on linear arrays with respect to the number of wavelengths.

5.3 Conclusion

In this chapter, we proposed a new scheme, lattice embedding, for wavelength assignment of parallel FFT (dimensional hypercubes) on WDM linear arrays. By lattice embedding, the number of wavelengths required to realize parallel FFT on WDM linear arrays significantly improves the known result in [31] and [29]. Our results have a clear significance for applications because FFT represents a common communication

pattern shared by a large class of scientific and engineering problems and WDM optical networks as a promising technology in networking has an increasing popularity. Our proposed embedding method also provides a new approach to the hypercube layout problem considering connections dimension by dimension rather than all connections as in the traditional approach.

5.4 Application Extensions

In the case if the the number of nodes in dimensional hypercube (parallel FFT) is larger than that on linear array, it is easy to divide the nodes for parallel FFT computation into small groups such that the number of groups in the partitioned parallel FFT is equal to that on the linear array. In this way, it is easy to see the similar embedding scheme can be implemented. For example, given a $2^{n'}$ node FFT computation and a 2^n node linear array, where $n' > n$, the $2^{n'}$ FFT computation nodes can be divided into a 2^n FFT groups, with each group containing $2^{n'-n}$ FFT nodes. Thus, the lattice embedding can be easily applied by embedding all the nodes in each group on one node of linear array.

Another interesting issue is to extend the lattice embedding and derive the number of wavelengths required for dimensional hypercube on other types of WDM optical networks. An open problem is to find the lower bounds for this problem and the improving schemes which can achieve the lower bounds.

Chapter 6

Conclusion and Future Work

This chapter provides a summary of this thesis. Possible extensions of this work are also discussed.

6.1 Summary

We studied network embedding problems of meshes on a family of double-loop networks and hypercubes on a class of array-based WDM optical networks, both of which are promising future networks architectures. This thesis is mainly composed of two parts. By evaluating the traditional embedding metrics, the first part is focused on systematically solving the problems of embedding meshes and tori on a family of double-loop networks, which have desirable characteristics and great potential to be widely used in the future. The second part is focused on addressing the embedding of hypercubes on a class of array-based optical networks by analyzing the metric of wavelength requirement which has been an important problem with the increasing of the popularity of optical networks. The main contents and contributions are summarized as follows:

6.1.1 Embedding Meshes/Tori on Double-loop Networks

In Chapter 2, we designed the embedding scheme for meshes and tori on a family of double-loop networks. Different with the traditional tessellation approach of L-shape

[28], we proposed a novel tessellation approach to partition the geometric plane of double-loop networks into a set of parallelogram tiles, called *P-shape*. Based on the characteristics of P-shape, we designed a simple embedding scheme, namely *P-shape embedding*, that embeds meshes and tori on double-loop networks in a systematic way resulting in a low average dilation. The major differences between the traditional L-shape and our proposed P-shape are listed as follows:

(1) L-shape is asymmetric, whereas P-shape is centrosymmetric, thus enabling other regular graphs to be embedded on double-loop networks in a regular and systematic way.

(2) L-shape concerns double-loop network's own properties, whereas P-shape is designed to exploit the relationships between double-loop networks and other regular networks. Therefore, P-shape can act as a bridge between double-loop networks and other regular networks.

(3) For a given double-loop network, there is a unique L-shape, whereas different P-shape constructions can be made on different base lengths for the same double-loop network, thus providing more choices on the construction of P-shape.

We constructed P-shape for $DL(N; 1, s)$, and showed that meshes and tori can be embedded on $DL(N; 1, s)$ by simply embedding the nodes of meshes and tori on the nodes in P-shape, called P-shape embedding, which significantly improves the previous scheme [50] on $DL(N; 1, s)$. We further extended the construction of P-shape to the general case of $DL(N; s_1, s_2)$. To the best of our knowledge, this is the first result for embedding meshes and tori on $DL(N; s_1, s_2)$. Our results show that a large fraction of edges in meshes and tori have dilation 1 by P-shape embedding, resulting in a low average dilation. Advantages of P-shape embedding compared with simple and snake-like embedding [50] can be demonstrated as follows.

(1) P-shape embedding is more scalable. Simple and snake-like embedding can only be implemented on $DL(N; 1, s)$, and P-shape embedding can be used on both $DL(N; 1, s)$ and $DL(N; s_1, s_2)$.

(2) P-shape embedding has a larger number of edges with dilation 1 than simple and snake-like embedding.

	H_n^b	H_n^u
L_n^b	$\lfloor 2N/3 \rfloor$	$\lfloor N/3 \rfloor$ ($\log N$ is even), $\lceil N/3 \rceil$ ($\log N$ is odd)
R_n^b	$\lfloor 5N/12 \rfloor$	$\lfloor 5N/24 \rfloor$ ($\log N$ is even), $\lceil 5N/24 \rceil$ ($\log N$ is odd)
R_n^u	$(NlogN)/2$	$\lceil logN/2 \rceil \times N/4$
$M_{n_1,n_2,\ldots,n_r}^b$	$\lfloor 2^{n_r+1}/3 \rfloor$	$\lfloor 2^{n_r}/3 \rfloor$ (n_r is even), $\lceil 2^{n_r}/3 \rceil$ (n_r is odd)
$T_{n_1,n_2,\ldots,n_r}^b$	$\lfloor 5 \times 2^{n_r}/12 \rfloor$	$\lfloor 5 \times 2^{n_r}/24 \rfloor$ (n_r is even), $\lceil 5 \times 2^{n_r}/24 \rceil$ (n_r is odd)
$T_{n_1,n_2,\ldots,n_r}^u$	$n_r \times 2^{n_r-1}$	$\lceil n_r/2 \rceil \times 2^{n_r-2}$

Table 6.1: Directional hypercubes on optical WDM networks

(3) P-shape embedding has more optimal cases than simple and snake-like embedding.

6.1.2 Embedding Hypercubes on WDM Optical Networks

In Chapter 3, we studied routing and wavelength assignment for realizing hypercubes on WDM optical networks including linear arrays and rings, meshes and tori with the consideration of communication directions for both bidirectional and unidirectional hypercube communications. For each case, we identified a lower bound on the number of wavelengths required, and designed the embedding scheme and wavelength assignment algorithm that uses a provably near-optimal number of wavelengths. The related results are listed in Table 6.1.

In Chapter 4, we designed embedding scheme for hypercubes on optical chordal ring networks of degree 3, and derived the number of wavelengths required for different chord length. We also designed the embedding schemes of symmetric embedding and cyclic permutation embedding schemes for 4-degree chordal ring networks, and derived the numbers of wavelengths required. The results of the two embedding schemes on 4-degree chordal rings are shown in Table 6.2.

In Chapter 5, we designed an embedding scheme for realizing parallel FFT (dimensional hypercubes) on optical linear arrays by considering the hypercubes dimension by dimension different with the consideration of all dimensions in Chapter 3 and 4. Based on our proposed embedding scheme, called *lattice embedding*, the number of wavelengths required to realize dimensional hypercubes on linear arrays has been sig-

	Scheme 1	Scheme 2
chord length	2^m	$2^m - 1$
embedding	symmetric	cyclic permutation
$\lambda(m < \frac{n}{2})$	$\lfloor 5 \times 2^{n-m-2}/3 \rfloor$	$2 \times \lfloor 5 \times 2^{n-m}/12 \rfloor$
$\lambda(m = \frac{n}{2})$	$\lfloor 2^{n/2+1}/3 \rfloor$	$2 \times \lfloor 5 \times 2^{n/2}/12 \rfloor$
$\lambda(m = \frac{n+1}{2})$	$\lfloor 2^{(n+3)/2}/3 \rfloor$	$2 \times \lfloor 5 \times 2^{(n+1)/2}/12 \rfloor$
$\lambda_{min}(m > \frac{n+1}{2})$	$\lfloor 2^{m+1}/3 \rfloor$	$\lfloor 5 \times 2^m/12 \rfloor$
λ_{min} (n is even)	$\lfloor 2\sqrt{N}/3 \rfloor$	$2 \times \lfloor 5\sqrt{N}/12 \rfloor$
M_{min}(n is even)	$\sqrt{N}$	$\sqrt{N}-1, 2\sqrt{N}-1$
m_{min}(n is even)	$n/2$	$n/2, n/2+1$
λ_{min}(n is odd)	$\lfloor 5\sqrt{2N}/12 \rfloor$	$\lfloor 5\sqrt{2N}/12 \rfloor$
M_{min}(n is odd)	$\sqrt{N}/2$	$\sqrt{2N}-1$
m_{min}(n is odd)	$(n-1)/2$	$(n+1)/2$

Table 6.2: Hypercubes embedded onto optical 4-degree chordal rings

nificantly reduced compared with the previous results [31][29].

6.2 Future Research

The research of this thesis can be extended in various ways. Additional work may either extend the applicability of the techniques or improve the results. The Following are a number of future research directions that are related to this thesis.

- Further Research on P-shape Properties

  Our designed P-shape is a helpful tool for constructing the embedding of regular graphs on double-loop networks. For future research, it is of great interest to further investigate the properties of P-shape, which may help to analyze other routing and embedding problems. Some embedding problems for other topologies on double-loop networks may be studied by using P-shape tessellation approach. One open problem is to extend our methods to the embedding of high dimensional meshes on multi-loop networks $DL(N; s_1, s_2, ..., s_{n-1}, s_n)$, which has a higher degree of technical complexity.

- State-of-art Implementation on Optical Networks

As mentioned in Chapter 1, state-of-art technology allows for a limited number of wavelengths, and the engineering problem is to establish communication between pairs of nodes so that the total number of wavelengths used is minimized. For increasing the efficiency of wavelength-routed optical networks, our proposed solutions are based on the definition of *Routing and Wavelength Assignment* (RWA) [134]. If the number of wavelengths required to realize an all-optical process in one round is greater than the available number of wavelengths, then several all-optical rounds are accomplished [8]. In this case, the efficiency of implementation need to be considered and the algorithms need to be designed for future research.

- Fault Tolerant All-to-All Communications on WDM Optical Networks

  It has been proven that hypercube has some desirable properties to simulate all-to-all communication with good fault tolerant characteristic. Another interesting application is to realize fault tolerant all-to-all communications on WDM optical networks by implementing hypercube communications on optical networks in $\log N$ steps. Since hypercube has good topological characteristics such as small diameter, high connectivity, simple routing and fault tolerance, future research can be conducted to analyze the wavelength requirement and fault tolerance performance for realizing all-to-all communications on WDM optical networks by combining and extending our results.

- Application on Large Meshes and Hypercubes

  According to the definitions of the embedding functions in this thesis, it is assumed that the number of nodes in the guest graphs (meshes and hypercubes) is equal to that in the host graphs. If the number of nodes in the meshes and hypercubes is larger than that of host graphs, our embedding can be extended to apply. This is because it is easy to partition a mesh or hypercube into a group of small meshes or hypercubes, such that the number of super nodes in the partitioned mesh or hypercube is equal to that in the host graph by considering each small mesh or hypercube as a super node. In this way, the embedding schemes can be constructed similarly. One of the most important reasons is that the partitioned

mesh or hypercube has the same topological properties with the original mesh or hypercube. This problem can be further studied to examine the expansion of the embedding.

- Realizing Other Topologies

  As mentioned in Chapter 1, many results have been obtained on the embedding problems for meshes and hypercubes. It is easy to see that the embedding of topology G_x on double-loop networks or optical networks may be constructed in two steps: firstly, embedding G_x on mesh/hypercube using the previous results; and secondly, embedding mesh/hypercbue on double-loop networks/optical networks using the results obtained in this thesis. By combining the previous results and our embedding schemes, future research can be conducted for realizing other topologies on double-loop networks and optical networks.

- Improvement of Results

  The improvement of our proposed embedding schemes need to be investigated, and optimal solutions for some of the problems need to be identified in the future. Future research can be conducted to determine whether the lower bound can be identified, and whether the embedding schemes are optimal.

Bibliography

[1] A. Aggarwal, A. Bar-Noy, D. Coppersmith, R. Ramaswami, B. Schieber, and M. Sudan, "Efficient routing in optical networks," *Journal of the ACM*, vol. 43, no. 6, pp. 973–1001, 1996.

[2] T. Andreae and M. Hintz, "On hypercubes in de bruijn graphs," *Parallel Processing Letters*, vol. 8, no. 2, pp. 259–268, 1998.

[3] B. Arden and H. Lee, "Analysis of chordal ring networks," *IEEE Transactions on Computers*, vol. 30, no. 4, pp. 291–295, 1981.

[4] R. Aschenbrenner, "A proof for the cyclic cutwidth of Q_5," California State University San Bernardino (CSUSB), Tech. Rep., 2001.

[5] Y. A. Ashir and I. A. Stewart, "Fault-tolerant embeddings of hamiltonian circuits in k-ary n-cubes," *SIAM Journal on Discrete Mathematics*, vol. 15, no. 3, pp. 317–328, 2002.

[6] N. Bagherzadeh, M. Dowd, and N. Nassif, "Embedding an arbitrary binary tree into the star graph," *IEEE Transactions on Computers*, vol. 45, no. 4, pp. 475–481, 1996.

[7] L. Barrière, J. Cohen, and M. Mitjana, "Gossiping in chordal rings under the line model," *Theoretical Computer Science*, vol. 264, no. 1, pp. 53–64, 2001.

[8] B. Beauquier, J. Bermond, L. Gargano, P. Hell, S. Pérennes, and U. Vaccaro, "Graph problems arising from wavelength routing in all optical networks," in

Proceedings of the 2nd Workshop on Optics and Computer Science, 1997, pp. 366–370.

[9] B. Beauquier, "All-to-all communication for some wavelength-routed all-optical networks," *Networks*, vol. 33, no. 3, pp. 179–187, 1999.

[10] J. Bermond, F. Comellas, and D. F. Hsu, "Distributed loop computer networks: a survey," *Journal of Parallel and Distributed Computing*, vol. 24, no. 1, pp. 2–10, 1995.

[11] J. Bermond, L. Gargano, S. Perennes, A. A. Rescigno, and U. Vaccaro, "Efficient collective communication in optical networks," *Theoretical Computer Science*, vol. 233, no. 1-2, pp. 165–189, 2000.

[12] S. Bettayeb, B. Cong, M. Girou, and I. H. Sudborough, "Embedding star networks into hypercubes," *IEEE Transactions on Computers*, vol. 45, no. 2, pp. 186–194, 1996.

[13] S. L. Bezrukov, B. Monien, W. Unger, and G. Wechsung, "Embedding ladders and caterpillars into the hypercube," *Discrete Applied Mathematics*, vol. 83, no. 1-3, pp. 21–29, 1998.

[14] S. Bezrukov, J. Chavez, L. Harper, M. Rottger, and U. Schroeder, "The congestion of n-cube layout on a rectangular grid," *Discrete Mathematics*, pp. 13–19, 2000.

[15] S. Bhatt and J. Cai, "Taking random walks to grow trees in hypercubes," *Journal of ACM*, vol. 40, no. 3, pp. 741–764, 1993.

[16] S. N. Bhatt, F. R. K. Chung, F. T. Leighton, and A. L. Rosenberg, "Efficient embeddings of trees in hypercubes," *SIAM Journal on Computing*, vol. 21, no. 1, pp. 151–162, 1992.

[17] M. Borella, B. Mukherjee, F. Jia, S. Ramamurthy, D. Banerjee, and J. Iness, "Optical interconnects for multiprocessor architectures using wavelength-division

multiplexing," in *Proceedings of the 27th Hawaii Internation Conference on System Science*, 1994, pp. 499 – 508.

[18] W. Bouknight, S. Denenberg, D. McIntyre, J. Randall, A. Sameh, and D. Slotnick, "The Illiac IV system," *Proceedings of IEEE*, vol. 60, pp. 369–379, 1972.

[19] F. Cao and A. Borchers, "Optimal transmission schedules for lightwave networks embedded with de bruijn graphs," *Theoretical Computer Science*, vol. 222, no. 1-2, pp. 113–131, 1999.

[20] F. Cao, D. H. C. Du, and A. Pavan, "Topological embedding into WDM optical passive star networks with tunable transmitters of limited tuning range," *IEEE Transactions on Computers*, vol. 47, no. 12, pp. 1404–1413, 1998.

[21] C. Castillo, "A proof for the cyclic cutwidth of Q_6," California State University San Bernardino (CSUSB), Tech. Rep., 2003.

[22] R. Chamberlain, M. Franklin, R. Krchnavek, and B. Baysal, "Design of an optically-interconnected multiprocessor," in *Proceedings of the 5th International Conference on Massively Parallel Processing*, 1998, pp. 114–122.

[23] R. D. Chamberlain, M. A. Franklin, and C. S. Baw, "Gemini: An optical interconnection network for parallel processing," *IEEE Transactions on Parallel and Distributed Systems*, vol. 13, no. 10, pp. 1038–1055, 2002.

[24] M. Y. Chan, "Embedding of d-dimensional grids into optimal hypercubes," in *SPAA '89: Proceedings of the first annual ACM symposium on Parallel algorithms and architectures*, 1989, pp. 52–57.

[25] M. Y. Chan and F. Y. L. Chin, "On embedding rectangular grids in hypercubes," *IEEE Transactions on Computers*, vol. 37, no. 10, pp. 1285–1288, 1988.

[26] M. Y. Chan, "Embedding of grids into optimal hypercubes," *SIAM Journal on Computing*, vol. 20, no. 5, pp. 834–864, 1991.

[27] C. Chen and F. K. Hwang, "The minimum distance diagram of double-loop networks," *IEEE Transactions on Computers*, vol. 49, no. 9, pp. 977–979, 2000.

[28] C. Chen, J. K. Lan, and W.-S. Tang, "An efficient algorithm to find a double-loop network that realizes a given L-shape," *Theoretical Computer Science*, vol. 359, no. 1, pp. 69–76, 2006.

[29] Y. Chen and H. Shen, "An improved scheme of wavelength assignment for parallel fft communication pattern on a class of regular optical networks," in *Proceedings of the IFIP International Conference on Network and Parallel Computing*, 2005, pp. 189–196.

[30] ——, "Wavelength assignment for directional hypercube communications on a class of WDM optical networks," in *International Conference on Parallel Processing (ICPP 2007)*, 2007, p. 71.

[31] Y. Chen, H. Shen, and F. Liu, "Wavelength assignment for realizing parallel FFT on regular optical networks," *The Journal of Supercomputing*, vol. 36, no. 1, pp. 3–16, 2006.

[32] Y. Cheng and F. K. Hwang, "Diameters of weighted double loop networks," *Journal of Algorithms*, vol. 9, no. 3, pp. 401–410, 1988.

[33] C. H. Chou and D. H. C. Du, "Uni-directional hypercubes," in *Proceedings of conference on Supercomputing*, 1990, pp. 254–263.

[34] X. Chu and B. Li, "Dynamic routing and wavelength assignment in the presence of wavelength conversion for all-optical networks," *IEEE/ACM Transactions on Networking*, vol. 13, no. 3, pp. 704–715, 2005.

[35] M. M. de Azevedo, N. Bagherzadeh, and S. Latifi, "Low expansion packings and embeddings of hypercubes into star graphs: A performance-oriented approach," *IEEE Transactions on Parallel and Distributed Systems*, vol. 9, no. 3, pp. 261–274, 1998.

[36] H. P. Dharmasena and X. Yan, "An optimal fault-tolerant routing algorithm for weighted bidirectional double-loop networks," *IEEE Transactions on Parallel and Distributed Systems*, vol. 16, no. 9, pp. 841–852, 2005.

[37] J. Díaz, J. Petit, and M. Serna, "A survey of graph layout problems," *ACM Computing Surveys*, vol. 34, no. 3, pp. 313–356, 2002.

[38] A. Ding and G. S. Poo, "A survey of optical multicast over WDM networks," *Computer Communications*, vol. 26, no. 2, pp. 193–200, 2003.

[39] T. Dobravec, B. Robič, and J. Žerovnik, "Permutation routing in double-loop networks: design and empirical evaluation," *Journal of Systems Architecture: the EUROMICRO Journal*, vol. 48, no. 13-15, pp. 387–402, 2003.

[40] T. Dobravec, J. Žerovnik, and B. Robič, "An optimal message routing algorithm for circulant networks," *Journal of Systems Architecture: the EUROMICRO Journal*, vol. 52, no. 5, pp. 298–306, 2006.

[41] Q. Dong, X. Yang, J. Zhao, and Y. Y. Tang, "Embedding a family of disjoint 3D meshes into a crossed cube," *Information Sciences*, vol. 178, no. 11, pp. 2396–2405, 2008.

[42] P. W. Dowd, "Wavelength division multiple access channel hypercube processor interconnection," *IEEE Transactions on Computers*, vol. 41, no. 10, pp. 1223–1241, 1992.

[43] R. Dutta and G. N. Rouskas, "A survey of virtual topology design algorithms for wavelength routed optical networks," Tech. Rep., 1999.

[44] K. Efe, A. L. Broadwater, and A. Fernández, "Embedding complete binary trees in product graphs," *Telecommunication Systems*, vol. 13, no. 1, pp. 99–109, 2000.

[45] J. Ellis, "Embedding rectangular grids into square grids," *IEEE Transactions on Computers*, vol. 40, no. 1, pp. 46–52, 1991.

[46] J. A. Ellis, S. Chow, and D. Manke, "Many to one embeddings from grids into cylinders, tori, and hypercubes," *SIAM Journal on Computing*, vol. 32, no. 2, pp. 386–407, 2003.

[47] J. A. Ellis and M. Markov, "Embedding grids into grids: Dilation four suffices," *Parallel Processing Letters*, vol. 8, no. 2, pp. 243–250, 1998.

[48] J. Erbele, "The cyclic cutwidth of Q_n," California State University San Bernardino (CSUSB), Tech. Rep., 2003.

[49] J. Fan and X. Jia, "Embedding meshes into crossed cubes," *Information Sciences*, vol. 177, no. 15, pp. 3151–3160, 2007.

[50] J. Fang, J. Hsiao, and C. Tang, "Embedding meshes and torus networks onto degree four chordal rings," in *IEE Proceedings:Computers and Digital Technieques*, 1998, pp. 73–80.

[51] M. Fiol, J. L. A. Yebra, I. Alegre, and M. Valero, "A discrete optimization problem in local networks and data alignment," *IEEE Transactions on Computers*, vol. 36, no. 6, pp. 702–713, 1987.

[52] M. M. Freire, R. M. F. Coelho, and J. J. P. C. Rodrigues, "The role of nodal degree in the optical core of IP-over-WDM networks." in *Proceedings of the 8th IEEE International Symposium on Computers and Communication*, 2003, pp. 661–665.

[53] M. M. Freire and H. J. A. da Silva, "Influence of chord length on the blocking performance of wavelength-routed chordal ring networks." in *Proceedings of the IFIP TC6 Fifth Working Conference on Optical Network Design and Modeling*, 2001, pp. 79–88.

[54] ——, "Performance comparison of wavelength routing optical networks with chordal ring and mesh-torus topologies." in *Proceedings of the First International Conference on Networking*, 2001, pp. 358–367.

[55] M. Freire, R. Coelho, and J. Rodrigues, "High performance optical backbones for next generation internet," in *International Conference on Information Technology: Computers and Communications*, 2003, p. 170.

[56] L. Gardner, Z. Miller, D. Pritikin, and I. H. Sudborough, "Embedding hypercubes into pancake, cycle prefix and substring reversal networks," in *Proceedings of the 28th Hawaii International Conference on System Sciences*, 1995, pp. 537–545.

[57] L. Gargano, P. Hell, and S. Perennes, "Colouring paths in directed symmetric trees with applications to WDM routing," in *Proceedings of the 24th International Colloquium on Automata, Languages and Programming*, 1997, pp. 505–515.

[58] L. Gargano and U. Vaccaro, "Routing in all-optical networks: Algorithmic and graph-theoretic problems," in *Information and Complexity*. Kluwer Academic Publishers, 2000, pp. 555–578.

[59] J. Gu, X. Hu, X. Jia, and M. Zhang, "Routing algorithm for multicast under multi-tree model in optical networks," *Theoretical Computer Science*, vol. 314, no. 1, pp. 293–301, 2004.

[60] Q. Gu and S. Peng, "Multihop all-to-all broadcast on WDM optical networks." *IEEE Transactions on Parallel and Distributed Systems*, vol. 14, no. 5, pp. 477–486, 2003.

[61] D. J. Guan, "An optimal message routing algorithm for double-loop networks," *Information Processing Letters*, vol. 65, no. 5, pp. 255–260, 1998.

[62] A. K. Gupta and S. E. Hambrusch, "Embedding complete binary trees into butterfly networks," *IEEE Transactions on Computers*, vol. 40, no. 7, pp. 853–863, 1991.

[63] A. K. Gupta, D. Nelson, and H. Wang, "Efficient embeddings of ternary trees into hypercubes," *Journal of Parallel and Distributed Computing*, vol. 63, no. 6, pp. 619–629, 2003.

[64] M. Hamdi and S. W. Song, "Efficient embeddings into the hypercube using matrix transformations," in *Proceedings of the 9th international conference on Supercomputing*, 1995, pp. 280–288.

[65] ——, "Embedding hierarchical hypercube networks into the hypercube," *IEEE Transactions on Parallel and Distributed Systems*, vol. 8, no. 9, pp. 897–902, 1997.

[66] R. Heckmann, R. Klasing, B. Monien, and W. Unger, "Optimal embedding of complete binary trees into lines and grids," *Journal of Parallel and Distributed Computing*, vol. 49, no. 1, pp. 40–56, 1998.

[67] V. Heun and E. W. Mayr, "Efficient dynamic embeddings of binary trees into hypercubes," *Journal of Algorithms*, vol. 43, no. 1, pp. 51–84, 2002.

[68] C. T. Ho and S. L. Johnsson, "Embedding hyperpyramids into hypercubes," *IBM Journal of Research and Development*, vol. 38, no. 1, pp. 31–45, 1994.

[69] C. Ho and S. L. Johnsson, "Embedding three-dimensional meshes in boolean cubes by graph decomposition," in *Proceedings of the International Conference on Parallel Processing*, 1990, pp. 319–326.

[70] ——, "Dilation *d* embedding of a hyper-pyramid into a hypercube," in *Supercomputing '89: Proceedings of the 1989 ACM/IEEE conference on Supercomputing*. New York, NY, USA: ACM, 1989, pp. 294–303.

[71] J.-W. Hong, K. Mehlhorn, and A. L. Rosenberg, "Cost trade-offs in graph embeddings, with applications," *Journal of ACM*, vol. 30, no. 4, pp. 709–728, 1983.

[72] H. Huang, C. Yang, and K. Tseng, "Broadcasting on uni-directional hypercubes and its applications," *Journal of Information Science and Engineering*, vol. 19, no. 2, pp. 183–203, 2003.

[73] F. K. Hwang, "A complementary survey on double-loop networks," *Theoretical Computer Science*, vol. 263, no. 1-2, pp. 211–229, 2001.

[74] ——, "A survey on multi-loop networks." *Theoretical Computer Science*, vol. 1-3, no. 299, pp. 107–121, 2003.

[75] B. James, "The cyclical cutwidth of the three-dimensional and four-dimensional cubes," CSUSB McNair Scholars Program Summer Research Journal, Tech. Rep., 1996.

[76] H. Kaplan and R. Shamir, "Embedding one interconnection network in another," *Computing Supplement*, vol. 7, p. 257282, 1990.

[77] ——, "Pathwidth, bandwidth, and completion problems to proper interval graphs with small cliques," *SIAM Journal on Computing*, vol. 25, no. 3, pp. 540–561, 1996.

[78] R. Klasing, R. Luling, and B. Monien, "Compressing cube-connected cycles and butterfly networks," in *Proc. 2nd IEEE Symposium on Parallel and Distributed Processing*, 1990, pp. 858–865.

[79] H. Lee, H. Choi, S. Subramaniam, and H.-A. Choi, "Survivable embedding of logical topologies in WDM ring networks," *Information SciencesInformatics and Computer Science*, vol. 149, no. 1-3, pp. 151–160, 2003.

[80] F. T. Leighton, *Introduction to Parallel Algorithms and Architectures: Arrays, Trees, Hypercubes*. Morgan Kaufmann, 1992.

[81] D. Li, X. Du, X. Hu, L. Ruan, and X. Jia, "Minimizing number of wavelengths in multicast routing trees in WDM networks," *Networks*, vol. 35, no. 4, pp. 260–265, 2000.

[82] K. Li, *Parallel Computing Using Optical Interconnections*, Y. Pan and S. Q. Zheng, Eds. Kluwer Academic Publishers, 1998.

[83] Y. Li, S. B. Rao, and A. W. Lohmann, "Free-space optical mesh-connected bus networks using wavelength-division multiple access," *Applied Optics*, vol. 32, pp. 6425–6437, Nov. 1993.

[84] W. Liang and H. Shen, "Multicasting and broadcasting in large WDM networks," in *Proceddings of the 11th International Parallel Processing Symposium*, 1998, pp. 365–369.

[85] W. Liang and X. Shen, "A general approach for all-to-all routing in multihop WDM optical networks." *IEEE/ACM Transactions on Networking*, vol. 14, no. 4, pp. 914–923, 2006.

[86] C. C. Lin, X. Ma, and S. Huang, "(R) edge embedding of two-dimensional grids in hypercubes with dilation two and congestion three," *Proceedings of the International Conference on Parellel Processing*, vol. 02, pp. 62 – 69, 1996.

[87] Y. Liu, Y. Wang, and D. J. Guan, "An optimal fault-tolerant routing algorithm for double-loop networks," *IEEE Transactions on Computers*, vol. 50, no. 5, pp. 500–505, 2001.

[88] A. Louri and S. Furlonge, "Feasibility study of a scalable optical interconnection network for massively parallel processing systems," *Applied Optics*, vol. 35, no. 8, p. 1296, 1996.

[89] A. Louri, B. Weech, and C. Neocleous, "A spanning multichannel linked hypercube: A gradually scalable optical interconnection network for massively parallel computing," *IEEE Transactions on Parallel and Distributed Systems*, vol. 9, no. 5, pp. 497–512, 1998.

[90] E. Ma and L. Tao, "Embeddings among meshes and tori," *Journal of Parallel and Distributed Computing*, vol. 18, no. 1, pp. 44–55, 1993.

[91] A. Mei and R. Rizzi, "Hypercube computations on partitioned optical passive stars networks." *IEEE Transactions on Parallel and Distributed Systems*, vol. 17, no. 6, pp. 497–507, 2006.

[92] R. G. Melhem and G. Hwang, "Embedding rectangular grids into square grids with dilation two," *Interconnection networks for high-performance parallel computers*, pp. 577–586, 1994.

[93] Z. Miller, D. Pritikin, and I. H. Sudborough, "Near embeddings of hypercubes into cayley graphs on the symmetric group," *IEEE Transactions on Computers*, vol. 43, no. 1, pp. 13–22, 1994.

[94] B. Monien, "Simulating binary trees on x-trees (extended abstract)," in *SPAA '91: Proceedings of the third annual ACM symposium on Parallel algorithms and architectures*, 1991, pp. 147–158.

[95] B. Mukherjee, D. Banerjee, S. Ramamurthy, and A. Mukherjee, "Some principles for designing a wide-area WDM optical network," *IEEE/ACM Transactions on Networking*, vol. 4, no. 5, pp. 684–696, 1996.

[96] S. Nakano, N. Kamiura, Y. Hata, and N. Matsui, "Reconfiguration of two-dimensional meshes embedded in faulty hypercubes," *Proceedings of international Symposium on Defect and Fault Tolerance in VLSI Systems*, pp. 395 – 403, 1999.

[97] L. Narayanan, J. Opatrny, and D. Sotteau, "All-to-all optical routing in optimal chordal rings of degree four," in *Proceedings of the 10th Annual ACM-SIAM Symposium on Discrete algorithms*, 1999, pp. 695–703.

[98] J. Newsome and D. Song, "Gem: Graph embedding for routing and data-centric storage in sensor networks without geographic information," in *Proceedings of the 1st international conference on Embedded networked sensor systems*, 2003, pp. 76–88.

[99] C. Nomikos, A. Pagourtzis, K. Potika, and S. Zachos, "Routing and wavelength assignment in multifiber WDM networks with non-uniform fiber cost," *Computer Networks*, vol. 50, no. 1, pp. 1–14, 2006.

[100] J. Opatrny, "Uniform multi-hop all-to-all optical routings in rings," in *LATIN '00: Proceedings of the 4th Latin American Symposium on Theoretical Informatics*. London, UK: Springer-Verlag, 2000, pp. 237–246.

[101] D. A. Patterson and J. L. Hennessy, *Computer architecture: a quantitative approach*. San Francisco, CA, USA: Morgan Kaufmann Publishers Inc., 1990.

[102] J. M. Peha and F. A. Tobagi, "Analyzing the fault tolerance of double-loop networks," *IEEE/ACM Transactions on Networking*, vol. 2, no. 4, pp. 363–373, 1994.

[103] S. Ponnuswamy, S. Ponnuswamy, V. Chaudhary, and V. Chaudhary, "Embedding of meshes on rotator graphs," in *Proceedings of the 36th Midwest Symposium on Circuits and Systems*, 1993, pp. 5–8.

[104] G. S. Poo and Y. Zhou, "A, new multicast wavelength assignment algorithm in wavelength-routed WDM networks," *IEEE Journal on Selected Areas in Communications*, vol. 24, no. S-4, pp. 2–12, 2006.

[105] C. Qiao and Y. Mei, "On the multiplexing degree required to embed permutations in a class of networks with direct interconnects," in *Proceedings of the 2nd IEEE Symposium on High-Performance Computer Architecture*, 1996, p. 118.

[106] ——, "Off-line permutation embedding and scheduling in multiplexed optical networks with regular topologies," *IEEE/ACM Transactions on Networking*, vol. 7, no. 2, pp. 241–250, 1999.

[107] X. Qin and Y. Yang, "Multicast connection capacity of WDM switching networks with limited wavelength conversion," *IEEE/ACM Transactions on Networking*, vol. 12, no. 3, pp. 526–538, 2004.

[108] P. Raghavan and E. Upfal, "Efficient routing in all-optical networks," in *Proceedings of the 26th annual ACM Symposium on Theory of Computing*, 1994, pp. 134–143.

[109] R. Ramaswami and K. N. Sivarajan, "Routing and wavelength assignment in all-optical networks," *IEEE/ACM Transactions on Networking*, vol. 3, no. 5, pp. 489–500, 1995.

[110] S. Ranka, J. Wang, and N. Yeh, "Embedding meshes on the star graph," in *Supercomputing '90: Proceedings of the 1990 ACM/IEEE conference on Supercomputing*, 1990, pp. 476–485.

[111] A. Raspaud and O. S. Ykora, "Congestion and dilation, similarities and differences - a survey," in *In Proceedings of the 7th International Colloquium on Structural Information and Communication Complexity*, 2000, pp. 269–280.

[112] M. Röttger and U. Schroeder, "Embedding 2-dimensional grids into optimal hypercubes with edge-congestion 1 or 2," *Parallel Processing Letters*, vol. 8, no. 2, pp. 231–242, 1998.

[113] M. Röttger, U. Schroeder, and W. Unger, "Embedding 3-dimensional grids into optimal hypercubes," in *Canada-France Conference on Parallel and Distributed Computing*, 1994, pp. 81–94.

[114] Y. Saad and M. H. Schultz, "Topological properties of hypercubes," *IEEE Transactions on Computers*, vol. 37, no. 7, pp. 867–872, 1988.

[115] P. Saengudomlert, E. Modiano, and R. G. Gallager, "Lightpath communications: an approach to high bandwidth optical WAN's," *IEEE Transactions on Communications*, vol. 40, no. 7, pp. 1171–1182, 1992.

[116] H. Schroder, H. Schroder, O. Sykora, and I. Vrto, "Cyclic cutwidths of the mesh," in *Proceedings of International Conference on Current Trends in Theory and Practice of Computer Science*, 1999, pp. 443–452.

[117] H. Schröder, O. Sýkora, and I. Vrto, "Optical all-to-all communication for some product graphs," in *Proceedings of the 24th Seminar on Current Trends in Theory and Practice of Informatics*, 1997, pp. 555–562.

[118] H. Shen, F. Chin, and Y. Pan, "Efficient fault-tolerant routing in multihop optical WDM networks," *IEEE Transactions on Parallel and Distributed Systems*, vol. 10, no. 10, pp. 1012–1025, 1999.

[119] X. Shen, W. Liang, and Q. Hu, "On embedding between 2D meshes of the same size," *IEEE Transactions on Computers*, vol. 46, no. 8, pp. 880–889, 1997.

[120] S.K.Lee, A. Oh, and H. Choi, "Transmission schedules for hypercube interconnection in WDM optical passive star networks," *Discrete Applied Mathematics*, vol. 117, pp. 133–148(16), 2002.

[121] T. Sung, C. Lin, Y. Chuang, and L. H. Hsu, "Fault tolerant token ring embedding in double loop networks," *Information Processing Letters*, vol. 66, no. 4, pp. 201–207, 1998.

[122] T. Tan and D. H. Du, "Embedded unidirectional incomplete hypercubes for optical networks," *IEEE Transactions on Communications*, vol. 41, no. 9, pp. 1284–1289, 1993.

[123] C. Tsai, "Embedding of meshes in möbius cubes," *Theoretical Computer Science*, vol. 401, no. 1-3, pp. 181–190, 2008.

[124] Y. Tseng, S. Chang, and J. Sheu, "Fault-tolerant ring embedding in a star graph with both link and node failures," *IEEE Transactions on Parallel and Distributed Systems*, vol. 08, no. 12, pp. 1185–1195, 1997.

[125] L. G. Valiant, "Universality considerations in VLSI circuits." *IEEE Transactions on Computers*, vol. 30, no. 2, pp. 135–140, 1981.

[126] T. S. Wailes and D. G. Meyer, "Multiple channel architecture: a new optical interconnection strategy for massively parallel computers," *Journal of Lightwave Technology*, vol. 9, pp. 1702–1716, 1991.

[127] C. K. Wong and D. Coppersmith, "A combinatorial problem related to multimodule memory organizations," *Journal of ACM*, vol. 21, no. 3, pp. 392–402, 1974.

[128] P. E. Wright and F. K. Hwang, "Survival reliability of some double-loop networks and chordal rings," *IEEE Transactions on Computers*, vol. 44, no. 12, pp. 1468–1471, 1995.

[129] C. Xin, "Blocking analysis of dynamic traffic grooming in mesh WDM optical networks," *IEEE/ACM Transactions on Networking*, vol. 15, no. 3, pp. 721–733, 2007.

[130] M.-C. Yang, J. J. M. Tan, and L.-H. Hsu, "Highly fault-tolerant cycle embeddings of hypercubes," *Journal of Systems Architecture*, vol. 53, no. 4, pp. 227–232, 2007.

[131] Y. Yang and J. Wang, "Cost-effective designs of WDM optical interconnects," *IEEE Transactions on Parallel and Distributed Systems*, vol. 16, no. 1, pp. 51–66, 2005.

[132] X. Yuan and R. Melhem, "Optimal routing and channel assignments for hypercube communication on optical mesh-like processor arrays," in *Proceedings of the The Fifth International Conference on Massively Parallel Processing Using Optical Interconnections*, 1998, pp. 110–118.

[133] X. Yuan, "Dynamic and compiled communication in optical time-division-multiplexed point-to-point networks," Ph.D. dissertation, Pittsburgh, PA, USA, 1998.

[134] H. Zang, J. P. Jue, and B. Mukherjee, "A review of routing and wavelength assignment approaches for wavelength-routed optical networks," *Optical Network Magazine*, vol. 1, no. 1, pp. 47–60, 2000.

[135] X. Zhang and C. Qiao, "On scheduling all-to-all personalized connections and cost-effective designs in WDM rings," *IEEE/ACM Transactions on Networking*, vol. 7, no. 3, pp. 435–445, 1999.

[136] X. Zhang, J. Wei, and C. Qiao, "Constrained multicast routing in WDM networks with sparse light splitting," in *Proceedings of the IEEE Conference on Computer Communications(INFOCOM)*, 2000, pp. 1781–1790.

[137] Y. Zhang, X. He, G. Zhou, W. Liu, Y. Wang, and Z. Yin, "Optical fiber interconnection system for massively parallel processor arrays," in *Proceedings of the*

Second Workshop on Massively Parallel Processing Using Optical Interconnections, 1995, p. 57.

[138] Z. Zhang and Y. Yang, "On-line optimal wavelength assignment in WDM networks with shared wavelength converter pool," *IEEE/ACM Transactions on Networking*, vol. 15, no. 1, pp. 234–245, 2007.

[139] C. Zhou and Y. Yang, "Multicast communication in a class of rearrangeable optical WDM networks," in *MPPOI '98: Proceedings of the The Fifth International Conference on Massively Parallel Processing Using Optical Interconnections*. Washington, DC, USA: IEEE Computer Society, 1998, p. 68.

[140] Y. Zhou and G. S. Poo, "Multicast wavelength assignment for sparse wavelength conversion in WDM networks," in *Proceedings of the IEEE Conference on Computer Communications(INFOCOM)*, 2006.

[141] T. F. Znati, T. Alrabiah, and R. Melhem, "Low-cost, delay-bounded point-to-multipoint communication to support multicasting over WDM networks," *Computer Networks*, vol. 38, no. 4, pp. 423–445, 2002.